

Lithocholic Acid and Macromitophagy Regulate the Dynamics of Lipid Metabolism and Storage
to Modulate Chronological Aging in *Saccharomyces cerevisiae*

Vincent Roy Richard

A Thesis
In
The Department
Of
Biology

Presented in Partial Fulfillment of the Requirement
For the Degree of Doctor of Philosophy in Biology
Concordia University
Montreal, Quebec, Canada

May 2014

© Vincent Roy Richard, 2014

Concordia University
School of Graduate Studies

This is to certify that the thesis prepared

By: Vincent Roy Richard

Entitled: **Lithocholic Acid and Macromitophagy Regulate the Dynamics of Lipid Metabolism and Storage to Modulate Chronological Aging in *Saccharomyces cerevisiae***

and submitted in partial fulfillment of the requirements for the degree of

Doctor of Philosophy (Biology)

complies with the regulations of the University and meets the accepted standards with respect to originality and quality.

Signed by the final Examining Committee:

_____	Chair
Dr. Monica Mulrennan	
_____	External Examiner
Dr. Nancy Braverman	
_____	Examiner
Dr. Catherine Bachewich	
_____	Examiner
Dr. Patrick Gulick	
_____	Examiner
Dr. Dajana Vuckovic	
_____	Thesis Supervisor
Dr. Vladimir Titorenko	

Approved by _____

Chair of Department or Graduate Program Director

_____ 2014

Dean of Faculty

Abstract

Aging is a complex biological phenomenon that is caused by a multitude of extrinsic and intrinsic factors. At the level of the organism aging can be defined as the loss of resistance to factors promoting pathologies over time, while at the population level it is more accurately reflected by the increased mortality rate with the age of the population. Understanding the underlying intrinsic and extrinsic factors is key to understanding, and perhaps mitigating age-related functional decline. In our lab we use *Saccharomyces cerevisiae* as a model organism for studying the cellular and molecular mechanisms that regulate cellular aging. In the course of my project I sought to investigate the role of mitochondrial quality control, as well as lipid metabolism and storage in regulating the aging process in yeast. We found that deletion of Atg32p shortened yeast chronological lifespan (CLS) under caloric restriction growth conditions and abrogated the life-extending capabilities of lithocholic acid (LCA) – a bile acid that extends CLS even under caloric restriction conditions. Deletion of Atg32p also resulted in aberrant morphology, membrane lipid composition, and a reduction in the mitochondrial functional state. To address why deletion of Atg32p negated the beneficial effects of LCA we sought to first locate into which subcellular compartment LCA accumulates. It was found that LCA enters yeast cells and accumulates largely in the inner mitochondrial membrane. I observed that treatment with LCA alters mitochondrial lipid composition, size, and morphology. In the *atg32Δ* deletion background, mitochondrial lipid composition was aberrant, and these cells were highly susceptible to both H₂O₂ induced apoptosis and fatty acid induced liponecrotic cell death. From this I sought to understand the mechanisms through which exogenous monounsaturated fatty acids induced cell death. Using a combination of electron microscopy, biochemical assays, and mass spectrometry it was found that exogenous palmitoleic acid (POA) causes a type of cell death which is characterized by morphological and biochemical features which are unique from the three best characterized types of programmed cell death- apoptosis, necrosis, and autophagic cell death – and has henceforth been referred to as liponecrotic cell death. In addition to this, we showed that mitophagy as well as lipid storage pathways and peroxisomal beta-oxidation of free fatty acids are protective processes against POA induced programmed cell death. Together this data allowed for the formulation of a working model integrating mitochondrial quality control processes and those involved in lipid metabolism and storage in mediating the regulation of chronological lifespan in yeast.

Acknowledgements

I would like to acknowledge the tremendous guidance and support of my supervisor Dr. Vladimir Titorenko, who was instrumental in the design and troubleshooting of much of the work shown in this thesis. I would also like to thank the members of my graduate committee Dr. Catherine Bachewich and Dr. Patrick Gulick for valuable questions and constructive criticism. In addition I would like to thank the Center For Biological Applications of Mass Spectrometry (CBAMS) and especially Jean-Pierre Falguyret and Alain Tessier for invaluable assistance and expertise with training and assistance in method development and instrumentation for my various uses of mass spectrometry. My doctoral studies were funded by the Canadian Institutes of Health Research (CIHR).

I'd like to thank my friends and fellow graduate students Adam Beach, Michelle Burstein, Anna Leonov, Pavlo Kyryakov, Alex Goldberg, Simon Bourque, Alejandra Gomez-Perez, Rachel Feldman and Olivia Koupaki. I would also like to acknowledge the large number of undergraduate students, volunteers, summer research students, and international exchange students who made the lab a vibrant and diverse work environment.

Most importantly I'd like to acknowledge my family and friends for their unwavering support over the course of my doctoral studies.

My sincerest thanks,
Vincent R. Richard

Table of Contents

List of Figures	VI
Abbreviations	XII
1. Introduction	1
1.1 Aging can be mitigated through genetic, dietary, and chemical interventions	1
1.2 Yeast as a model for studying programmed cell death and aging	2
1.3 Interorganellar dynamics of lipid metabolism and storage as a key mediator of cell death and aging in yeast	3
1.4 Thesis Outline and Contributions	6
2. Chemical genetic screen identifies lithocholic acid as an anti-aging compound	10
2.1 Introduction	10
2.2 Materials and Methods	11
2.3 Results	13
2.3.1 LCA extends the CLS of WT yeast under CR by modulating the storage of FFA	14
2.3.2 LCA extends yeast CLS independent of TOR by modulating housekeeping longevity assurance pathways	14
2.4 Discussion and Conclusion	17
3. Mitochondrial membrane lipidome defines yeast longevity	19
3.1 Introduction	19
3.2 Materials and Methods	20
3.3 Results	22
3.3.1 Mitochondrial membranes of yeast cultured in the presence of LCA exhibit altered concentrations of various glycerophospholipid species	22
3.3.2 Mitochondrial membranes of yeast cultured in the presence of LCA display reduced concentration of non-bilayer forming glycerophospholipids and elevated concentrations of their bilayer forming species	29
3.3.3 Mitochondria of yeast cultured in the presence of LCA are enlarged, their number is reduced and their morphology is altered	31
3.4 Discussion	34

3.5 Conclusions.....	35
4. Macromitophagy is a longevity assurance process that in chronologically aging yeast limited under caloric restriction conditions maintains cellular lipid homeostasis	38
4.1 Introduction	38
4.2 Materials and Methods	39
4.3 Results.....	42
4.3.1 Macromitophagy is required for maintaining the homeostasis of membrane lipids in the mitochondria, ER, and PM.....	42
Discussion	47
Conclusion	49
5. Macromitophagy protects yeast from liponecrotic programmed cell death	51
5.1 Abstract.....	51
5.2 Introduction	51
5.3 Materials and Methods	53
5.4 Results.....	55
5.4.1 Macromitophagy protects yeast from a mode of cell death triggered by exogenous palmitoleic fatty acid (POA)	55
5.4.2 POA induces “liponecrosis”, a mode of cell death that differs from apoptotic, regulated necrotic and autophagic cell death subroutine	57
5.4.3 Macromitophagy, functional mitochondria, and neutral lipids synthesis protect yeast from liponecrotic cell death elicited by POA	62
5.4.4 Peroxisomal fatty acid oxidation protects yeast from liponecrotic cell death triggered by POA	64
5.4.5 Non-selective macroautophagy executes liponecrotic cell death elicited by POA...64	
5.5 Discussion.....	67
5.6 Conclusions.....	68
6. Mechanism of Liponecrosis, a distinct mode of programmed cell death	72
6.1 Introduction	72
6.2 Materials and Methods	73
6.3 Results.....	74

6.3.1 The extent of POA incorporation into neutral lipids and phospholipids defines the susceptibility of yeast to liponecrotic PCD.....	74
6.3.2 The alkaline pH and lipid asymmetry responsive Rim101 signalling pathway commits yeast to liponecrotic PCD by reducing the level of PE in the extracellular leaflet of the PM.....	84
6.3.3 The commitment of yeast to liponecrotic PCD elevates the extent of oxidative damage to cellular proteins and lipids	91
6.3.4 Various pathways of macroautophagy differ in their roles in POA-induced liponecrotic PCD.....	93
6.4 Discussion.....	101
7. Conclusions and Future Directions	105
8. References.....	110
9. Appendix	
A - Metabolomic and Lipidomic Analyses of Chronologically Aging Yeast.....	124

List of Figures

Figure 1: Mechanism linking non-CR conditions to FFA induced PCD.....	3
Figure 2: CR and LCA extend yeast CLS by remodelling lipid metabolism in the peroxisome, ER, and LD	5
Figure 3 In chronologically aging WT yeast that entered the non-proliferative stationary (ST) phase under CR, LCA alters the levels of lipids and protects cells from lipid-induced necrotic death.....	12
Figure 4 In spite of a partial reduction in the life-extending efficacy of LCA in yeast lacking Ras2p, LCA still significantly increases their mean and maximum life spans under CR and non-CR conditions	14
Figure 5 Although the life-extending efficacy of LCA in yeast lacking Rim15p is partially reduced, LCA still significantly increases their mean and maximum life spans under CR and non-CR conditions	15

Figure 6 Outline of pro- and anti-aging processes that are controlled by the TOR and/or cAMP/PKA signaling pathways and are modulated by LCA or rapamycin (RAP) in chronologically aging yeast	17
Figure 7 - In yeast cultures containing exogenously added LCA, this bile elevates the glycerophospholipid/protein ratio of mitochondrial membranes in an age-dependent manner.....	24
Figure 8 - LCA exhibits age-dependent differential effects on the concentrations (calculated as nanomoles of glycerophospholipid/mg of protein) of different species of mitochondrial membrane glycerophospholipids	27
Figure 9 - LCA exhibits age-dependent differential effects on the relative levels (calculated as molar percentage of all glycerophospholipids) of different molecular forms of mitochondrial membrane glycerophospholipids.....	28
Figure 10 - LCA does not cause a significant change in the “unsaturation index” for any of the glycerophospholipid species	29
Figure 11 - LCA reduces the relative levels of non-bilayer forming glycerophospholipids and elevates the relative levels of their bilayer forming species	31
Figure 12 LCA enlarges mitochondria, reduces their number and alters their morphology.	34
Figure 13 - A model for a mechanism underlying the ability of LCA to extend yeast longevity by accumulating in mitochondria, altering mitochondrial membrane lipidome, and affecting mitochondrial morphology and function.	37
Figure 14 - Lipid synthesis in the ER and mitochondria and lipid transport via mitochondria-ER and PM-ER junctions.....	45
Figure 15 - Under CR conditions, the atg32Δ mutation alters levels of several membrane lipid species in mitochondria, the ER and the PM.	47
Figure 16 - A working model for a mechanism that in atg32Δ cells underlies the spatiotemporal dynamics of age-related changes in lipid synthesis in the ER and mitochondria as well as in lipid transport via mitochondria-ER (MAM) and PM-ER (PAM) junctions.....	51
Figure 17 – Deletion of Atg32p increases yeast susceptibility of cell death induced by palmitoleic acid (POA) as well as hydrogen peroxide.....	58
Figure 18 - Morphological traits characteristic of the cell death subroutines triggered by a short-term exposure to exogenous POA or hydrogen peroxide.	60

Figure 19 - Percentage of WT and *atg32Δ* cells that display nuclear fragmentation (A), plasma membrane rupture (B), LD accumulation (C) or lack of all cellular organelles (D). 61

Figure 20 - Percentage of WT and *atg32Δ* cells that display nuclear fragmentation (A), phosphatidylserine (PS) externalization (B), propidium iodide (PI) positive staining (C) or LDaccumulation (D).. 62

Figure 21 - WT, *dga1Δ*, *are2Δ*, *cyc3Δ* and *fox1Δ* cells were recovered at days 1, 2 and 4 of culturing in a nutrient-rich YP medium initially containing 0.2% glucose as carbon source. 64

Figure 22 - A non-selective en masse autophagic degradation of cellular organelles and macromolecules executes an orchestrated by Atg1p form of POA-induced liponecrotic cell death, whereas such degradation operates as a pro-survival process in yeast committed to apoptotic death that is triggered by cell exposure to exogenous hydrogen peroxide. 67

Figure 23 - A model for molecular mechanisms underlying programmed liponecrotic cell death elicited by POA. An incorporation of POA into POA-containing phospholipids (PL) and their consequent accumulation in various cellular membranes may operate as pro-death processes that create excessive cellular stress, thereby triggering liponecrosis. 72

Figure 24 - An exposure of WT cells to various concentrations of exogenous POA elicits differential age-dependent effects on the relative levels of all molecular species of phospholipids and TAG, and the *atg32Δ*-dependent mutational block of mitophagy alters these effects..... 79

Figure 25 - An exposure of WT cells to various concentrations of exogenous POA elicits differential age-dependent effects on the relative levels of C16:1 molecular species (i.e., POA-containing species) of phospholipids and TAG, and the *atg32Δ*-dependent mutational block of mitophagy alters these effects..... 80

Figure 26 - An exposure of WT cells to various concentrations of exogenous POA elicits differential age-dependent effects on the relative levels of C16:1 molecular species (i.e., POA-containing species) of all major forms of PL, and the *atg32Δ*-dependent mutational block of mitophagy alters these effects..... 81

Figure 27 An exposure of WT cells to various concentrations of exogenous POA elicits differential age-dependent effects on the relative levels of all molecular species of all major

forms of PL, and the atg32Δ-dependent mutational block of mitophagy alters these effects.	82
Figure 28 Outline of the flow of exogenous POA into pathways for phospholipids synthesis in the ER and mitochondria, phospholipids transport via mitochondria-ER and PM-ER junctions, TAG synthesis in the ER, and TAG deposition within LD.....	83
Figure 29 - Various single-gene-deletion mutations (each eliminating an enzyme involved in POA transport to the ER or in POA incorporation into phospholipids and/or neutral lipids within the ER) elicit differential age-dependent effects on the susceptibility of yeast to POA-induced liponecrotic PCD.....	84
Figure 30 The alkalinisation of culture medium by yeast exposed to POA is not essential for the ability of POA to trigger liponecrotic PCD.	86
Figure 31 - Outline of the alkaline-pH- and lipid-asymmetry-responsive Rim101 signaling pathway operating in yeast cells. (A) This signaling pathway can be induced by alkalinisation of culture medium and/or in response to certain changes in asymmetrical distribution of some species of phospholipids across the PM bilayer.	88
Figure 32 - Various single-gene-deletion mutations eliminating different protein components of the Rim101 signaling pathway reduce the susceptibility of yeast to POA-induced liponecrotic PCD if they decrease the extent of PE depletion in the extracellular leaflet of the PM, a hallmark event of this PCD subroutine	91
Figure 33 - Various single-gene-deletion mutations eliminating different protein components of the Rim101 signaling pathway make yeast more susceptible to POA-induced liponecrotic PCD if they increase the degree of PE depletion in the extracellular leaflet of the PM, a hallmark event of this PCD modality.....	92
Figure 34 - Yeast cells committed to liponecrotic PCD exhibit elevated oxidative damage to cellular proteins and lipids.....	93
Figure 35 - Outline of the pathways for non-selective and selective macroautophagic delivery of cellular organelles and macromolecules to the vacuole in yeast.	96
Figure 36 – Various pathways of autophagy play different roles in POA-induced liponecrotic PCD.....	97

Figure 37 - The spermidine-inducible autophagy pathway for non-selective degradation of various cellular organelles and macromolecules plays an essential role in executing POA-induced liponecrotic PCD.....	99
Figure 38 - A model for molecular mechanisms that in yeast underlie the opposing roles of various autophagy pathways in POA-induced liponecrotic PCD.....	101
Figure 39 - A model for a mechanism underlying POA-induced liponecrotic PCD in yeast.....	104
Figure 40 - Import setting for LipidXplorer	141

Abbreviations

ADHAP	Alkyldihydroxyacetonephosphate
AMPK/TOR	AMP-activated protein kinase/target of rapamycin
cAMP/PKA	cAMP/protein kinase A
CDP-DAG	cytidine diphosphate-diacylglycerol
CFU	Colony forming units
CL	Cardiolipin
CLS	Chronological Lifespan
CR	Caloric Restriction
CvT	Cytoplasm-to-vacuole targeting pathway
DG	Diglyceride
EE	Ergosteryl esters
EM	Electron microscopy
ESCRT-III	Endosomal sorting complex (type III) required for transport
FFA	Free Fatty Acids
FM	Fluorescence microscopy
IGF-1	Insulin/insulin-like growth factor 1
IMM	Inner mitochondrial membrane
LCA	Lithocholic Acid
LD	Lipid droplets
LPA	Lysophosphatidic acid
MAM	Mitochondria associated membrane
MLCL	Monolysocardiolipin
Mol%	Molar percentage
OMM	Outer mitochondrial membrane
PA	Phosphatidic acid
PAM	Plasma membrane associated membrane
PC	Phosphatidyl choline
PCD	Programmed cell death
PE	Phosphatidyl ethanolamine
PG	Phosphatidyl glycerol
PI	Phosphatidyl inositol
PL	Phospholipid
POA	Palmitoleic Acid
PS	Phosphatidyl serine
TAG	Triacylglycerols

1. Introduction

Aging is a complex biological phenomenon that is caused by a multitude of extrinsic and intrinsic factors. At the level of the organism aging can be defined as the loss of resistance to factors promoting pathologies and disease over time, while at the population level it is more accurately reflected by the increased in mortality rate with the age of the cohort ¹. Understanding the underlying intrinsic and extrinsic factors is key to understanding why the rate of aging is apparently different amongst organisms. In itself, this is very interesting – but this should also give valuable insight not just to our understanding of the aging process but also to our understanding of various human pathologies – including cancers, cardiovascular diseases, Alzheimer’s disease, etc. – since age is the predominant risk factor for the majority of them ^{2,3}.

1.1 Aging and age related dysfunction can be mitigated through genetic, dietary, and chemical interventions

Aging of multicellular and unicellular eukaryotic organisms is a multifactorial biological phenomenon that has various causes, and affects a plethora of cellular activities. Yet despite the seeming complexity of the aging process there are a number of interventions that can slow down its progression. Mutations in close to 100 genes have been found to increase the lifespan of *Saccharomyces cerevisiae* and the same is true for the evolutionarily distant worm *C. elegans* ⁴⁻⁷. Many of these mutations, which increase lifespan, target components of a relatively narrow set of nutrient- and energy-sensing signaling pathways that are conserved across phyla. These include the insulin/insulin-like growth factor 1 (IGF-1), AMP-activated protein kinase/target of rapamycin (AMPK/TOR) and cAMP/protein kinase A (cAMP/PKA) pathways. By sharing many protein kinases and adaptor proteins, the insulin/IGF-1, AMPK/TOR and cAMP/PKA form a network that regulates lifespan ^{3,8-10}. Of interest, humans with dwarfism that harbour mutations in the GHR gene (which would reduce IGF-1 signalling) have an extremely low incidence of cancers and diabetes ¹¹.

In addition to the various pro-longevity mutations, diet plays an important role in defining organismal energy and nutrient status, which has been shown to be critical in influencing the aging process in a number of organisms. Caloric restriction (CR) is a diet that extends lifespan of a number of evolutionarily distant species which is based on the lowering of caloric intake but maintaining a healthy level of amino acids, vitamins and other nutrients ³. It is

also important to note that starvation is not a condition for CR to extend lifespan. For yeast cultures this is implemented by lowering the concentration of glucose in the growth medium from 2% to 0.2-0.5%^{12,13}. In yeast this has been shown to greatly slow the aging process in part by attenuating adaptable pro-aging pathways¹⁴⁻¹⁷.

In addition to genetic and dietary interventions that extend longevity, treatment with certain small molecules can extend longevity and/or increase health-span of evolutionarily diverse organisms. The majority of the known compounds that extend longevity of yeast only work under non-CR or normal conditions. For this reason it is thought that these compounds simply mimic the effects of CR on gene expression, metabolic processes, and stress response pathways¹⁸⁻²⁰. The majority of these compounds are thought to act on the aforementioned limited set of nutrient responsive signal transduction pathways including the insulin/IGF-1 and AMPK/TOR pathways as well as the sirtuin pathway. In addition to this, some CR mimetics have been shown to only be able to increase life span under non-CR conditions²¹⁻²⁴. Some evidence suggests this is also the case for humans²⁰. This observation leads to the idea that most, if not all, longevity pathways are adaptable in that they modulate longevity only in response to certain extrinsic signals – for example the concentration of glucose in the culture media. In contrast to this a number of compounds have been identified that extend lifespan even under CR conditions²⁵⁻²⁷, indicating that some non-adaptable processes may also play a critical role in defining the longevity of organisms. Lithocholic acid which is an extremely hydrophobic bile acid, was demonstrated to greatly increase lifespan in both normal and under CR conditions²⁷. Of interest, elevated levels of a variety of bile acids and bile acid derivatives have been found in higher concentrations in the plasma of humans with longer leukocyte telomere length which is known to be involved in regulating the aging process and age related diseases^{28,29}.

1.2 Yeast as a model for studying programmed cell death and aging

The budding yeast *Saccharomyces cerevisiae* is a unicellular eukaryote, which is amenable to biochemical, genetic, and systems analyses. Because many of the genes and pathway that are already implicated in regulating aging and programmed cell death (PCD) are found in yeast, this model organism serves as an ideal model for their further elucidation. Yeast has already contributed a wealth of information about the various processes that underlie the regulation of PCD and aging^{2,6,14,27,30}.

Yeast as a model organism for the study of aging can be classified into two general paradigms- namely the replicative aging model and the chronological model. In the replicative model of yeast aging, lifespan is defined by how many buds a mother cell can produce before senescing. This system is meant to model the way that mitotically active cells in higher eukarya might age³¹. The chronological model of yeast aging studies how long cells can remain viable after entering into a non-dividing state (stationary phase). This is measured by measuring clonogenicity by comparing the total number of cells in a culture to the total number of colony forming units (CFU) over time. This paradigm models the way that post-mitotic or non-dividing cells in higher eukarya might age- for example human neurons^{6,13}.

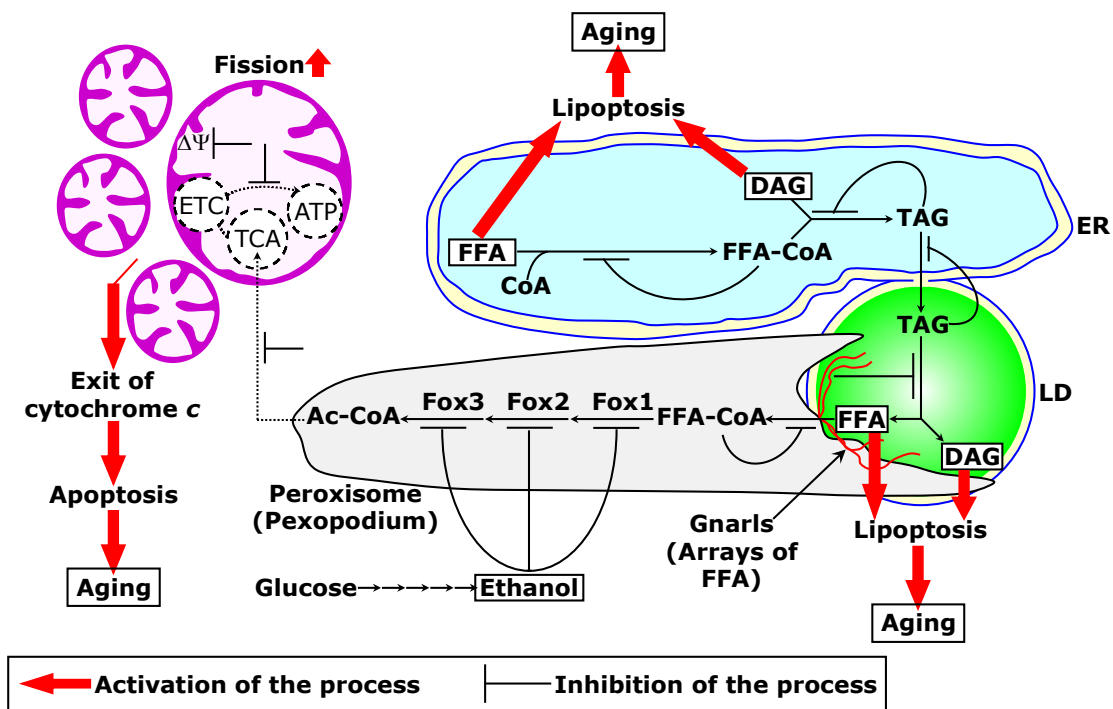


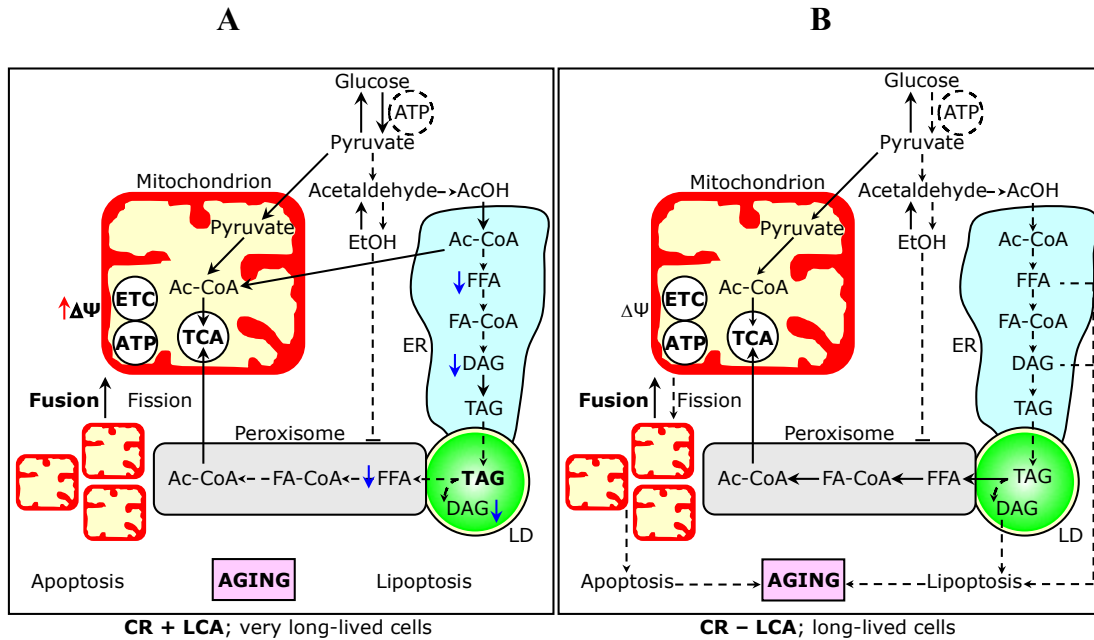
Figure 1: Mechanism linking non-CR conditions to FFA induced PCD. Caloric restriction (CR) and lithocholic acid delay aging by remodeling lipid dynamics in the endoplasmic reticulum (ER), lipid bodies (LB) and peroxisomes. The thickness of arrows correlates with the rates of metabolic processes in yeast entered stationary growth phase in nutrient-rich medium. T-bars denote inhibition of the process. The metabolites accumulated in bulk quantities are shown in bold. Red arrows connote the reduction of a metabolite concentration. Reproduced with permission from³².

1.3 Interorganellar dynamics of lipid metabolism and storage as a key mediator of cell death and aging in yeast

In addition to having conserved components of the mammalian apoptotic machinery, yeast also undergo a variety of other forms of PCD including autophagic, necrotic, and other uncharacterized types of cell death³³. This makes yeast a suitable model for studying the mechanisms that regulate PCD.

The term “PCD” refers to a genetically programmed and regulated form of cell death³⁴. Several PCD subroutines are presently known; these subroutines have different underlying mechanisms, display different morphological and biochemical traits, and are controlled by different (although partially overlapping) signalling pathways^{34–36}. The most well characterized examples of PCD subroutines include extrinsic apoptosis, caspase-dependent or -independent intrinsic apoptosis, regulated necrosis, and autophagic cell death.

Our lab has published and unpublished data that shows that one of the key processes mediating cell death and aging in yeast is lipid metabolism in the peroxisomes, lipid droplets (LD), and the ER (ER)³². Under non-CR conditions yeast primarily ferment glucose to ethanol^{13,37}. The accumulation of ethanol impinges on the ability of the peroxisome to metabolize free fatty acids (FFA) derived from the lipolytic degradation of triglycerides (TAG) in LD by decreasing the expression of enzymes involved in peroxisomal β -oxidation³⁷. This causes an accumulation of FFA within the ER and LD, ultimately leading to FFA induced PCD (Figure 1). CR reduces the amount of ethanol that is accumulated, and thus prevents the inhibition of peroxisomal oxidation of FFA. This reduces the amount of FFA in the ER and LD and decreases the cellular susceptibility to FFA induced PCD (Figure 2B). Likewise CR yeast cultures treated with lithocholic acid (LCA) exhibit increased expression of enzymes involved in TAG biosynthesis and decreased levels of enzymes involved in lipolytic degradation of TAG to FFAs. This in turn reduces the amount of FFA to a more optimal level than in CR alone. In addition to this LCA induces the increased import of acetyl-CoA into the mitochondria thereby supplying the mitochondria with a key metabolic intermediate as well as sequestering it from ER confined FFA biosynthetic processes (Figure 1, Figure 2A). In addition to this, both CR and LCA induce changes to the functional state of the mitochondria resulting in increased mitochondrial membrane potential into stationary phase, increased expression of proteins involved in the citric acid cycle and electron transport chain, and reduced mitochondrial fragmentation resulting in a reduction in the release of cytotoxic factors like cytochrome C (Figure 2AB)³⁸.



Cell Cycle (2011) 10:3042-3044

Figure 2: CR and LCA extend yeast CLS by remodelling lipid metabolism in the peroxisome, ER, and LD. See figure legend of Figure 1 for details. Reproduced with permission from ³².

Together this model implicates lipid metabolism – specifically the levels of FFA – in causing PCD in yeast, as well as illustrating the importance of mitochondrial functionality in defining processes involved in PCD and aging. However the exact mechanisms linking the accumulation of FFA to cell death, and how mitochondrial fitness is important in mitigating PCD have not been established.

We previously published that treating yeast cultures with palmitoleic acid (POA) - a mono unsaturated sixteen carbon FFA - induces cell death in yeast in a concentration dependent manner ^{27,39}. What was unknown was the mechanisms underlying POA induced PCD and whether it fit into one of the three major PCD subroutines – namely apoptotic, autophagic, or necrotic cell deaths. Based on this we were interested in understanding if POA induced cell death represented an age dependent type of cell death, and whether or not it is programmed or accidental in terms of how it is carried out. We sought to find out if certain genetic mutations could either increase or decrease a population’s susceptibility to POA induced cell death, and last we wanted to understand whether the cell death could be part of a subroutine corresponding to previously characterized types of PCD. Additionally, if POA induced cell death represents a novel form of PCD; we sought to understand if it could exist as complex network between

various other PCD subroutines. My findings contributed to the discovery that exogenously added POA causes PCD in a concentration and age-dependent fashion, and that this type of PCD has a unique set of morphological and biochemical features which suggest that it is an as yet previously uncharacterized type of PCD. My findings also gave valuable insight into the role that mitochondrial quality control processes play in (I) mitigating POA induced PCD by sustaining a functional pool of mitochondria which are necessary for generating energy for the storage of FFAs as TAGs in LDs as well as maintaining respiratory fitness into stationary phase while producing an optimal level of ROS, (II) modulating the lipid composition of various biomembranes and thus affecting a variety of biophysical properties including permeability and curvature, and (III) being essential for Lithocholic acid to increase yeast CLS. Together these data intricately link regulation of lipid metabolism to the regulation of longevity in yeast.

Thesis Outline and Contributions

Chapter 2 of this thesis deals with the initial discovery of lithocholic acid (LCA), a bile acid which greatly extends yeast chronological lifespan (CLS) under both normal and caloric restriction growth conditions. Specifically, the data I present in this chapter illustrates our attempt to gain a mechanistic understanding of how the beneficial effects of LCA are attained. LCA extends yeast CLS by modulating certain housekeeping longevity assurance pathways that modulate a number of cellular activities- among them are those involved in the metabolism and storage of lipids. In addition to this, I also present our finding that LCA actually utilizes parts of known adaptive signalling pathways (nutrient responsive signal transduction pathways) in a surprising way to extend CLS under normal growth media conditions (2% glucose).

Chapter 2 of this thesis is adapted from published work in Goldberg, A.*, Richard, V.*, Kyryakov, P.*, Bourque, S. D.*, Beach, A., Burstein, M. T., Titorenko, V. I. (2010). Chemical genetic screen identifies lithocholic acid as an anti-aging compound that extends yeast chronological life span in a TOR-independent manner, by modulating housekeeping longevity assurance processes. Aging. * Denotes an equally contributing author. All presented data was primarily done by myself with the assistance of Simon Bourque in the measurement of various lipid species.

Chapter 3 is essentially a continuation of chapter 2 where I describe our efforts to attain a mechanistic understanding of the effects of LCA at the subcellular level. Specifically, we used

subcellular fractionation followed by mass spectrometry to discover that of the majority of the intracellular, organelle localized pool of LCA was localized to the inner mitochondrial and outer mitochondrial membranes⁴⁰. Based on this and our understanding of the integration of mitochondria into processes involved in the biosynthesis and transport of membrane phospholipids, we hypothesized and demonstrated that LCA modulates the lipid composition of the mitochondrial membrane. In addition to this, we demonstrated that alterations to the mitochondrial lipid composition correlated with changes in the size, number, and structure of these organelles. Together the presented data contribute to the establishment of the importance of the mitochondrial membrane lipidome in regulating chronological lifespan in yeast.

The work presented in chapter 3 is adapted from our published data in Beach, A.*, Richard, V. R.*, Leonov, A.*, Burstein, M. T., Bourque, S. D., Koupaki, O.*, Titorenko, V. I. (2013). Mitochondrial membrane lipidome defines yeast longevity. *Aging*. I conducted the lipidomic analyses with the assistance of Simon Bourque. Electron micrographs were acquired by Mylene Juneau (NSERC summer student).

Chapter 4 investigates a potential physiological role for mitochondria specific macroautophagy (mitophagy) in defining yeast CLS under CR conditions. We made use of the *atg32Δ* deletion mutant, which is incapable of carrying out this type of macroautophagy to discover that loss of mitophagy results in (I) insensitivity to the beneficial effects of LCA, and (II) pleiotropic alterations to the lipid composition of the mitochondria, but also the plasma membrane and the endoplasmic reticulum. This suggests that the maintenance of proper membrane lipid homeostasis under caloric restriction is dependent on the maintenance of a functional population of mitochondria, and that this contributes to defining longevity in yeast.

The work presented in chapter 4 is adapted from our published data in Richard, V. R., Leonov, A., Beach, A., Burstein, M. T., Koupaki, O., Gomez-Perez, A., Titorenko, V. I. (2013). Macromitophagy is a longevity assurance process that in chronologically aging yeast limited in calorie supply sustains functional mitochondria and maintains cellular lipid homeostasis. *Aging*. I conducted all of the experimental work shown in this chapter.

Chapter 5 discusses the discovery of liponecrosis, which is a newly identified PCD subroutine in yeast. Liponecrosis is induced artificially by adding an excessive quantity of free fatty acids to the culture medium. In these studies we used palmitoleic acid, which is a sixteen-carbon monounsaturated fatty acid, which had been known to cause cell death from our previous

studies. We hypothesized that this mode of cell death is distinct from previously characterized forms of cell death due to a number of unique morphological, as well as physiological and biochemical parameters, which do not coincide with the major three known types of PCD. In connection with chapter 4, we investigated the importance of mitophagy in mitigating this PCD subroutine and found it to be critical for preventing POA induced cell death.

The data presented in chapter 5 is adapted from the following publication Sheibani, S., Richard, V., & Beach, A. Vladimir, Titorenko. (2013). Macromitophagy, neutral lipids synthesis, and peroxisomal fatty acid oxidation protect yeast from “liponecrosis”, a previously unknown form of programmed cell death. *Cell Cycle*. Sevan Mattie and Sara Sheibani acquired the electron micrographs presented in this chapter. Alejandra Gomez assisted in measurement of CLS of all strains tested as well as measurement of all parameters in figure 20.

Chapter 6 continues from chapter 5 to further develop a mechanistic understanding of how exactly an abnormal accumulation of fatty acids – namely palmitoleic acid – within yeast cells commits them to liponecrotic cell death. What we discovered was that the cells capacity to shunt exogenously added fatty acids into lipid storage pathways (*i.e.* for the biosynthesis of sterol esters and triacylglycerols), determines the cellular susceptibility to liponecrotic cell death. What was also discovered was that this buffering capacity due to the biosynthesis of “storage” lipids is ablated in cells deficient in mitochondria specific autophagy. This phenomenon was also found to be age related – thus indicating that this cell death modality may play an important part in cellular aging. Furthermore, this chapter illustrates a “pro-death” role for the alkaline pH and membrane phospholipid homeostasis responsive Rim101 pathway in committing cells to liponecrotic cell death. Finally a model is constructed integrating interorganellar lipid metabolism and storage with a model implicating the mitochondrial functional state and maintenance through mitophagy in regulating CLS in yeast.

The data presented in this chapter is from a manuscript, which is in the process of submission as Richard, V. R., Beach, A., Leonov, A., Piano, A., Titorenko, V. I. (2014). Mechanism of liponecrosis, a distinct mode of programmed cell death. *Microbial Cell*. I conducted all of the mass spectrometry work in this chapter, as well as all the assays for oxidatively damaged biomolecules. Measurement of culture pH was performed by Pavlo Kyryakov. Alejandra Gomez assisted in measurement of CLS of all strains tested.

The data shown in this thesis is primarily my own work, but I would like to acknowledge contributions/support from Simon Bourque with assistance in training in the use of mass spectrometry. I should also acknowledge Pavel Kyryakov and Alex Goldberg for their assistance with development/training in the use of assays for clonogenic survival and measurement of CLS. I would like to specifically acknowledge Adam Beach for his work on the localization of LCA within yeast cells (which I have not presented here). I would also like to acknowledge Sara Sheibani (visiting graduate student), Sevan Mattie, (NSERC summer student), and Mylene Juneau (NSERC summer student) who assisted in the acquisition of electron micrographs (see chapters 3 and 5) at the Facility for Electron Microscopy Research (FEMR) at McGill University. Finally I would like to acknowledge the intellectual input of my supervisor, Dr. Vladimir Titorenko who was instrumental in the experimental design and data interpretation of much of the data presented in this thesis.

2. Chemical genetic screen identifies lithocholic acid as an anti-aging compound that extends yeast chronological life span in a TOR-independent manner, by modulating lipid storage pathways

2.1 Introduction

The extension of lifespan caused by caloric restriction was previously shown to be mediated by both adaptable – nutrient responsive - and non-adaptable or “housekeeping” processes within the cell ^{9,27}. In previous studies from our lab, a mechanism of how caloric restriction increases yeast chronological lifespan was found to be mitigated through the regulation of storage and metabolism of fatty acids within the endoplasmic reticulum (ER), lipid droplets (LD), and peroxisomes. This model posited that because under caloric restriction yeast produce less ethanol via fermentation than under normal conditions, fatty acid metabolism in the peroxisome could be carried out more efficiently. Ethanol had been shown to repress the expression of FOX1, FOX2, and FOX3 involved in free fatty acid metabolism via β -oxidation in the peroxisome. Under caloric restriction conditions fatty acid oxidases 1-3 as well as triacylglycerol lipases 1-4 show increased expression. This is evidenced by the observation of increased lipolytic degradation of lipid droplets (LD) via BODIPY fluorescence microscopy, as well as increased consumption of triacylglycerol (TAG) and ergosteryl ester (EE) species via thin layer chromatography (TLC) as well as quantitative mass spectrometry based shotgun lipidomics ¹³.

With this in mind we sought to identify small molecules that increase the CLS of yeast under CR conditions by targeting lipid metabolism and modulating cellular processes that are not considered to be the primary adaptable signalling pathways involved in longevity regulation. A chemical genetic screen was carried out which identified lithocholic acid (LCA) as a potent regulator of yeast CLS ⁹.

The chemical genetic screen was carried out in the *pex5Δ* mutant background. Pex5p is a peroxisomal matrix import receptor necessary for the import of fatty acid oxidases to the peroxisomal matrix ⁴¹. The *pex5Δ* deletion results in shortened CLS and changes in lipid metabolism, lipid-induced necrotic cell death, mitochondrial morphology and fitness, stress resistance, mitochondria-controlled apoptosis, and stability of nuclear and mitochondrial DNA

²⁷. It was discovered that a group of bile acids could significantly extend the CLS of the *pex5Δ*, amongst these lithocholic acid was the most efficacious ²⁷. We found that LCA also greatly increases the mean and maximum CLS of WT yeast both under normal and caloric restriction conditions ²⁷. Treatment with LCA also altered various parameters of mitochondrial fitness; perhaps contributing to the compounds beneficial effect on yeast CLS. This finding prompted us to investigate how the exposure of WT cells to LCA under CR conditions influences other longevity-related processes impaired in the *pex5Δ* mutant – namely the regulation of lipid metabolism.

I provided evidence that LCA extends longevity of chronologically aging yeast through two different mechanisms. In one mechanism, this bile acid targets a set of “housekeeping” longevity assurance processes regulating lipid storage. These processes are not known to be directly regulated by the adaptable TOR and cAMP/PKA pathways and yet have been implicated in the regulation of longevity. In the other mechanism, the longevity extending capacity of LCA is dependent on the adaptable cAMP/PKA pathway under non-CR conditions implying a surprising pro-longevity role for the PKA pathway.

2.2 Materials and Methods

2.2.1 Yeast strains and growth conditions

The WT strain BY4742 (*MATα his3Δ1 leu2Δ0 lys2Δ0 ura3Δ0*) and single-gene-deletion mutant strains in the BY4742 genetic background (all from Open Biosystems) were grown in YP medium (1% yeast extract, 2% peptone) containing 0.2% 0.5%, 1% or 2% glucose as carbon source, 2% glucose representing “normal” culture conditions, and 0.2% and 0.5% glucose representing caloric restriction conditions. Cells were cultured at 30°C with rotational shaking at 200 rpm in Erlenmeyer flasks at a “flask volume/medium volume” ratio of 5:1.

2.2.2 Pharmacological manipulation of CLS

CLS analysis was performed as previously described ¹³. Briefly, samples of yeast cells were taken and a fraction of the sample was diluted in order to determine the cell titer using a hemacytometer. Another fraction of sample was then serially diluted and plated in duplicate on YP plates containing 2% glucose as carbon source. Plates were cultured at 30°C After 2 days of

incubation at 30°C, the number of colony forming units (CFU) per plate was counted. The number of CFU was defined as the number of viable cells in a sample. For each culture, the percentage of viable cells was calculated as follows: (number of viable cells per ml/total number of cells per ml) x 100. The percentage of viable cells in mid-logarithmic phase was set at 100%. Lithocholic acid (L6250) and all other tested bile acids were from Sigma. Their stock solutions in DMSO were made on the day of adding each of these compounds to cell cultures. Compounds were added to growth medium at the indicated concentration immediately following cell inoculation. The final concentration of DMSO in yeast cultures supplemented with a bile acid (and in control cultures supplemented with DMSO) was 1% (v/v).

2.2.3 Quantitative Analysis of Yeast Lipids by Mass Spectrometry

Mass spectrometry based lipidomics was conducted as previously described⁴². Briefly, yeast cells were harvested from culture ($\sim 5 \times 10^7$ cells) by centrifugation at 3000 x g for 1 minute. Cells were washed twice with ice cold water, spiked with an internal standard mix prepared in LC-MS grade chloroform:methanol (1:1) according to Table 1, and then subjected to lipid extraction by a modified Bligh & Dyer method^{42,43}. Yeast lipid extracts were directly infused into a Micromass Q-ToF 2 (Waters, Milford, MA, USA) mass spectrometer equipped with a nano-electrospray source. The mass spectrometer was operated in both positive and negative ion modes at a flow rate of 1 μ L/min. Spectra were converted to centroid format. Lipid species were identified and quantified using deconvoluted spectral data processed in homemade excel sheets. Putative lipid identities were validated by MSMS.

2.2.4 Fluorescence Microscopy

The Annexin V / Propidium Iodide assay kit (Invitrogen) for apoptotic/necrotic cell death was used according to established protocols.

2.3 Results

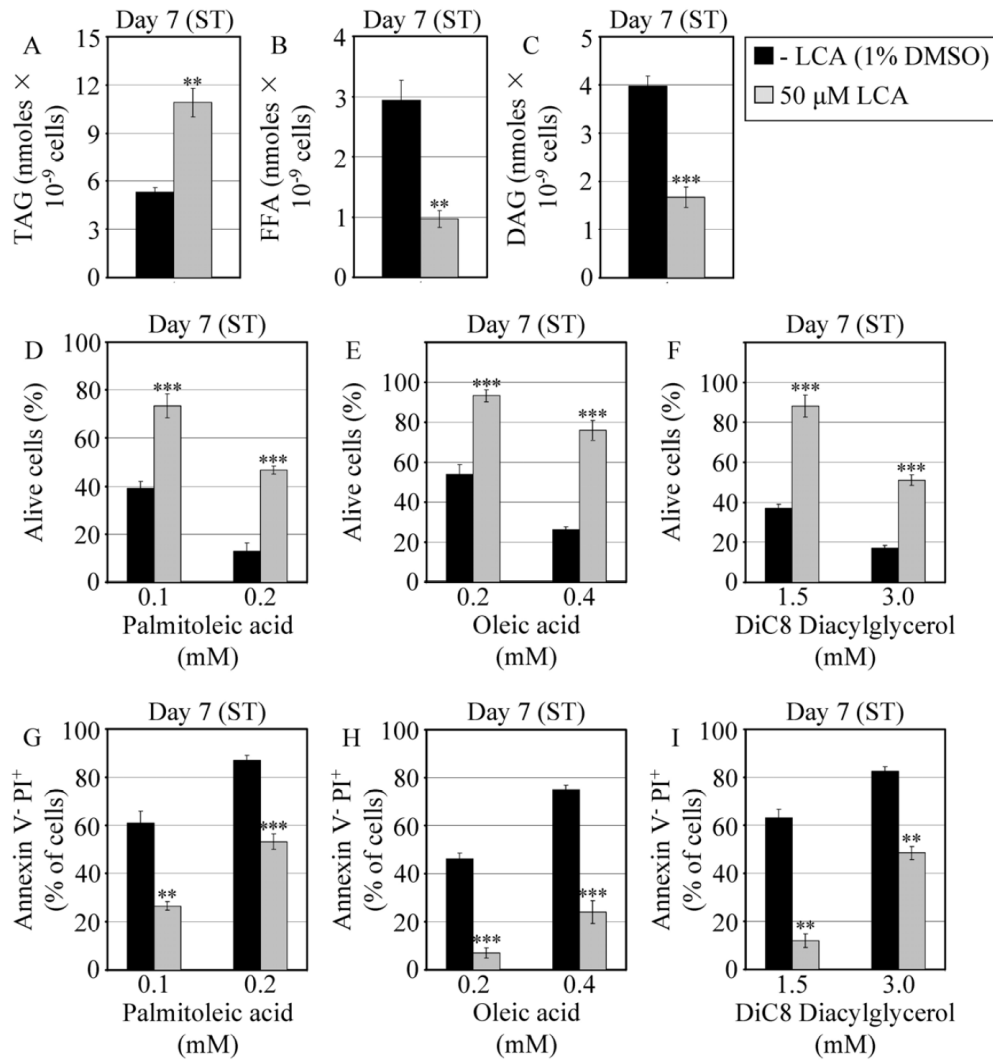


Figure 3 LCA alters the levels of various lipid classes and prevents fatty acid induced cell death in chronologically aging yeast grown under CR conditions into stationary phase. (A - C) Levels of triacylglycerols and free fatty acids measured by mass spectrometry (A and B) and of diacylglycerols monitored by TLC (C) in WT cells grown in medium with or without LCA. (D - F) Viability of WT cells pre-grown in medium with or without LCA and then treated for 2 h with palmitoleic acid (D), oleic acid (E) or DiC8 diacylglycerol (F). (G - I) Percent of WT cells (pre-grown in medium with or without LCA) that following their treatment with palmitoleic acid (G), oleic acid (H) or DiC8 diacylglycerol (I) displayed Annexin V negative and PI positive (Annexin V⁻ and PI⁺) staining characteristic of necrotic cell death. Data are presented as means \pm SEM (n = 3-9; ***p < 0.001; **p < 0.01). WT cells grown on 0.2% glucose in the presence or absence of LCA were taken for analyses at day 7, when they reached reproductive maturation by entering into ST phase. Reproduced from ²⁷.

2.3.1 LCA extends the CLS of WT yeast under CR by modulating free fatty acid storage pathways

In order to evaluate whether the observed effects of LCA were due to alterations to processes involved in lipid metabolism, I quantitatively profiled the yeast lipidome using mass spectrometry. The method that was used allowed for the comprehensive analysis of the yeast lipidome including most of the major phospholipids, free fatty acids, and neutral lipids were measured in a quantitative manner. From this analysis it was observed that LCA elevated the concentration of TAG in WT cells that entered the non-proliferative ST phase under CR at 0.2% glucose (Figure 3A). Furthermore, under these conditions LCA also substantially reduced the intracellular levels of FFA and DAG in WT yeast that reached reproductive maturation by entering into ST phase (Figure 3B,C). Moreover, LCA greatly reduced the susceptibility of reproductively mature WT cells under CR to necrotic cell death that was caused by a short-term exposure to exogenous FFA or DAG and defined by Annexin V/PI⁺ staining (Figure 3D-I). These findings were consistent with what we hypothesized – namely that the compound rescues the *pex5Δ* mutant by targeting lipid metabolism in the ER, lipid bodies and peroxisomes since these are the principal sites of synthesis, storage, and degradation of lipids within the cell.

2.3.2 LCA extends yeast CLS independent of TOR, by modulating housekeeping longevity assurance pathways

To assess whether the effects of LCA were dependent on “adaptable” or nutrient responsive signal transduction pathways which are known to regulate chronological lifespan in yeast we assessed how the cAMP/PKA pathway influences the ability of LCA to extend CLS in yeast under normal as well as caloric restriction conditions. To do this we measured viability of several mutants of the cAMP/PKA pathway with or without LCA. Among these, was *ras2Δ* - a GTP-binding protein that activates adenylate cyclase and is responsible for the synthesis of the PKA activator cAMP⁴⁴, resulting in loss of PKA kinase activity. Deletion of *ras2Δ* resulted in a partial reduction in the effect of LCA, however it still significantly increased CLS under CR and non-CR conditions (Figure 4).

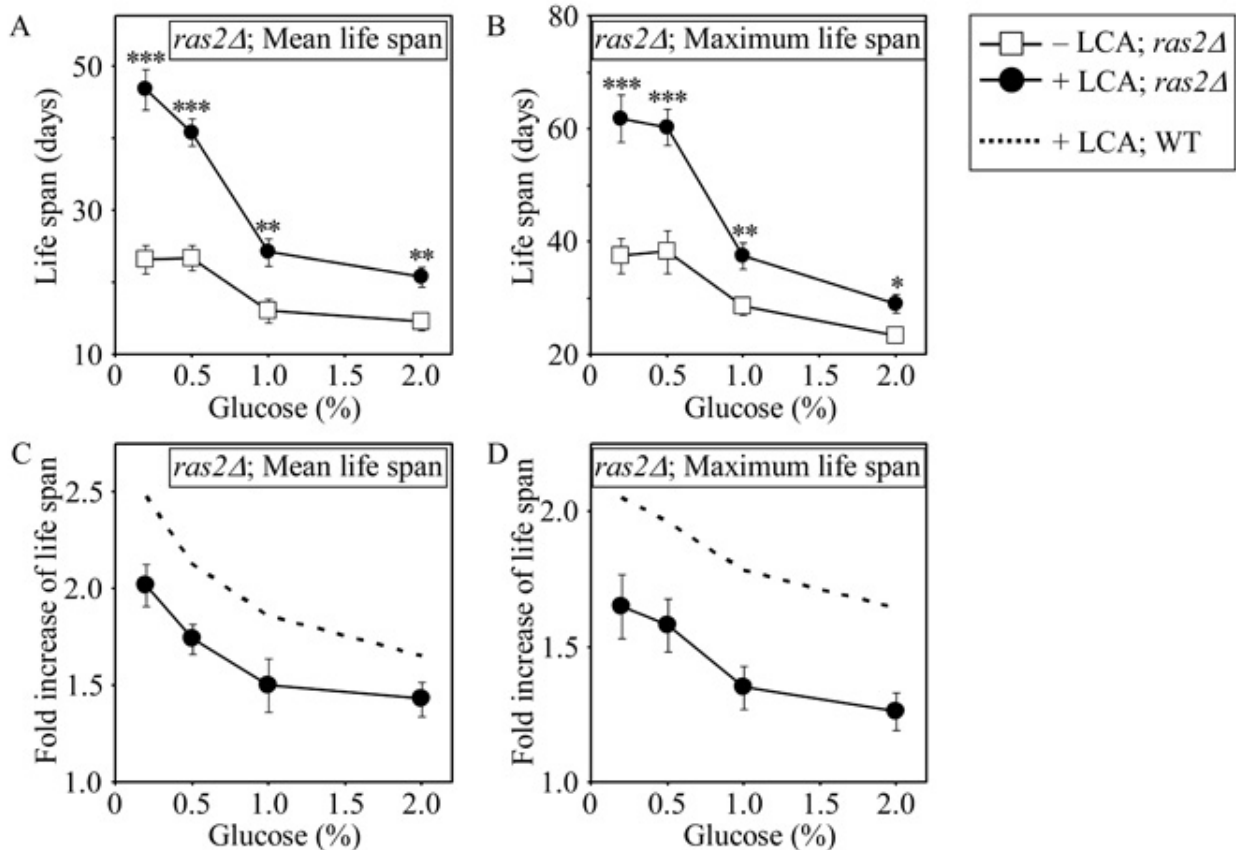


Figure 4 LCA partially increases the mean and maximum CLS of yeast lacking Ras2p under both CR and Non-CR conditions. (A and B) Effect of LCA on the mean (A) and maximum (B) life spans of chronologically aging *ras2Δ* strain. Data are presented as means \pm SEM (n = 4-7; ***p < 0.001; **p < 0.01; *p < 0.05). (C and D) Effect of LCA on the fold increase in the mean (C) or maximum (D) life spans of chronologically aging *ras2Δ* and WT strains. Data are presented as means \pm SEM (n = 4-7). Cells in A to D were cultured in medium initially containing 0.2%, 0.5%, 1% or 2% glucose in the presence of LCA (50 μ M) or in its absence. Reproduced from ²⁷.

From this, it would seem that LCA modulates lifespan of yeast through two different mechanisms. In the first mechanism LCA targets certain housekeeping longevity assurance pathways that act to positively regulate longevity. These targets would be independent of the adaptable cAMP/PKA pathway modulated by calorie availability (Figure 6B). Because of the partial reduction in the effect of LCA on yeast CLS, we propose that a second mechanism might involve PKA acting surprisingly as a prolongevity factor by activating PKA-dependent phosphorylation of the cytosolic pool of Rim15p (Figure 6B). While phosphorylation of Rim15p inactivates its protein kinase activity ⁴⁴, and the nuclear pool of Rim15p has a well established anti-aging function ^{3,10,14,44}, it is possible that the cytosolic pool of this nutrient-sensory protein

kinase plays an important pro-aging role by phosphorylating a number of proteins that promote aging only if phosphorylated (Figure 6B). In fact, some of the cytosolic phosphorylation targets of Rim15p are involved in longevity regulation⁴⁵. We hypothesized that under non-CR conditions, activated PKA is involved in some of the anti-aging effects of LCA, perhaps through regulation of Rim15p kinase activity. This is consistent with the fact that lack of Ras2p only partially reduced the ability of LCA to extend lifespan, and this occurred to an equal extent under both CR and non-CR conditions (Figure 4C,D). The loss of PKA activity resulting from the *ras2Δ* deletion would thus inhibit the ability of PKA to regulate the pro-aging effects of the cytosolic Rim15p pool.

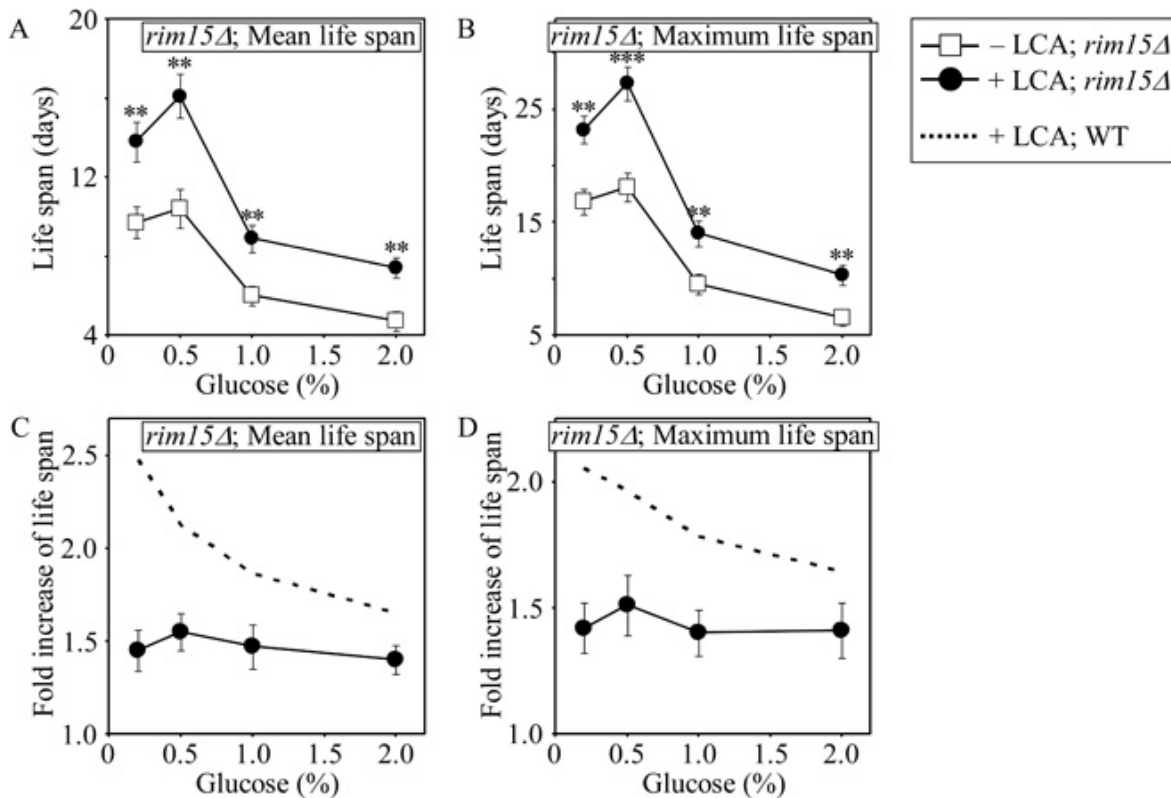


Figure 5 LCA partially increases the mean and maximum CLS of yeast lacking Rim15p under both CR and Non-CR conditions. Effect of LCA on the mean (A) and maximum (B) life spans of chronologically aging *rim15Δ* strain. Data are presented as means \pm SEM (n = 5-7; ***p < 0.001; **p < 0.01). Effect of LCA on the fold increase in the mean (C) or maximum (D) life spans of chronologically aging *rim15Δ* and WT strains. Data are presented as means \pm SEM (n = 5-7). Cells in A to D were cultured in medium initially containing 0.2%, 0.5%, 1% or 2% glucose in the presence of LCA (50 μ M) or in its absence. . Adapted from²⁷.

The TOR and cAMP/PKA pathways both act to phosphorylate Rim15p when nutrients are abundant^{10,44}. The Rim15p nuclear pool plays an important role in regulating the life-extending effect of CR by enabling the establishment of a pro-longevity transcriptional program which activates various stress responsive factors including Msn2p, Msn4p and Gis1p (Figure 6A)^{3,10,14,44}. Interestingly, LCA was still able to extend lifespan in the *rim15Δ* mutant, although only partially (Figure 5A,B). Also worth noting is that by eliminating a key nutrient-sensory protein kinase on which the adaptable TOR and cAMP/PKA pathways converge to regulate longevity in a calorie availability-dependent fashion, the *rim15Δ* mutation abolished the dependence of the anti-aging efficacy of LCA on the number of available calories (Figure 5C,D).

2.4 Discussion

2.4.1 LCA extends yeast CLS by modulating housekeeping longevity assurance processes that are not regulated by the adaptable TOR and cAMP/PKA signaling pathways

These findings imply that LCA extends longevity of chronologically aging yeast by targeting two distinct mechanisms. One mechanism extends longevity in a manner that is independent of the availability of nutrients outside the cell (i.e. glucose). This mechanism involves the LCA-governed modulation of certain housekeeping longevity assurance pathways that do not overlap with the adaptable TOR and cAMP/PKA pathways (Figure 6B). The data presented here shows evidence of at least one such pathway, in that LCA modulates the regulation of lipid storage and metabolism. This effectively suppresses the pro-aging process^{13,37,46} of lipid-induced necrotic cell death, likely by reducing the intracellular levels of FFA and DAG that trigger programmed necrotic cell death.

In addition to modulation of myriad of housekeeping pathways, LCA appears to be able to utilize the PKA pathway to promote longevity specifically under non-CR conditions. This mechanism is devised of a regulatory relationship between LCA and PKA, a key player in the adaptable cAMP/PKA pathway. We propose that LCA causes PKA to act as a pro-longevity factor by activating PKA-dependent phosphorylation of the cytosolic pool of Rim15p, a key nutrient-sensory protein kinase on which the adaptable TOR and cAMP/PKA pathways converge to regulate longevity in a calorie availability-dependent fashion (Figure 6B). Of note, the nuclear pool of Rim15p is well known for its anti-aging role in governing the life-extending effect of CR by enabling a pro-longevity transcriptional program driven by Msn2p, Msn4p and Gis1p (Figure

6B)^{10,44}. Based on the presented data we hypothesized that 1) unlike Rim15p in the nucleus, the cytosolic pool of Rim15p acts as a pro-aging factor presumably by phosphorylating target proteins within the cytosol⁴⁵ that promote aging when phosphorylated (Figure 6B). In addition to this, under non-CR conditions LCA may somehow enhance the PKA-dependent phosphorylation of Rim15p (Figure 6B); causing inactivation of the kinase activity of Rim15p allowing for the dephosphorylation of its cytosolic targets⁴⁴. However, it remains to be tested whether deletion of the cytosolic targets of Rim15p has an effect on the ability of LCA to modulate lifespan.

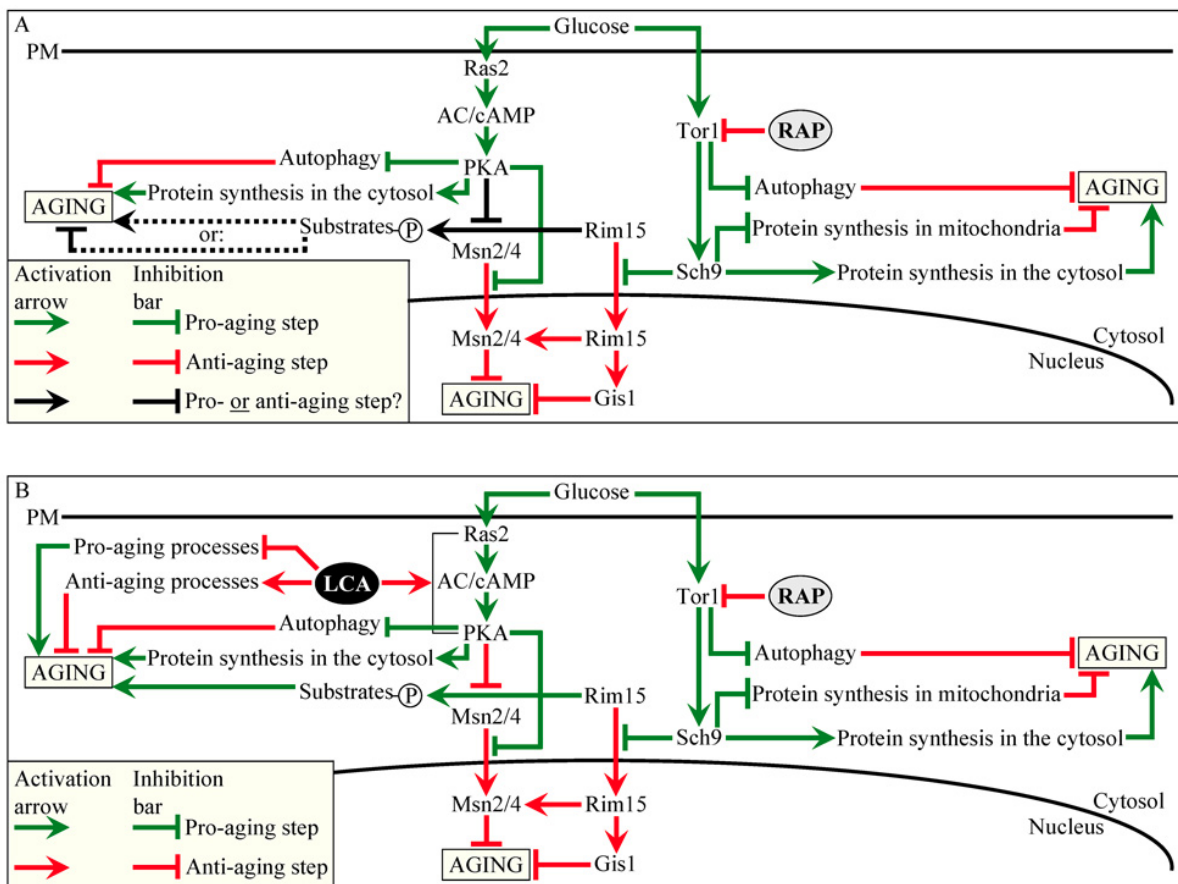


Figure 6 Outline of pro- and anti-aging processes that are controlled by the TOR and/or cAMP/PKA signalling pathways and are modulated by LCA or rapamycin (RAP) in chronologically aging yeast. The currently accepted (A) and updated, based on this study (B), outlines of pro- and anti-aging processes are shown. Activation arrows and inhibition bars denote pro-aging processes (displayed in green color), anti-aging processes (displayed in red color) or processes whose role in longevity regulation was unknown (displayed in black color). Dotted lines denote hypothetical processes. Reproduced from²⁷.

3. Mitochondrial membrane lipidome defines yeast longevity

3.1 Introduction

As mentioned previously, we identified lithocholic acid (LCA), a bile acid, as a natural compound that acts synergistically with CR to cause a substantial increase in yeast chronological lifespan under longevity-extending CR conditions. In addition to the ability of LCA to protect yeast from cell death caused by the exposure to exogenously added fatty acids in the culture medium by altering lipid metabolism and storage, LCA also induced a number of beneficial effects including alterations in mitochondrial morphology, functionality, stress resistance, mitochondria-controlled apoptosis, and stability of both nuclear and mitochondrial genomes⁴⁷.

Based on this we decided to examine a mechanism underlying the potent anti-aging effect of LCA in yeast cultured under CR. What was found was that exogenously added LCA enters yeast cells and primarily accumulates in the mitochondria. This was discovered through use of subcellular fractionation followed by mass spectrometry to quantitatively assess in which subcellular fraction LCA would accumulate⁴⁰. Of the pool of LCA that gets into yeast cells, it primarily associated with the inner mitochondrial membrane (IMM), and to a lesser extent in the outer mitochondrial membrane (OMM). From this we decided to conduct another mass spectrometry based lipid-profiling experiment – this time of purified mitochondria. What we found was that LCA greatly affected glycerophospholipid synthesis and movement within both mitochondrial membranes, causing significant age-related changes in the mitochondrial membrane lipidome. These changes coincided with altered size, number and morphology, as well as mitochondrial respiration, membrane potential, ATP synthesis and reactive oxygen species (ROS) homeostasis⁴⁷. Together this data suggests that the ability of LCA to extend yeast CLS is at least partly dependent on its capacity to reconfigure the mitochondrial membrane lipidome.

Based on an expanding knowledge-base about the basic science of cellular aging, it is now widely accepted that the functional state of the mitochondria in eukaryotic cells plays an important role in regulating cellular and organismal aging⁴⁸⁻⁵¹. The age-related decline in mitochondrial function is considered to be one of the major hallmarks of aging in eukaryotic organisms across evolutionarily distinct organisms⁵². Mitochondria play a key role in the aging process because they are responsible for supplying the cell with the majority of its requirement

for ATP, which is synthesized via oxidative phosphorylation coupled to the electron transport chain in the inner mitochondrial membrane (IMM)^{48,53,54}. This process is known to generate reactive oxygen species (ROS) which play a critical role in the development of a pro- or anti-aging cellular routines⁵⁵⁻⁶⁰. The mitochondria is also involved in producing and releasing a plethora of metabolites, iron-sulphur clusters (ISC), proteins, peptides and DNA fragments that are essential for establishing cellular commitment to certain cell death modalities, and thus necessarily determining the rate of cellular aging⁶¹.

3.2 Materials and Methods

Yeast strains, media and growth conditions

The wildtype strain *Saccharomyces cerevisiae* BY4742 (*MAT α his3 Δ 1 leu2 Δ 0 lys2 Δ 0 ura3 Δ 0*) [Thermo Scientific/Open Biosystems; #YSC1054] was grown in YP medium (1% yeast extract, 2% peptone) [both from Fisher Scientific; #BP1422-2 and #BP1420-2, respectively] containing 0.2% glucose [#D16-10; Fisher Scientific] as carbon source. Cells were cultured at 30°C with rotational shaking at 200 rpm in Erlenmeyer flasks at a “flask volume/medium volume” ratio of 5:1.

Pharmacological manipulation of chronological lifespan

Chronological lifespan assay and pharmacological manipulation of chronological lifespan by addition of lithocholic acid (LCA) [Sigma; #L6250] were performed as previously described^{27,62}. LCA was added to growth medium in DMSO or water at the final concentration of 50 μ M immediately following cell inoculation into the medium. The final concentration of DMSO in yeast cultures supplemented with LCA (and in the corresponding control cultures supplemented with compound vehicle) was 1% (v/v).

Mitochondrial Lipidomics

Purification and sub fractionation of mitochondria was carried out as previously described⁶³. Extraction of lipids from purified mitochondria was conducted by a modified Bligh & Dyer method as described previously⁴². The following mass spectrometric identification and quantitation of various lipid species were performed according to established procedures⁶².

The “unsaturation index” for each molecular form of glycerophospholipids was calculated as previously described⁶⁴. For the PA, PG, PS, PE, PC and PI species of

glycerophospholipids, the unsaturation index was calculated as the “glycerophospholipids with one or two unsaturated acyl chains (*i.e.*, C_{n:1} and C_{n:2} species)/glycerophospholipids without unsaturated acyl chains (*i.e.*, C_{n:0} species)” ratio. For the MLCL species of glycerophospholipids, the unsaturation index was calculated as the “glycerophospholipids with one, two or three unsaturated acyl chains (*i.e.*, C_{n:1}, C_{n:2} and C_{n:3} species)/glycerophospholipids without unsaturated acyl chains (*i.e.*, C_{n:0} species)” ratio. For the CL species of glycerophospholipids, the unsaturation index was calculated as the “glycerophospholipids with unsaturated acyl chains /glycerophospholipids without unsaturated acyl chains (*i.e.*, C_{n:0} species)” ratio.

Subcellular Fractionation and Purification of Organelles

Subcellular fraction followed by purification of Mitochondria ⁶³, was conducted according to established protocols that are summarized below.

Isolation of crude mitochondrial fractions

Yeast cells were harvested at 3,000 × g for 5 min at room temperature, washed with water and resuspended in DTT buffer (100 mM Tris-H₂SO₄, pH 9.4, 10 mM dithiothreitol [DTT]). Cells were incubated in DTT buffer incubated for 20 min at 30°C to weaken the cell wall. The cells then were washed with Zymolyase buffer (1.2 M sorbitol, 20 mM potassium phosphate, pH 7.4) and centrifuged at 3,000 × g for 5 min at room temperature. Cells were then incubated with 3 mg/g (wet weight) of Zymolyase-100T in 7 ml/g (wet weight) Zymolyase buffer for 45 min at 30°C. Following an 8-min centrifugation at 2,200 × g at 4°C, the isolated spheroplasts were washed in ice-cold homogenization buffer (5 ml/g) (0.6 M sorbitol, 10 mM Tris-HCl, pH7.4, 1 mM EDTA, 0.2% (w/v) BSA) and centrifuged at 2,200 × g for 8 min at 4°C. Spheroplasts were homogenized in ice-cold homogenization buffer using glass dounce homogenizer 15 strokes. Cell debris was removed by centrifuging the resulting homogenates at 3,000 × g for 10 min at 4°C. The resulting supernatant was then centrifuged at 12,000 × g for 15 min at 4°C to pellet mitochondria. The remnant cell debris was removed by centrifuging the mitochondrial fraction at 3,000 × g for 5 min at 4°C. The resulting supernatant was then centrifuged at 12,000 × g for 15 min at 4°C to obtain the crude mitochondrial pellet, which was then resuspended in 3 ml of SEM Buffer (250 mM sucrose, 1 mM EDTA, 10 mM MOPS, pH 7.2) and used for the purification of mitochondria as described below.

Purification of mitochondria devoid of microsomal and cytosolic contaminations

A sucrose gradient was made by overlaying 1.5 ml of 60% sucrose with 4 ml of 32% sucrose, 1.5 ml of 23% sucrose, and then 1.5 ml of 15% sucrose (all in EM buffer; 1 mM EDTA, 10 mM MOPS, pH 7.2). Finally, a 3-ml aliquot of the crude mitochondrial fraction in SEM buffer was applied to the gradient and centrifuged at $134,000 \times g$ (33,000 rpm) for three hours at 4°C in vacuum (Rotor SW40Ti, Beckman). The purified mitochondria found at the 60%/32% sucrose interface were carefully removed and stored at - 80°C until lipids were extracted for mass spectrometry.

Miscellaneous procedures

Electron microscopy and the morphometric analysis of the resulting images were performed as previously described ⁶⁵. Protein concentration in samples of purified mitochondria was determined with an RC DC protein assay kit (#500-0122; Bio-Rad) following the manufacturer's instructions.

3.3 Results

3.3.1 Mitochondrial membranes of yeast cultured in the presence of LCA exhibit altered concentrations of various glycerophospholipid species

The phospholipid composition of both the inner and outer mitochondrial membranes is related to the membrane composition of the endoplasmic reticulum (ER) through a network of highly dynamic processes. These processes include the synthesis of the glycerophospholipids phosphatidic acid (PA), cytidine diphosphate-diacylglycerol (CDP-DAG), phosphatidylserine (PS), phosphatidylcholine (PC) and phosphatidylinositol (PI) by enzymes residing in the ER. Additionally, the enzymes involved in the biosynthesis of CDP-DAG, phosphatidylglycerol (PG), cardiolipin (CL) and monolysocardiolipin (MLCL) are located in the IMM. The result is such that a bidirectional movement of glycerophospholipids via mitochondria-ER junctions (also called mitochondria-ER contact sites) is necessary to maintain proper membrane lipid composition. The mitochondria-ER junctions represent zones of close apposition between the OMM and the mitochondria-associated membrane (MAM) domain of the ER. To complicate matters, there also exists a CL-dependent inhibition of PA transport from the OMM to the IMM by Ups1p, a protein that shuttles PA between the two mitochondrial membranes ⁶⁶⁻⁶⁹.

Based on our observation that LCA accumulates in the IMM and is also present in the OMM⁴⁰, we hypothesized that LCA may alter the relative concentrations of various glycerophospholipid species in mitochondrial membranes – perhaps by affecting the activity of enzymes involved in glycerophospholipid synthesis within the IMM, affecting glycerophospholipid exchange between the mitochondrial and ER membranes via mitochondria-ER junctions, and/or impinging on the Ups1p-driven shuttling of PA between the two mitochondrial membranes.

To determine whether mitochondria-confined LCA alters the glycerophospholipid composition of the mitochondrial membranes, we used mass spectrometry to compare the membrane lipidomes of mitochondria purified from yeast cultured under CR conditions with or without LCA, either dissolved in water or DMSO. We found that, regardless of the presence of DMSO, exogenously added LCA increased the glycerophospholipid/protein ratio of mitochondrial membranes in an age dependent manner (Figure 7). In fact, LCA had no effect on the glycerophospholipid/protein ratio of mitochondrial membranes in cells recovered at diauxic (D) growth phase on day 2 of cell culturing, but caused a moderate (but significant) increase in this ratio in cells recovered at post-diauxic (PD) growth phase. This ratio was significantly elevated in cells recovered upon entering stationary (ST) phase on day 7 of cell culturing (Figure 7).

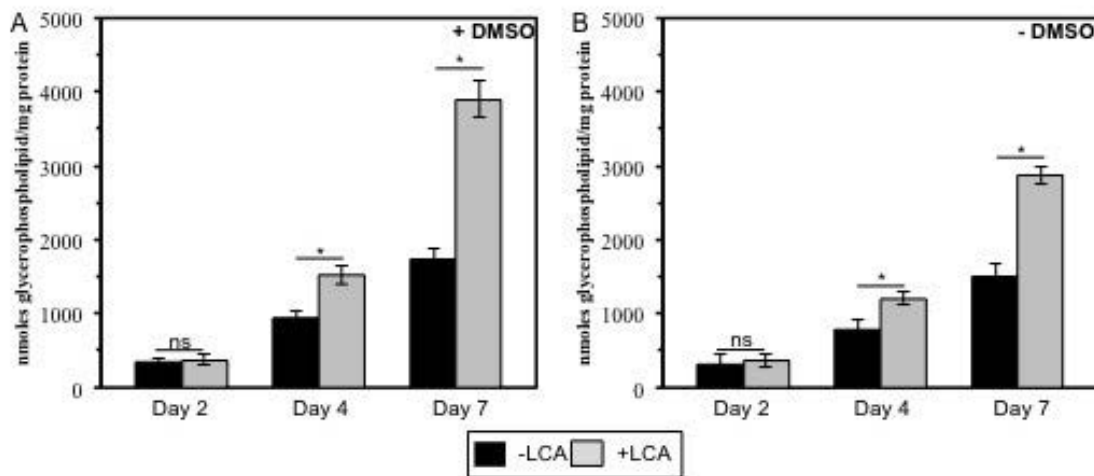


Figure 7 In yeast cultures containing exogenously added LCA, this bile elevates the glycerophospholipid/protein ratio of mitochondrial membranes in an age-dependent manner. Cells were cultured in the nutrient-rich YP medium initially containing 0.2% glucose with 50 μ M LCA or without it, in the presence of 1% DMSO (A) or in its absence

(B). Mitochondria were purified from cells recovered on day 2, 4 or 7 of cell culturing. Protein concentration measurement in samples of purified mitochondria, extraction of mitochondrial membrane lipids, and mass spectrometric identification and quantitation of the extracted glycerophospholipid species were carried out as described in Methods. Based on these data, the “total membrane glycerophospholipids /total membrane protein” ratios were calculated as nanomoles of glycerophospholipid/mg of protein for mitochondria that were purified from cells recovered on day 2, 4 or 7 of cell culturing. Data are presented as means \pm SEM (n = 3; *p < 0.01; ns, not significant). Adapted from ⁴⁰.

In addition to this, LCA treatment induced differential effects on the concentrations of different molecular forms of mitochondrial membrane glycerophospholipids; moreover, these effects of LCA were age-dependent. Indeed, we found that LCA causes a rise in the levels of mitochondrial PA, PG, PS, PC and PI calculated as nanomoles of glycerophospholipid/mg of protein. These effects increased with the chronological age of yeast cells yet for the PG and PI species of mitochondrial membrane glycerophospholipids, this effect of LCA can be seen only in cells recovered at PD or ST growth phase on day 4 or 7 (Figure 8). In contrast, our mass spectrometric identification and quantitation of mitochondrial membrane glycerophospholipids revealed that (I) LCA elicits a decline in the levels of mitochondrial CL, MLCL and PE calculated as nanomoles of glycerophospholipid/mg of protein; (II) the extent of such effect of LCA on CL, MLCL and PE levels (calculated as nanomoles of glycerophospholipid/mg of protein) decreases with the chronological age of yeast cells; and (III) for the MLCL species of mitochondrial membrane glycerophospholipids, this effect of LCA can be seen only in cells recovered at PD or ST growth phase on day 4 or 7 (respectively) of cell culturing (Figure 8). These effects were not dependent on whether LCA was solubilized in water or DMSO.

Although a similar trend of the differential effect of LCA on the concentrations of different molecular forms of mitochondrial membrane glycerophospholipids was observed if their relative levels were calculated as molar percentage of all glycerophospholipids, the extent to which LCA increased the relative levels of mitochondrial PA, PG, PS and PC or decreased the relative levels of mitochondrial CL, MLCL and PE gradually progressed with the chronological age of yeast cells (Figure 9). Moreover, LCA did not alter the relative level of PI if it was calculated as molar percentage of all glycerophospholipids (Figure 9).

Importantly, while LCA elicited substantial differential effects on the relative levels of different molecular forms of mitochondrial membrane glycerophospholipids (calculated as molar

percentage of all glycerophospholipids), it did not cause a significant change in the “unsaturation index” for any of the glycerophospholipid species (Figure 10). This index is calculated as the ratio of glycerophospholipids with one, two, three or four unsaturated acyl chains / glycerophospholipids without unsaturated acyl chains (*i.e.*, C_{n:0} species)” ratio⁷⁰. We found that the unsaturation index was high for each molecular form of mitochondrial membrane glycerophospholipids, ranging from 4.2 to 63.3 (Figure 10). For PG, PS, PC, PI and PE, the unsaturation index is known to play a pivotal role in defining whether each of these glycerophospholipid species acquires the bilayer forming shape of a cylinder or it attains the non-bilayer forming shape, either that of a cone or an inverted cone (Figure 11A-D)^{66,71,72}. Of note, PA, CL and MLCL are known to be always present in the non-bilayer forming shape of a cone, regardless of their unsaturation indexes (Figure 11A-D)^{66,71,72}. Thus, the observed differential effects of LCA on the relative levels of different molecular forms of mitochondrial membrane glycerophospholipids (Figure 9) and the demonstrated lack of its effect on the unsaturation index for each of these molecular forms (Figure 10) imply that this bile acid alters only the relative levels of bilayer forming and non-bilayer forming glycerophospholipid species, but does not affect the molecular shape of any of them. The observed unsaturation indices were within the normal ranges that have been reported in the literature⁷³.

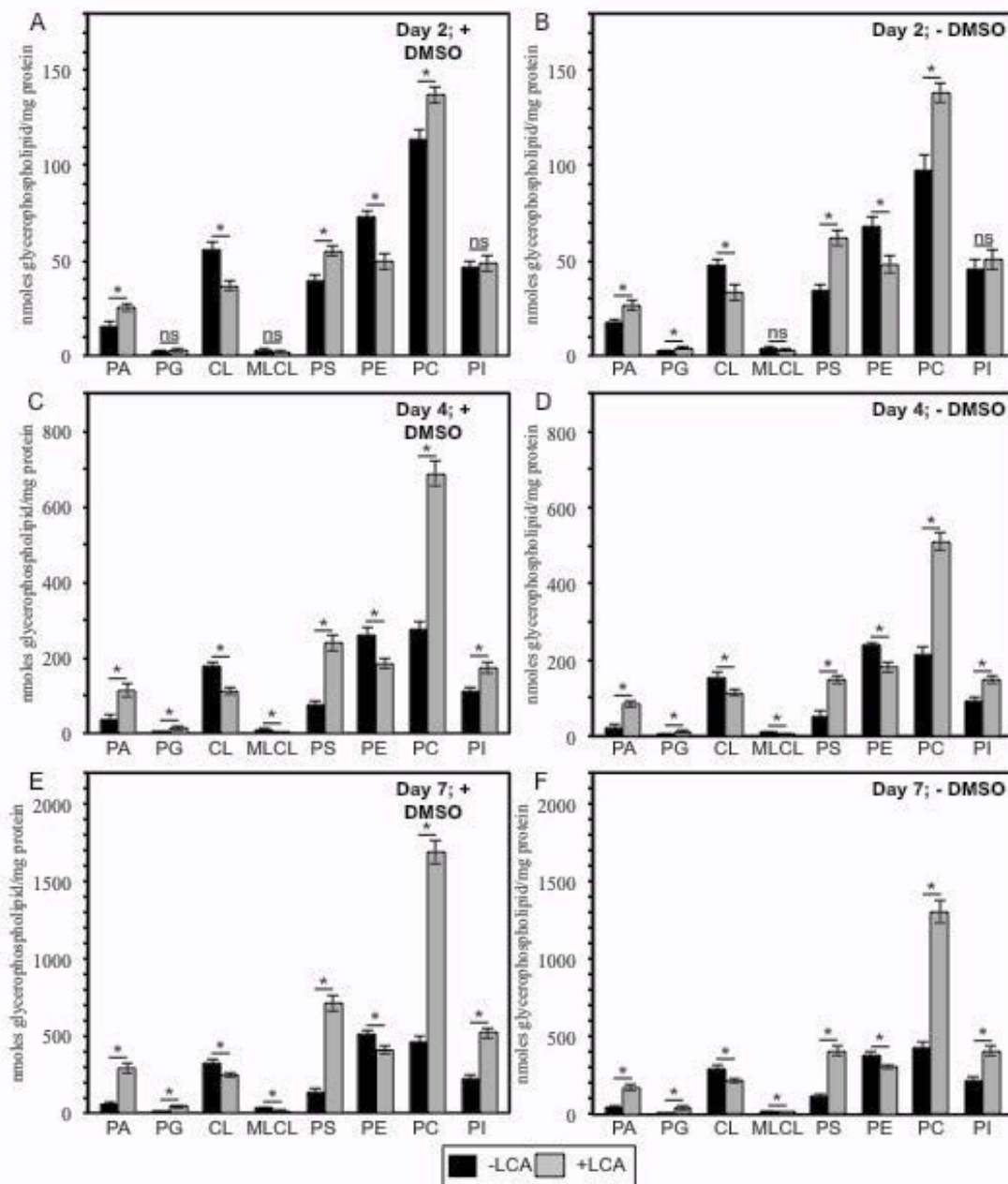


Figure 8 LCA exhibits age-dependent differential effects on the concentrations of different species of mitochondrial membrane glycerophospholipids. Cells were cultured in the nutrient-rich YP medium initially containing 0.2% glucose with 50 μ M LCA or without it (A, C and E) or in its absence (B, D and F). Mitochondria were purified from cells recovered on day 2, 4 or 7 of culturing. Based on these data, the concentrations of different molecular forms of mitochondrial membrane glycerophospholipids were calculated as nanomoles of glycerophospholipid/mg of protein for mitochondria that were purified from cells recovered on day 2, 4 or 7 of cell culturing. Data are presented as means \pm SEM (n = 3; *p < 0.01; ns, not significant). Reproduced from⁴⁰.

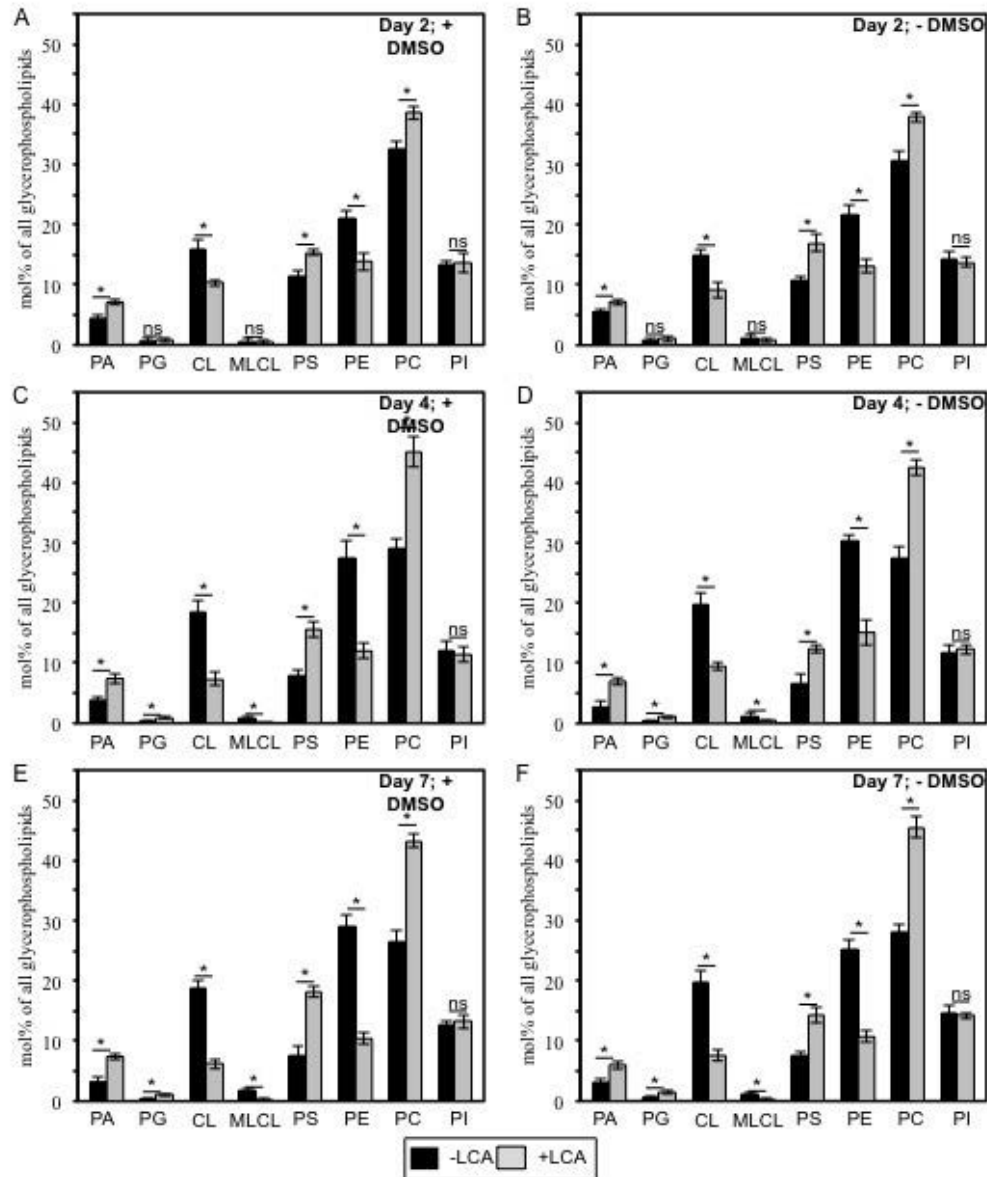


Figure 9 LCA exhibits age-dependent differential effects on the molar percentage of different molecular forms of mitochondrial membrane glycerophospholipids. Cells were cultured in the nutrient-rich YP medium initially containing 0.2% glucose with 50 μ M LCA or without it, in the presence of 1% DMSO (A, C and E) or in its absence (B, D and F). Mitochondria were purified from cells recovered on day 2, 4 or 7 of cell culturing. Based on these data, the relative levels of different species of mitochondrial membrane glycerophospholipids were calculated as molar percentage of all glycerophospholipids for mitochondria that were purified from cells recovered on day 2, 4 or 7 of cell culturing. Data are presented as means \pm SEM (n = 3; *p < 0.01; ns, not significant). Reproduced from ⁴⁰.

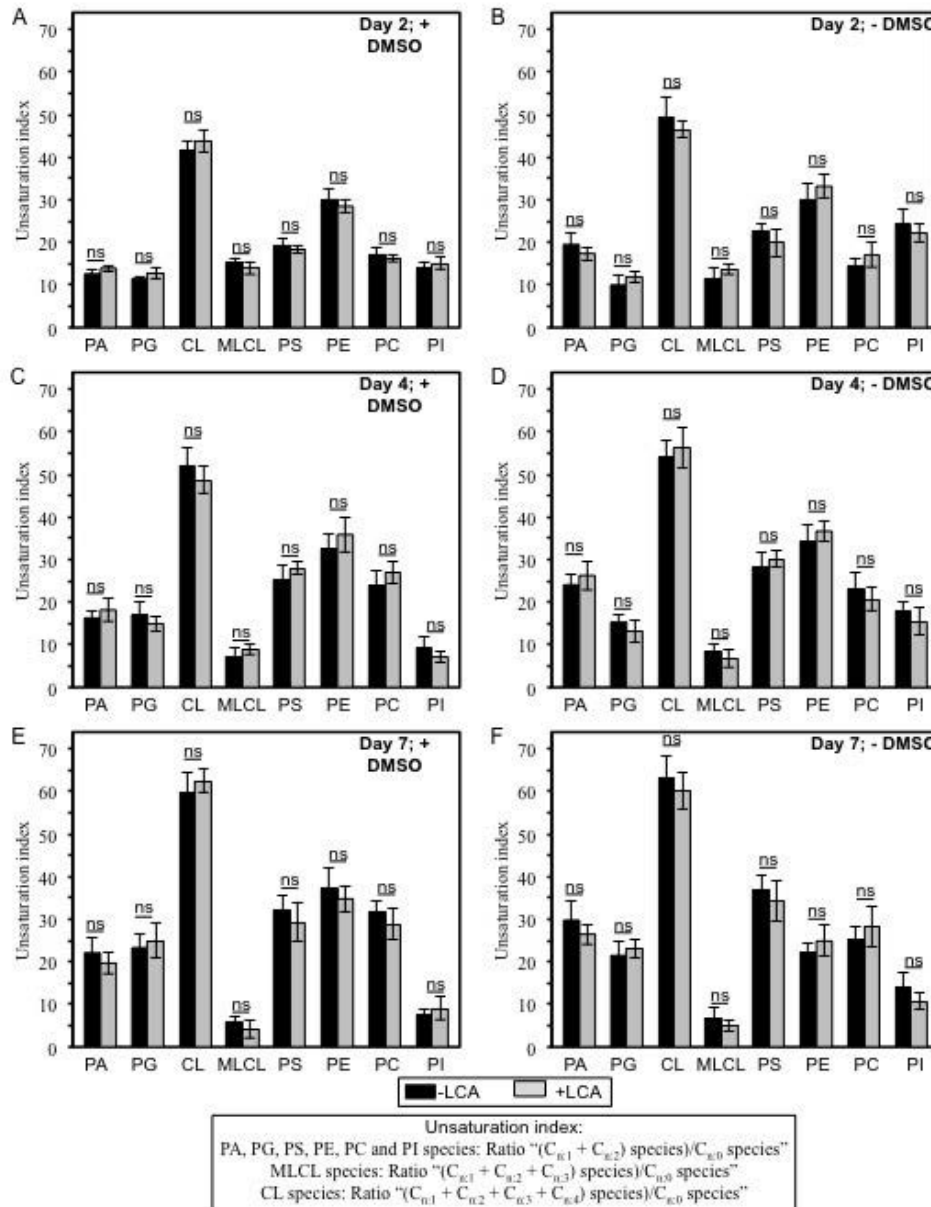


Figure 10 LCA does not cause a significant change in the “unsaturation index” for any of the glycerophospholipid species. Cells were cultured in the nutrient-rich YP medium initially containing 0.2% glucose with 50 μ M LCA or without it, in the presence of 1% DMSO (A, C and E) or in its absence (B, D and F). Based on these data, the unsaturation index for each molecular form of mitochondrial membrane glycerophospholipids was calculated as detailed in Methods. This index represents the “glycerophospholipids with one, two, three or four unsaturated acyl chains (i.e., Cn:1, Cn:2, Cn:3 and Cn:4 species)/glycerophospholipids without unsaturated acyl chains (i.e., Cn:0 species)” ratio. Data are presented as means \pm SEM (n = 3; ns, not significant). Reproduced from ⁴⁰.

3.3.2 Mitochondrial membranes of yeast cultured in the presence of LCA display reduced concentration of non-bilayer forming glycerophospholipids and elevated concentrations of their bilayer forming species

Glycerophospholipids have a shape that is defined by the relative sizes of the cross-sectional areas of its hydrophilic head group and hydrophobic acyl chains (Figure 11A-C) ^{66,71,72}. If the cross-sectional areas of the hydrophilic head group and hydrophobic acyl chains of a glycerophospholipid are equally sized, it has a cylindrical shape (Figure 11C) ^{66,71,72}. A glycerophospholipid with a hydrophilic head group that is smaller than the cross-sectional area of the hydrophobic acyl chains has a cone shape, whereas a glycerophospholipid that exhibits the opposite trend is shaped as an inverted cone (Figure 11C) ^{66,71,72}.

The relative levels of cylinder-, cone- and inverted cone-shaped glycerophospholipids in a membrane are known to define membrane curvature; thus, changes in the relative levels of the differently shaped lipids within a membrane can alter its curvature ^{66,71,72}. For the IMM, a rise in the relative levels of glycerophospholipids having the bilayer forming shape of a cylinder reduces the extent of membrane curving ^{66,71,72}. This causes a number of morphological changes including a reduction in positive and negative membrane curvature (that is either toward or away from the mitochondrial matrix respectively), as well as an increase in the proportion of membranes having a flat bilayer conformation. (Figure 11D) ^{66,71,72}. Likewise, an increase in the proportion of cone- and inverted cone-shaped glycerophospholipids increases the degree of membrane curvature, increasing the number of mitochondrial contact sites and mitochondrial cristae (Figure 11D) ^{66,71,72}

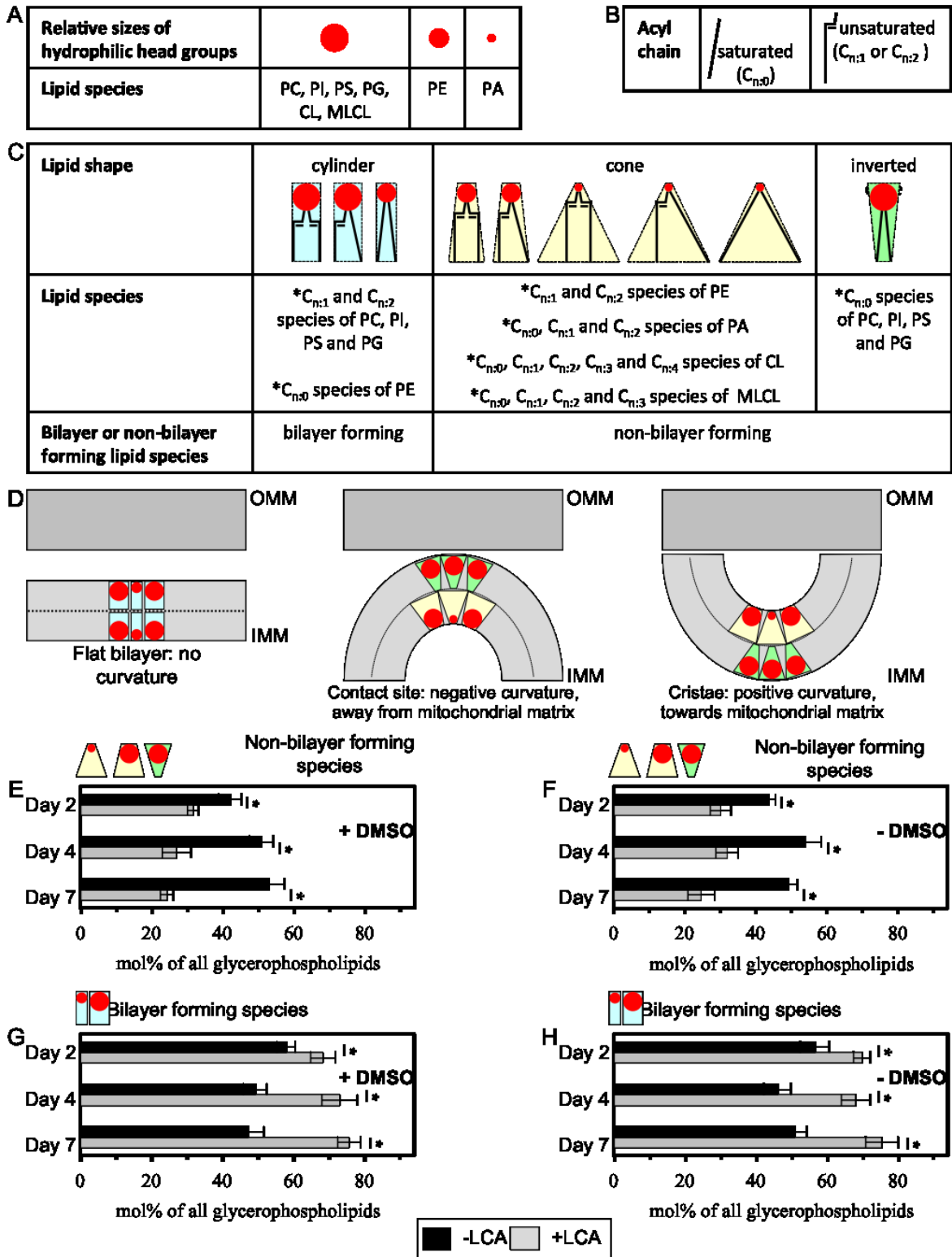


Figure 11 LCA reduces the relative levels of non-bilayer forming glycerophospholipids and elevates the relative levels of bilayer forming species. (A) Relative sizes of the cross-sectional areas of hydrophilic head group for different glycerophospholipid species. (B) Saturated and unsaturated hydrophobic acyl chains of

glycerophospholipids. (C) The shape of a glycerophospholipid molecule is defined by the relative sizes of the cross-sectional areas of its hydrophilic head group and hydrophobic acyl chains. (D) The relative levels of cylinder-, cone- and inverted cone-shaped glycerophospholipids in a membrane define membrane curvature, including that of the IMM. (E - H) Cells were cultured in the nutrient-rich YP medium initially containing 0.2% glucose with 50 μ M LCA or without it, in the presence of 1% DMSO (E and G) or in its absence (F and H). Data are presented as means \pm SEM (n = 3; *p < 0.01). Reproduced from ⁴⁰.

Mitochondria were purified from cells recovered on day 2, 4 or 7 of cell culturing. Extraction of mitochondrial membrane lipids, and mass spectrometric identification and quantitation of the glycerophospholipid species were performed as described in Methods. Based on these data, the relative levels of non-bilayer forming and bilayer forming glycerophospholipids were calculated as molar percentage of all membrane glycerophospholipids.

Based on our data on mass spectrometric identification and quantitation of mitochondrial membrane glycerophospholipids, we calculated the relative levels of their species having the non-bilayer forming shape of a cone or an inverted cone as well as the relative levels of glycerophospholipid species exhibiting the bilayer forming shape of a cylinder. The relative levels of non-bilayer forming and bilayer forming glycerophospholipids were calculated as molar percentage of all membrane glycerophospholipids. We found that, regardless of the presence of DMSO in yeast cultures containing exogenously added LCA, this bile acid reduces the relative levels of non-bilayer forming glycerophospholipids (Figure 11E,F) and elevates the relative levels of their bilayer forming species (Figure 11G,H). We therefore hypothesized that LCA may (I) reduce the abundance of the IMM domains displaying negative curvature characteristic of mitochondrial contact sites between the IMM and OMM; (II) decrease the abundance of the IMM domains exhibiting positive curvature typical of mitochondrial cristae formed by the IMM; and (III) increase the abundance of the IMM domains having flat bilayer conformation.

3.3.3 Mitochondria of yeast cultured in the presence of LCA are enlarged, their number is reduced and their morphology is altered

Membrane lipid composition is known to influence their structure and function ^{64,66,74,75}. In fact mitochondrial morphology is known to be determined by the phospholipid composition of its inner and outer membranes ^{66,76-78}. Treatment of yeast cultures with LCA causes an age-related increase in the glycerophospholipid/protein ratio of mitochondrial membranes and

induces an age related change in the relative levels of different molecular forms of glycerophospholipids within these membranes, we sought to investigate how LCA influences mitochondrial morphology and abundance in chronologically aging yeast. We used electron microscopy to reveal that in yeast cultures entering stationary phase (day 7 of culturing) grown under CR on 0.2% glucose, LCA induced a substantial increase in the size of mitochondria (Figure 12C, I), as well as significantly reduction in their number (Figure 12D, J). Whether LCA was dissolved in DMSO had no influence on this finding (Figure 12A-D, G-J).

From this, we deduced that what is most likely occurring is that the substantial enlargement of mitochondria and the resulting expansion of both mitochondrial membranes observed in yeast cultured with exogenously added LCA (Figure 12A-C and Figure 12G-I) was an effect of the age-related increase in the glycerophospholipid/protein ratio of mitochondrial membranes (Figure 7). It is possible that the decrease in mitochondrial number in yeast grown in the presence of exogenous LCA (Figure 12A,B, D, G, H, J) was caused by the differential effects of this bile acid on the relative levels of different glycerophospholipid species within mitochondrial membranes (Figure 9). In support of this, LCA increased the relative level of mitochondrial PA (Figure 9), a glycerophospholipid which is known to stimulate the fusion of small mitochondria^{66,79,80}.

In these cultures, LCA also significantly altered the morphology of the IMM and mitochondrial cristae. It was observed by electron microscopy that LCA treatment substantially lowered the proportion of mitochondria with cristae extending from the IMM by reducing the extent of connectivity between cristae and the inner boundary membrane (Figure 12A, B, E, G, H, K). This resulted in a significant increase in the total length of mitochondrial cristae relative to the total length of the OMM (Figure 12A, B, F, G, H and L). The formation of mitochondrial cristae by the IMM domains having positive curvature (*i.e.*, membrane curving towards the mitochondrial matrix) is known to require both glycerophospholipids having the non-bilayer forming shape of a cone and glycerophospholipids exhibiting the non-bilayer forming shape of an inverted cone (Figure 11D)^{66,72,81}. From this we hypothesized that the observed alterations to the morphology of the IMM and mitochondrial cristae were the result of the reduction of non-bilayer forming lipids in these membranes (Figure 12A, B, E-H, K and L). Moreover, it is plausible that the observed build-up of cristae disconnected from the IMM, and thus exhibiting

flat bilayer conformation was caused by the substantial rise in the relative levels of bilayer forming mitochondrial glycerophospholipids seen in these cells.

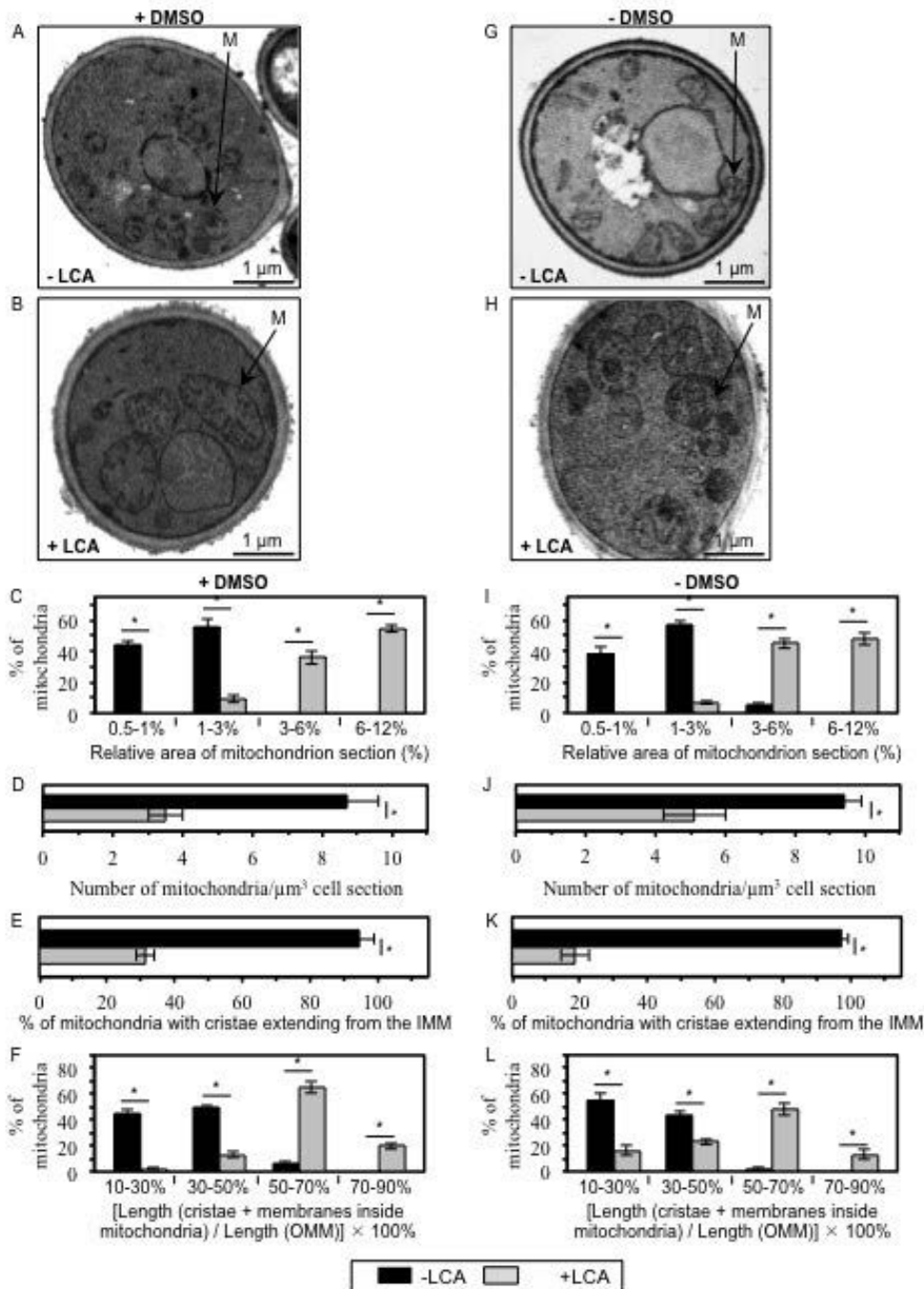


Figure 12 LCA enlarges the mitochondria, reduces their number and alters their morphology. Cells were cultured in the nutrient-rich YP medium initially containing 0.2% glucose with 50 μ M LCA or without it, in the presence of 1% DMSO (A - F) or in its absence (G - L). (A, B, G and H) Transmission electron micrographs of yeast cells recovered on day 7 of cell culturing. M, mitochondrion. Bar, 1 μ m. (C and I) Percentage of mitochondria having the indicated

relative area of mitochondrion section. The relative area of mitochondrion section was calculated as (area of mitochondrion section/area of cell section) \times 100%. Data are presented as means \pm SEM (transmission electron micrographs of at least 100 cells were subjected to morphometric analysis for each kind of culturing conditions; * $p < 0.01$). (D and J) Numbers of mitochondria in yeast cells. The data of morphometric analysis are expressed as the number of mitochondria per μm^3 of cell section \pm SEM (transmission electron micrographs of at least 100 cells were subjected to morphometric analysis for each kind of culturing conditions; * $p < 0.01$). (E and K) Percentage of mitochondria that exhibit cristae extending from the IMM. Data are presented as means \pm SEM (transmission electron micrographs of at least 100 cells were subjected to morphometric analysis for each kind of culturing conditions; * $p < 0.01$). (F and L) Percentage of mitochondria having the indicated relative length of mitochondrion cristae. The relative length of mitochondrion cristae was calculated as [the total length of mitochondrial cristae (including both cristae extending from the IMM and cristae disconnected from the inner boundary membrane)/the total length of the OMM] \times 100%. Data are presented as means \pm SEM (transmission electron micrographs of at least 100 cells were subjected to morphometric analysis for each kind of culturing conditions; * $p < 0.01$). Reproduced from ⁴⁰.

3.4 Discussion

In the data presented in this chapter, I contributed to some of the first evidence that the lipid composition of the mitochondrial membrane plays an essential role in defining the lifespan of yeast. What we now know is that LCA delays chronological aging in yeast by accumulating in both mitochondrial membranes and altering their lipid compositions. These alterations to the lipid composition of the IMM and OMM may be responsible for causing the observed changes in mitochondrial size, number and morphology. These changes coincide with alterations to various lifespan-defining cellular processes that are regulated by the mitochondria. In addition to this, LCA induces these changes under caloric restriction conditions. This signifies that LCA works synergistically with CR to induce an even greater extension of yeast CLS.

From this data, we developed a model to explain how LCA influences longevity by inducing changes to the mitochondrial lipidome and subsequently improving its functional state (Figure 13). First, exogenous LCA enters yeast cells and is sorted to mitochondria. Although in the presence of DMSO used as a vehicle for delivering exogenous LCA into a cell it also resides in the cytosol, the almost exclusive confinement of the intracellular pool of this bile acid to mitochondria if added without DMSO implies that, regardless of the presence of DMSO in yeast cultures, the potent anti-aging effect of LCA is due to its accumulation in mitochondria. Almost

75% of the total pool of mitochondrial LCA resides in the IMM, and approximately 25% of this pool is also confined to the OMM (Figure 13).

The model also posits that the IMM pool of LCA exerts an effect on activities of different enzymes involved in glycerophospholipid synthesis within the inner boundary membrane. The most likely explanation for these changes is that this bile acid specifically alters the hydrophobic environment within the IMM to slow down the Psd1p- and Crd1p-dependent reactions (Figure 13); the Psd1p reaction is known to lead to the conversion of PS to PE, whereas the Crd1p reaction produces CL from PG^{66,68}. The resulting reduction in the concentration of CL limits its availability for the later acyl chain remodeling steps (Figure 13), which involve the sequential action of the phospholipase Cld1p and the transacylase Taz1p^{66,68}. This, in turn, lowers the level of MLCL as well as reduces the flow and elevates the level of PC (Figure 13), the only known donor of acyl chains for the remodeling of newly synthesized CL^{66,68}. Our model also suggests that a reduction in CL within the IMM attenuates a negative feedback loop that involves a CL-dependent inhibition of PA transport from the OMM to the IMM by Ups1p, a protein that shuttles PA between the two mitochondrial membranes (Figure 13)^{66,68}. The acceleration of the Ups1p-driven transport of PA from the OMM to the IMM may in turn accelerate the movement of PA from the MAM domain of the ER to the OMM; such movement is known to occur via mitochondria-ER junctions⁶⁶⁻⁶⁸ and could be stimulated by the accumulated in the OMM pool of LCA (Figure 13). The transport of PA from the MAM domain of the ER to the OMM and then to the IMM acts synergistically with the aforementioned LCA-dependent deceleration of the Crd1p reaction to increase the levels of PA and PG within the IMM (Figure 13).

3.5 Conclusions

To summarize, the remodeling of glycerophospholipid synthesis within the IMM, attenuation of the CL-dependent inhibition of PA transport from the OMM to the IMM and acceleration of PA movement from the MAM domain of the ER to the OMM in cells cultured with LA cause: (I) a decline in the relative levels of PE, CL and MLCL within mitochondrial membranes; and (II) a rise in the relative levels of PA, PS, PC and PG within mitochondrial membranes (Figure 13). In our model, none of these LCA-driven processes in the IMM and OMM alters the relative level of PI within mitochondrial membranes (Figure 13), just as it was

demonstrated by our mass spectrometric quantitation of various molecular forms of mitochondrial membrane glycerophospholipids (Figure 9).

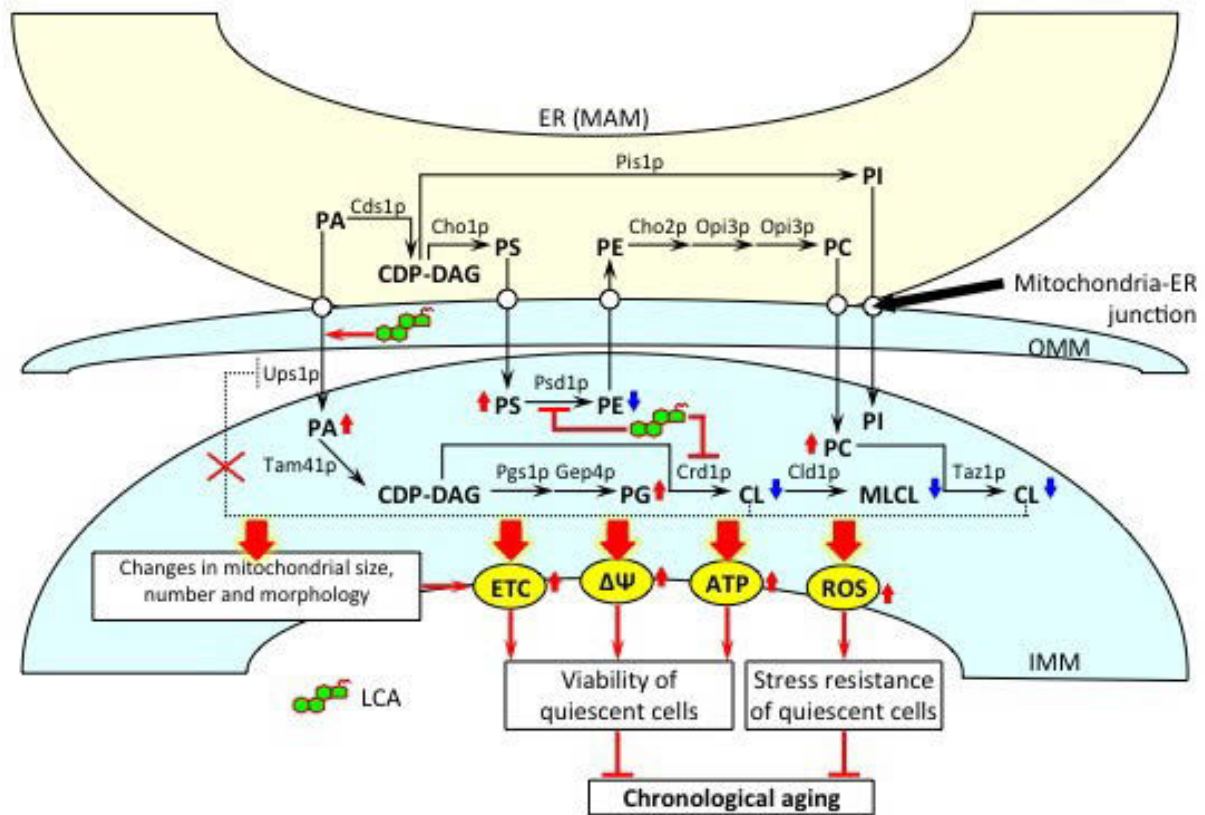


Figure 13 - A model for a mechanism underlying the ability of LCA to extend yeast longevity by accumulating in mitochondria, altering mitochondrial membrane lipidome, and affecting mitochondrial morphology and function. Exogenously added LCA enters yeast cells and accumulates mainly in the inner mitochondrial membrane (IMM). In so doing LCA causes a remodeling of glycerophospholipid synthesis within the IMM, attenuating the cardiolipin (CL)-dependent inhibition of phosphatidic acid (PA) transport from the OMM to the IMM and accelerating PA movement from the mitochondria-associated membrane (MAM) domain of the ER to the OMM via mitochondria-ER junctions. The LCA-driven progressive remodeling of mitochondrial membrane lipidomes with the chronological age of a yeast cell causes major changes in mitochondrial size, number and morphology. The elicited by LCA substantial changes in mitochondrial membrane lipidome and the resulting major changes in mitochondrial morphology act in synergy to alter the age-related chronology of mitochondrial respiration, electrochemical membrane potential, ATP synthesis and ROS homeostasis. Because of these LCA-dependent changes in the age-related dynamics of the four longevity-defining processes confined to mitochondria, chronologically “old” cells cultured with exogenous LCA exhibit higher mitochondrial respiration, electrochemical membrane potential, ATP level and ROS concentration. This increases their long-term viability and stress resistance and, thus, extends their longevity. Arrows next to the names of lipid species denote those of them whose concentrations are elevated (red arrows) or reduced (blue arrows) in cells cultured with exogenous LCA and therefore accumulating this bile acid in

the IMM and OMM. Activation arrows and inhibition bars displayed in red color denote anti-aging processes. Reproduced from ⁴⁰.

Our model indicates that by altering the biosynthesis and transport of several different membrane phospholipid species, LCA causes significant changes in the number and structure of mitochondria. These age-related changes include an increase in the abundance of mitochondrial glycerophospholipids (Figure 7), thereby leading to an expansion of both mitochondrial membranes and the resulting enlargement of mitochondria (Figure 12). In addition to this LCA causes a rise in the level of mitochondrial PA (Figure 9), which is likely involved in the apparent reduction in mitochondrial number (Figure 12) - perhaps by stimulating mitochondrial fusion which PA has been implicated in ^{66,79,80}. LCA also induced a decline in the relative levels of non-bilayer forming (*i.e.*, cone- and inverted cone-shaped) mitochondrial phospholipids (Figure 11), resulting in a decrease in the proportion of mitochondria with cristae extending from the IMM (Figure 12). This is possibly due to the fact that mitochondrial cristae formation by the IMM domains having positive curvature is known to require both these differently shaped non-bilayer forming glycerophospholipids ^{66,72,81}. Lastly, LCA induced a rise in the relative levels of bilayer forming (*i.e.*, cylinder-shaped) mitochondrial glycerophospholipids, thereby leading to an accumulation within the mitochondrial matrix of cristae disconnected from the IMM and thus exhibiting flat bilayer conformation - perhaps due to the known ability of bilayer forming glycerophospholipids to reduce the extent of membrane curving ^{66,72,81}.

4. Macromitophagy is a longevity assurance process that in chronologically aging yeast limited under caloric restriction conditions maintains cellular lipid homeostasis

Abstract

Macromitophagy controls mitochondrial quality and quantity. It involves the sequestration of dysfunctional or excessive mitochondria within double-membrane autophagosomes, which then fuse with the vacuole/lysosome to deliver these mitochondria for degradation. To investigate a physiological role of macromitophagy in yeast, we examined how the *atg32Δ*-dependent mutational block of this process influences the chronological lifespan of cells grown in a nutrient-rich medium containing low (0.2%) concentration of glucose. Under these longevity-extending conditions of caloric restriction (CR) yeast cells are not starving. Our findings imply that macromitophagy is a longevity assurance process underlying the beneficial effects of CR on yeast lifespan. Our analysis of how the *atg32Δ* mutation influences mitochondrial morphology, composition and function revealed that macromitophagy is required to maintain a network of healthy mitochondria. Our comparative analysis of the membrane lipidomes of organelles purified from wildtype and *atg32Δ* cells revealed that macromitophagy is required for maintaining cellular lipid homeostasis. We concluded that macromitophagy defines yeast longevity by modulating vital cellular processes inside and outside of mitochondria.

4.1 Introduction

Mitophagy is a key mechanism of mitochondrial quality and quantity control responsible for the autophagic degradation of aged, dysfunctional, damaged or excessive mitochondria⁸²⁻⁸⁴. Macromitophagy refers to the sequestration of targeted mitochondria into double-membrane-bounded structures known as autophagosomes^{2, 4}. Following fusion of these autophagosomes with the vacuole/lysosome, sequestered mitochondria are degraded by acid hydrolases⁸⁵.

A micromitophagic mode of mitophagy involves the engulfment of such mitochondria through direct invagination of the vacuolar/lysosomal boundary membrane^{85,86}, whereas its macromitophagic mode refers to the sequestration of targeted mitochondria into double-membrane-bounded structures known as autophagosomes^{85,87}. Following fusion of these autophagosomes with the vacuole/lysosome, sequestered mitochondria are degraded by acid

hydrolases^{88,89}.

Only the macromitophagic mode of mitophagy has been described in mammals^{90,91}. Macromitophagy in mammalian cells is known to play essential roles in several vital biological processes underlying organismal aging, development and differentiation, including (I) selective degradation of depolarized mitochondria in dopaminergic neurons in the substantia nigra, a PINK1/Parkin-dependent process impaired in autosomal recessive forms of Parkinson's disease; (II) massive elimination of mitochondria driven by Nix, a protein in the outer mitochondrial membrane, during reticulocyte-to-erythrocyte maturation; and (III) selective clearance of surplus mitochondria during white adipose tissue differentiation in an Atg5/Atg7-dependent manner^{87,90-93}.

The physiological role of mitophagy in yeast remains obscure. To provide further insight into the physiological functions of selective macroautophagic mitochondrial removal in the yeast *Saccharomyces cerevisiae*, in this study our lab examined how the *atg32Δ*-dependent mutational block of macromitophagy affects the chronological lifespan of yeast cultured in a nutrient-rich medium initially containing low (0.2%) concentration of glucose. It has been shown that under CR conditions yeast cells undergo an extensive remodeling of their metabolism in order to match the level of ATP produced under longevity-shortening non-CR conditions¹³. It has recently been demonstrated that LCA, a bile acid, is a potent anti-aging natural compound that acts in synergy with CR to enable a significant further extension of yeast lifespan under CR conditions²⁷. Specifically it was shown that the inhibition of mitochondrial specific macroautophagy (mitophagy) through deletion of Atg32p drastically impairs the ability of both a caloric restriction diet, as well as LCA to extend yeast CLS⁶². It was also demonstrated that Atg32p is necessary for maintaining a pool of functional mitochondria capable maintaining the efficiency of aerobic respiration⁶². Moreover, because mitochondria are known to be dynamically integrated into a network governing lipid metabolism and transport not only within these organelles but also within the endoplasmic reticulum (ER) and the plasma membrane (PM)^{66,67,78,94-96}, we investigated whether mitochondrial quality control via macromitophagy were critical for maintaining normal lipid homeostasis. I used mass spectrometry to compare the membrane lipidomes of purified mitochondrial, ER, and PM membranes from wildtype (WT) and *atg32Δ* cells that were cultured under CR on 0.2% glucose. The findings provide evidence that macromitophagy defines longevity of chronologically aging yeast limited in calorie supply

through the maintenance of normal organellar membrane lipid homeostasis.

4.2 Materials and Methods

Yeast strains, media and growth conditions.

The wildtype strain *Saccharomyces cerevisiae* BY4742 (*MAT α his3 Δ I leu2 Δ 0 lys2 Δ 0 ura3 Δ 0*) as well as the single-gene-deletion mutant strains *atg32 Δ* (*MAT α his3 Δ I leu2 Δ 0 lys2 Δ 0 ura3 Δ 0 atg32 Δ ::kanMX4*) [from Thermo Scientific/Open Biosystems; #YSC1054 and #YSC1021-550234 respectively] were grown in YP medium (1% yeast extract, 2% peptone) [both from Fisher Scientific; #BP1422-2 and #BP1420-2, respectively] containing 0.2% glucose [#D16-10; Fisher Scientific] as carbon source. Cells were cultured at 30°C with rotational shaking at 200 rpm in Erlenmeyer flasks at a “flask volume/medium volume” ratio of 5:1.

Subcellular Fractionation and Purification of Organelles

Subcellular fraction followed by purification of Mitochondria ⁶³, ER ⁹⁷, and plasma membrane ⁹⁸ were conducted according to established protocols that are summarized below.

Isolation of the crude ER and mitochondrial fractions

Yeast cells were harvested at $3,000 \times g$ for 5 min at room temperature, washed with water and resuspended in DTT buffer (100 mM Tris-H₂SO₄, pH 9.4, 10 mM dithiothreitol [DTT]). Cells were incubated in DTT buffer incubated for 20 min at 30°C to weaken the cell wall. The cells then were washed with Zymolyase buffer (1.2 M sorbitol, 20 mM potassium phosphate, pH 7.4) and centrifuged at $3,000 \times g$ for 5 min at room temperature. Cells were then incubated with 3 mg/g (wet weight) of Zymolyase-100T in 7 ml/g (wet weight) Zymolyase buffer for 45 min at 30°C. Following an 8-min centrifugation at $2,200 \times g$ at 4°C, the isolated spheroplasts were washed in ice-cold homogenization buffer (5 ml/g) (0.6 M sorbitol, 10 mM Tris-HCl, pH7.4, 1 mM EDTA, 0.2% (w/v) BSA) and centrifuged at $2,200 \times g$ for 8 min at 4°C. Spheroplasts were homogenized in ice-cold homogenization buffer using 15 strokes. Cell debris was removed by centrifuging the resulting homogenates at $3,000 \times g$ for 10 min at 4°C. The resulting supernatant was then centrifuged at $12,000 \times g$ for 15 min at 4°C to pellet mitochondria. The remnant cell debris was removed by centrifuging the mitochondrial fraction at $3,000 \times g$ for 5 min at 4°C. The

resulting supernatant was then centrifuged at $12,000 \times g$ for 15 min at 4°C to obtain the crude mitochondrial pellet, which was then resuspended in 3 ml of SEM Buffer (250 mM sucrose, 1 mM EDTA, 10 mM MOPS, pH 7.2) and used for the purification of mitochondria as described below.

Purification of mitochondria and ER devoid of microsomal and cytosolic contaminations

A sucrose gradient was made by overlaying 1.5 ml of 60% sucrose with 4 ml of 32% sucrose, 1.5 ml of 23% sucrose, and then 1.5 ml of 15% sucrose (all in EM buffer; 1 mM EDTA, 10 mM MOPS, pH 7.2). Finally, a 3-ml aliquot of the crude mitochondrial fraction in SEM buffer was applied to the gradient and centrifuged at $134,000 \times g$ (33,000 rpm) for three hours at 4°C in vacuum (Rotor SW40Ti, Beckman). The purified mitochondria found at the 60%/32% sucrose interface, and the purified ER found primarily at the 15%/23% sucrose interface were carefully removed and stored at -80°C until lipids were extracted for mass spectrometry.

Purification of Plasma Membrane

First, yeast cultures were harvested by centrifugation at $5,000 \times g$ (5,300 rpm) for 5 min at 4°C in a JA-10 rotor (Beckman). Cells were washed and resuspended in 13.7% sucrose in 25mM imidazole/HCl buffer (6.81g imidazole/100mL water adjusted to pH 7.0 w HCl). Cells were then pelleted at $5,000 \times g$ for 10 min at 4°C in a JA-17 rotor (Beckman). The supernatant was removed, and the cells were lysed with an equal volume of glass beads followed by 2 minute pulses by vortex and then placed on ice. This was repeated for a total of combined time of ~ 10 minutes. The cell suspension were diluted in 13.7% sucrose in 25 mM imidazole/HCl buffer and centrifuged at $1,000 \times g$ for 10 minutes to pellet unbroken cells in a JA-17 rotor (Beckman) at 4°C . Mitochondria were removed by centrifugation at $10,000 \times g$ (8,200 rpm) for 20 min at 4°C in a JA-17 rotor. Crude plasma membrane was then collected by centrifugation of the remaining supernatant at $30,000 \times g$ for 30 min at 4°C in a JA-17 rotor (Beckman). Crude plasma membrane was further purified by centrifugation on a sucrose gradient. The gradient was made by carefully overlaying 2.5 mL of 77% sucrose in imidazole/HCl (pH 7) with 2.5 mL of 56.5% sucrose in imidazole/HCl (pH 7), with 2.5 mL of 37.7% sucrose in imidazole/HCl (pH 7), with 2.5 mL of 13.7% sucrose in imidazole/HCl (pH 7). 1 mL of crude plasma membrane suspension was layered on each gradient made in tubes for the SW41Ti rotor (Beckman). Samples were

centrifuged at 200,000 x g for 3 hours at 4°C. The samples were fractionated and the fractions enriched in purified plasma membrane were stored at -80 °C until extraction of lipids for mass spectrometry.

Analysis of lipids by mass spectrometry

Extraction of lipids from purified mitochondria, ER and PM and following mass spectrometric identification and quantitation of various lipid species were carried out as previously described⁴². Mass spectrometric analyses were performed with a Thermo Orbitrap Velos mass spectrometer equipped with a HESI-II ion source (#10145339; Thermo Scientific) operating at a flow rate of 5 µl/minute. Lipid species were analyzed by top 10 data dependent FT-MS/MS at a resolution of 100,000 for MS scans and 30,000 for dependent MS/MS. Fragmentation was carried out using HCD at a normalized collision energy of 35 in negative ion mode and 65 in positive ion mode. Acquired mass spectra were converted from proprietary Thermo RAW format to either mzXML or mzML using MSConvert as part of the ProteoWizard suite (freely available from <http://proteowizard.sourceforge.net/>). The raw data were then imported into LipidXplorer (freely available from https://wiki.mpi-cbg.de/wiki/lipidx/index.php/Main_Page) for lipid identification. Data normalization, quantitation, and visualization were performed in Microsoft excel.

4.3 Results

4.3.1 Macromitophagy is required for maintaining the homeostasis of membrane lipids in mitochondria, the ER and the PM

Mitochondria are currently believed to be the only site within eukaryotic cells where cardiolipin (CL), the signature glycerophospholipid of these organelles, is synthesized^{66,78}. Additionally, yeast mitochondria house the synthesis of the glycerophospholipid phosphatidylethanolamine (PE), minor quantities of which are also formed in the Golgi apparatus⁷⁸. Both CL and PE are synthesized in the inner membrane of yeast mitochondria from their precursor lipid species cytidine diphosphate-diacylglycerol (CDP-DAG), which is formed exclusively in the ER. CDP-DAG also serves as a precursor for CL, whereas the glycerophospholipid phosphatidylserine (PS) is a precursor for PE (Figure 14)⁶⁶. Because of this, the biosynthesis of CL and PE in yeast cells relies on a delivery of their CDP-DAG and PS

precursors from the ER to the IMM^{66,99,100}. Moreover, the mitochondrially synthesized PE serves as a precursor for the glycerophospholipid phosphatidylcholine (PC), which is synthesized only in the ER (Figure 14)^{67,78}. For this reason ER synthesized PC must be transported to mitochondria – which is incapable of synthesizing this essential glycerophospholipid (Figure 14)^{66,99}. Additionally, the glycerophospholipids phosphatidic acid (PA) and phosphatidylinositol (PI) are synthesized in the ER but not in mitochondria of yeast cells; therefore, these two lipid species need to be translocated to these membranes from the site of their synthesis in the ER (Figure 14)^{66,78}. Altogether, this indicates that for the normal functioning of yeast mitochondria, a bidirectional exchange of lipids between the mitochondrial and ER membranes is required. Such an exchange occurs between zones of close apposition, known as membrane contact sites or junctions. These occur between the outer mitochondrial membrane and the mitochondria-associated membrane (MAM) domain of the ER. It is estimated that 80 to 110 of these mitochondria-ER junctions are believed to exist per yeast cell (Figure 14)^{67,100,101}. Of note, following their synthesis within the ER and inner mitochondrial membranes, lipids can be translocated to the PM; as many as 1,100 PM-ER junctions per yeast cell are involved in lipid transport from the PM-associated membrane (PAM) domain of the ER to the PM (Figure 14)^{94-96,100}.

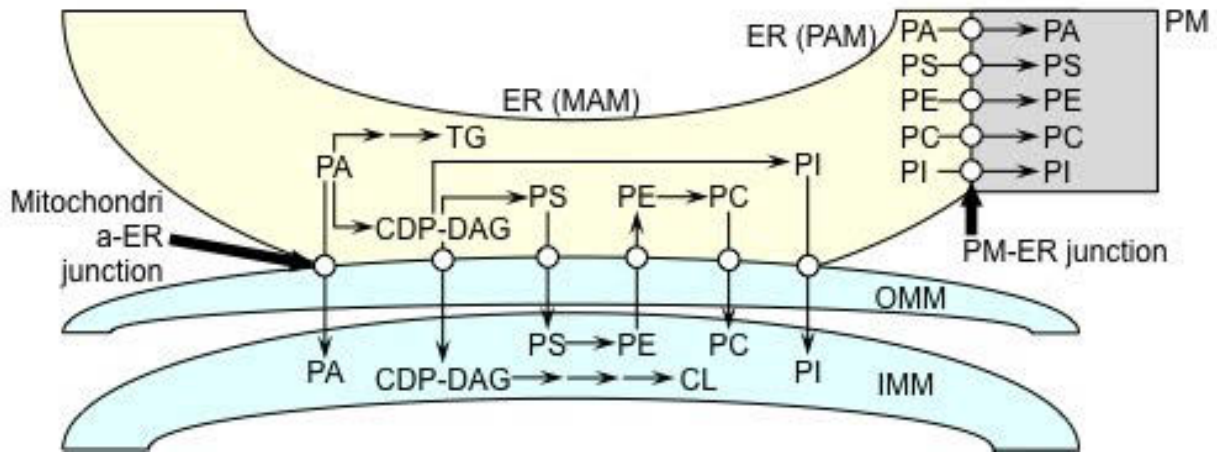


Figure 14 - Lipid synthesis in the ER and mitochondria and lipid transport via mitochondria-ER and PM-ER junctions. After being synthesized in the mitochondria-associated membrane (MAM) domain of the ER, cytidine diphosphate-diacylglycerol (CDP-DAG) and phosphatidylserine (PS) are transported via mitochondria-ER junctions to the outer mitochondrial membrane (OMM). Following their translocation from the OMM to the inner mitochondrial membrane (IMM), CDP-DAG and PS are used as substrates for the synthesis of cardiolipin (CL) and phosphatidylethanolamine (PE), respectively. PE is then transported through mitochondria-ER junctions to the

MAM domain of the ER, where it is converted to phosphatidylcholine (PC). After being formed in the MAM, PC is translocated via mitochondria-ER junctions to mitochondria, which are incapable of synthesizing this glycerophospholipid. The glycerophospholipids phosphatidic acid (PA) and phosphatidylinositol (PI) are also synthesized in the MAM domain of the ER, from which they are delivered through mitochondria-ER junctions to mitochondria known to lack enzymes required for the synthesis of these two glycerophospholipids. After being synthesized within the ER and inner mitochondrial membranes, lipids can be translocated via the PM-ER junctions from the PM-associated membrane (PAM) domain of the ER to the plasma membrane (PM). Unlike glycerophospholipids, various molecular forms of the neutral lipids triacylglycerols (TG) cannot be moved from the site of their synthesis in the ER to either mitochondria or the PM. Reproduced from ⁶².

With the role of the mitochondria in regulating lipid homeostasis within the mitochondria, ER, and the PM in mind, it was hypothesized that by inhibiting the ability of yeast cells to eliminate morphologically distinct, dysfunctional, or oxidatively damaged mitochondria through the deletion of Atg32p, yeast lipid homeostasis could be distorted. One could therefore expect that the *atg32Δ*-dependent mutational block of macromitophagy may alter membrane lipid composition not only in mitochondria but also in the ER and the PM.

The validity of this hypothesis was validated using mass spectrometry to compare the membrane lipidomes of mitochondria, ER and PM purified from WT and *atg32Δ* cells that were cultured under CR on 0.2% glucose and recovered on day 1, 2 or 4 of culturing. It was observed that the *atg32Δ* mutation altered the levels of several membrane lipid species in mitochondria, ER and PM. Additionally, the effect of *atg32Δ* on the membrane lipidomes of mitochondria, the ER, and the PM was different in cells recovered on day 1, 2 or 4 of culturing - indicating the effects are age-related (Figure 15).

In cells recovered at logarithmic growth phase (day 1), the *atg32Δ* mutation (I) increased the levels of PE (a glycerophospholipid delivered to the ER after its synthesis in the IMM) in mitochondria and the PM, and reduced its level in the ER; (II) lowered the level of CL (a mitochondrially synthesized and accumulated glycerophospholipid) in mitochondria; (III) decreased the level of PC (a glycerophospholipid synthesized in the ER membrane and then delivered to other membranes) in the PM, but did not alter its abundance in mitochondria or the ER; (IV) elevated the levels of PI (a glycerophospholipid synthesized in the ER membrane and then delivered to other membranes) in mitochondria and the ER, but did not alter its abundance in the PM; (V) lowered the level of TAG (neutral lipid species synthesized in the ER but not in mitochondria or the PM) in the ER; and (VI) did not affect the levels of PA and PS (two

glycerophospholipids synthesized in the ER membrane and then delivered to other membranes) in mitochondria, the ER and the PM (Figure 15 A, D, G).

Furthermore, in cells recovered at diauxic growth phase on day 2, the *atg32Δ* mutation (I) reduced the level of PE in the ER membrane but not in mitochondria or the PM; (II) elevated the level of CL in mitochondria; (III) decreased the levels of PC in mitochondria and the PM, but did not alter its abundance in the ER; (IV) reduced the level of PI in mitochondria and elevated the level of this glycerophospholipid in the ER, but did not alter its abundance in the PM; (V) lowered the level of TAG in the ER; (VI) increased the level of PA in the ER membrane, but did not alter its abundance in mitochondria or the PM; and (VII) reduced the level of PS in the ER and elevated the level of this glycerophospholipid in the PM, but did not alter its abundance in mitochondria (Figure 15 B, E and H).

Moreover, in cells recovered at post-diauxic growth phase on day 4, the *atg32Δ* mutation (I) elevated the levels of PE in mitochondria and the PM, and reduced its abundance in the ER; (II) decreased the level of CL in mitochondria; (III) reduced the level of PC in the ER and increased the level of this glycerophospholipid in the PM, but did not alter its abundance in mitochondria; (IV) lowered the levels of PI in mitochondria and the ER, but did not alter its abundance in the PM; (V) did not alter the level of TAG in the ER; (VI) elevated the levels of PA in mitochondria and the ER, and reduced its abundance in the PM; and (VII) decreased the level of PS in mitochondria, but increased the levels of this glycerophospholipid in the ER and the PM (Figure 15 C, F, I).

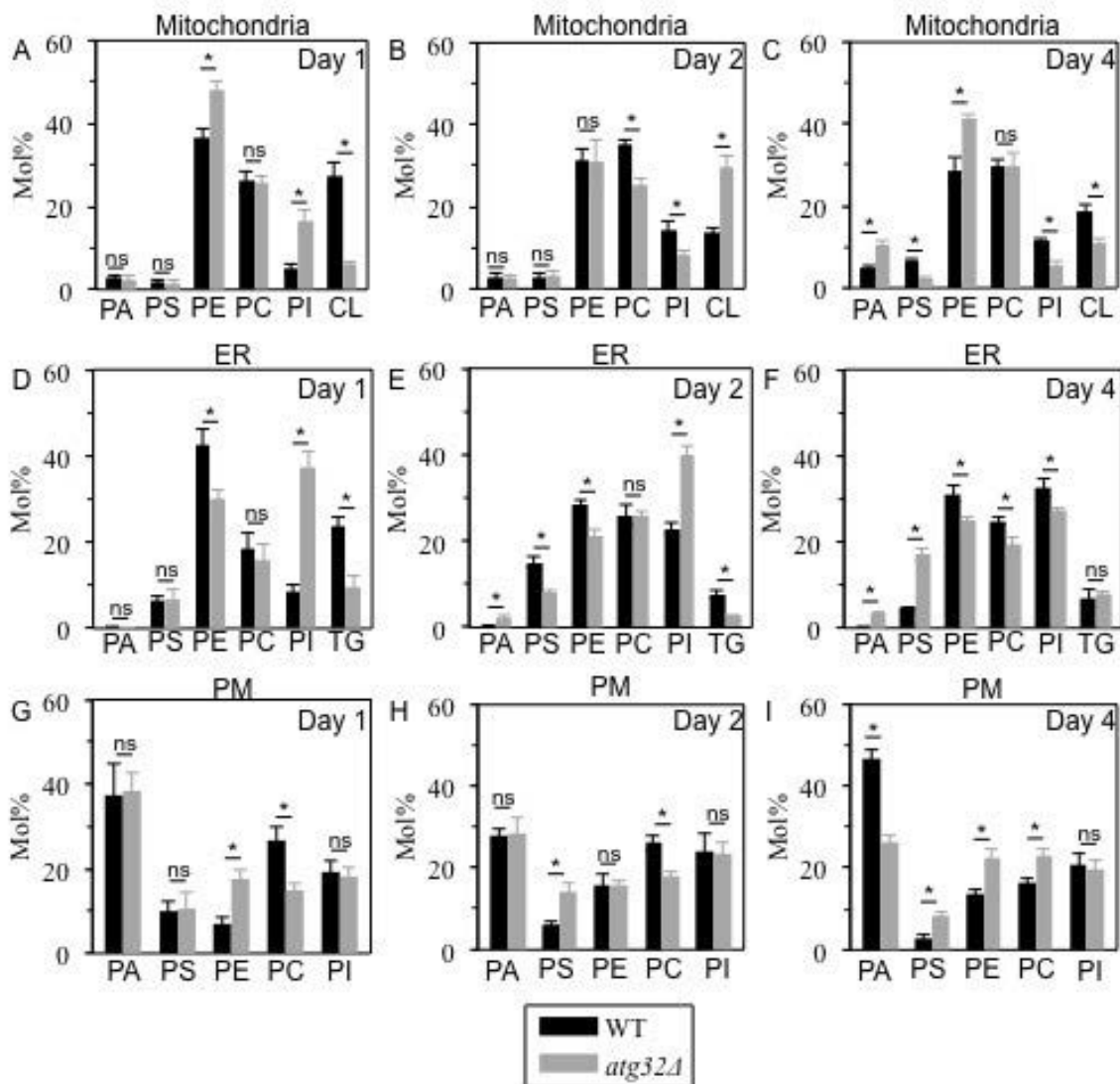


Figure 15 - Under CR conditions, the *atg32Δ* mutation alters levels of several membrane lipid species in mitochondria, the ER and the PM. WT and *atg32Δ* strains were cultured in the nutrient-rich YP medium initially containing 0.2% glucose. Mitochondria, the ER and the PM were purified from WT and *atg32Δ* cells recovered on day 1, 2 or 4 of culturing. Following extraction of membrane lipids from purified mitochondria, ER and PM, various lipid species were identified and quantitated by mass spectrometry as described in Methods. Data are presented as means \pm SEM (n = 3; *p < 0.01; ns, not significant). Reproduced from ⁶².

Altogether, these findings imply that under CR conditions macromitophagy is essential for sustaining the homeostasis of membrane lipids in mitochondria, the ER and the PM. It is plausible that the observed in macromitophagy-deficient *atg32Δ* cells age-related changes in the

membrane lipidomes of mitochondria, the ER and the PM may shorten yeast longevity by establishing a pro-aging cellular pattern.

4.4 Discussion

The observed age-related changes in the membrane lipidomes of mitochondria, the ER and the PM of the *atg32Δ* mutant imply that macromitophagy selectively eliminates mitochondria exhibiting an imbalance of their membrane lipidome. This is perhaps due to age-associated alterations in the synthesis, stability and/or oxidative state of some lipid species. Because mitochondria are convolutedly integrated into a network governing lipid dynamics not only within these organelles but also within the ER and the PM (Figure 14), it is reasonable to assume that the inability of macromitophagy-deficient *atg32Δ* cells to eliminate mitochondria exhibiting such an age-related imbalance of their membrane lipidome (I) can also compromise lipid metabolism and transport in the ER and the PM; and (II) could be responsible for the changes in the membrane lipidomes of the mitochondria, ER, and PM observed in *atg32Δ* cells.

Based on these observations, a working model for the mechanism underlying the age-dependent alteration to lipid synthesis in the ER and mitochondria was formulated (Figure 16). During logarithmic growth phase, lipid synthesis and transport is remodelled in *atg32Δ* cells leading to the following changes in the membrane lipidomes of mitochondria, the ER and the PM: (I) an activated conversion of PS into PE in the IMM and a simultaneous inhibition of PE transport from mitochondria to the MAM domain of the ER via mitochondria-ER (MAM) junctions elevate PE concentration in mitochondria and reduce its concentration in the ER; (II) an activated synthesis of PI from CDP-DAG in the MAM domain of the ER, along with an activation of PI transport from this ER domain to mitochondria via mitochondria-ER (MAM) junctions, rise PI concentration in both mitochondria and the ER; (III) an inhibition of TAG synthesis from PA in the MAM domain of the ER reduces TAG concentration in this organelle; (IV) an inhibition of CL synthesis from CDP-DAG in the IMM is responsible for the observed decline of CL concentration in mitochondria; (V) an activated transport of PE from the PAM domain of the ER to the PM via PM-ER (PAM) junctions increases PE concentration in the PM; and (VI) an inhibition of PC transport from the PAM domain of the ER to the PM via PM-ER (PAM) junctions reduces PC concentration in the PM (Figure 16A). During diauxic growth phase, *atg32Δ* cells undergo a remodelling of lipid synthesis and transport causing the following

alterations to membrane lipid concentrations in mitochondria, the ER and the PM: (I) an inhibited conversion of CDP-DAG into PS in the MAM domain of the ER and an inhibition of PE transport from mitochondria to this ER domain via mitochondria-ER (MAM) junctions reduce the concentrations of both PS and PE in the ER; (II) an inhibition of PC transport from the MAM domain of the ER to mitochondria via mitochondria-ER (MAM) junctions lowers the concentration of this glycerophospholipid in mitochondria; (III) an inhibited transport of PI from the MAM domain of the ER to mitochondria via mitochondria-ER (MAM) junctions reduces PI concentration in mitochondria and rises its level in the ER; (IV) an activation of CL synthesis from CDP-DAG in the IMM leads to the observed increase of CL concentration in mitochondria; (V) an inhibited conversion of PA into TAG in the MAM domain of the ER is responsible for the observed rise of PA and decline of TAG concentrations in this organelle; (VI) an activated transport of PS from the PAM domain of the ER to the PM via PM-ER (PAM) junctions increases its concentration in the PM; and (VII) an inhibition of PC transport from the PAM domain of the ER to the PM via PM-ER (PAM) junctions reduces PC level in the PM (Figure 16B). During post-diauxic growth phase, a remodelling of lipid synthesis and transport in *atg32Δ* cells alters the membrane lipidomes of mitochondria, the ER and the PM as follows: (I) an inhibition of PS transport from the MAM domain of the ER to mitochondria and a simultaneous inhibition of PE transport in the opposite direction via mitochondria-ER (MAM) junctions, along with an activated conversion of PS into PE in the IMM, not only rise the concentrations of PS in the ER and PE in mitochondria but also reduce the levels of PE in the ER and PS in mitochondria; (II) an inhibited synthesis of PC from PE in the MAM domain of the ER lowers PC concentration in this organelle; (III) an inhibition of the conversion of CDP-DAG into PI in the MAM domain of the ER reduces PI levels both in the ER and in mitochondria; (IV) an inhibited synthesis of CL from CDP-DAG in the IMM lowers CL concentration in mitochondria; (V) an activated transport of PS, PE and PC from the PAM domain of the ER to the PM via PM-ER (PAM) junctions increases their concentrations in the PM; and (VI) an inhibition of PA transport from the PAM domain of the ER to the PM via PM-ER (PAM) junctions not only reduces PA level in the PM but may also be responsible for the observed rise of PA concentrations in the ER and mitochondria (Figure 16C).

It has been previously established that the spatiotemporal dynamics of lipid synthesis, deposition and degradation play an essential role in longevity regulation in evolutionarily distant

organisms, including yeast^{13,32,37,102}. Therefore it is possible that these observed age-related alterations in these organellar lipidomes, and especially those seen in the short-lived *atg32Δ* mutant may lead to the establishment of a pro-aging cellular pattern and may ultimately shorten yeast longevity.

4.5 Conclusion

In conclusion it has now been established that macromitophagy is a longevity assurance process that is crucial to the beneficial effects of CR and LCA on yeast CLS. In addition to this we showed perhaps the first evidence that macromitophagy is necessary for maintaining normal lipid homeostasis in a variety of organellar membranes. We concluded that macromitophagy defines yeast longevity by modulating vital cellular processes inside and outside of mitochondria.

In the future, it would be important to identify longevity-defining cellular processes that are responsive to the observed in *atg32Δ* cells alterations in the repertoires of membrane lipids constituting mitochondria, the ER and the PM. These cellular processes may include (I) a mitochondria-controlled, age-related mode of apoptotic cell death known to be modulated in response to changes in CL concentration within the IMM^{103,104}; and (II) a non-selective pathway of macroautophagy shown to be responsive to certain alterations in lipid metabolism within and lipid exchange between several cellular membranes^{105–107}.

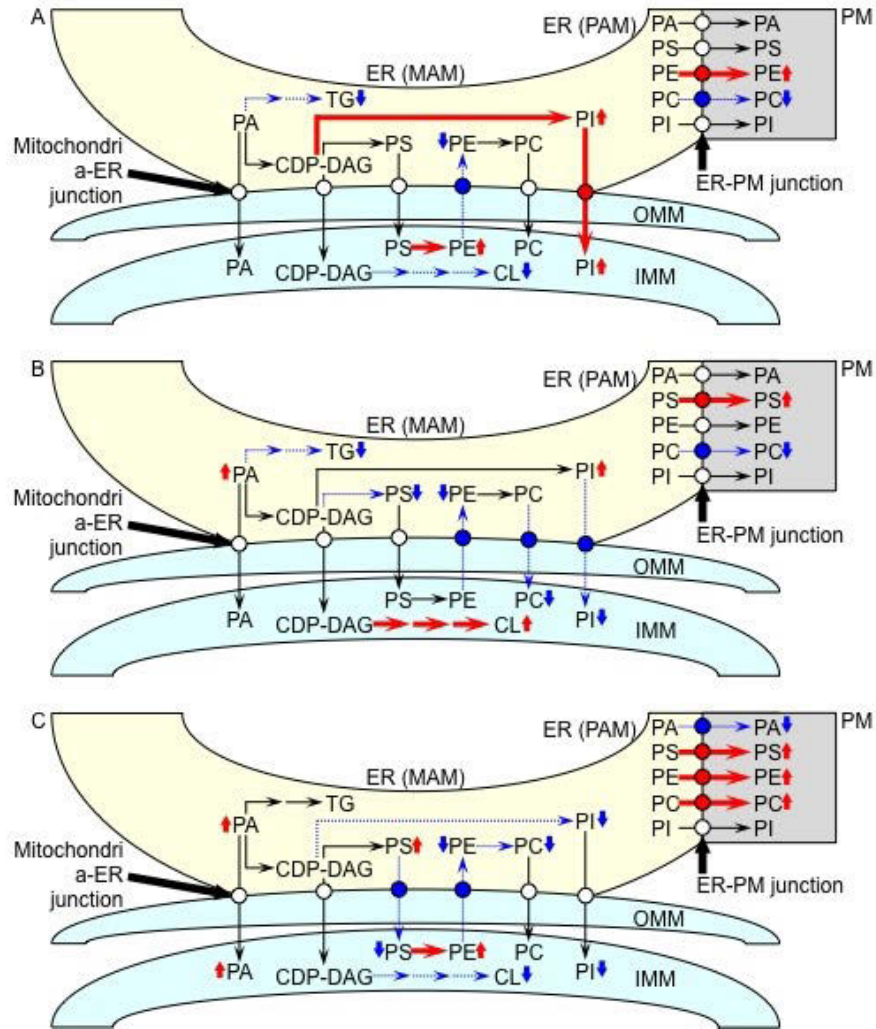


Figure 16 - A working model for a mechanism that in *atg32Δ* cells underlies the spatiotemporal dynamics of age-related changes in lipid synthesis in the ER and mitochondria as well as in lipid transport via mitochondria-ER (MAM) and PM-ER (PAM) junctions. During logarithmic (A), diauxic (B) and post-diauxic (C) phases of growth under CR conditions, a remodelling of lipid synthesis and transport in *atg32Δ* cells alters the membrane lipidomes of mitochondria, the ER and the PM. From the data of lipidomic analysis, we inferred an outline of lipid synthesis and transport processes that were activated (red arrows) or inhibited (blue arrows) by the *atg32Δ*-dependent mutational block of macromitophagy; the thickness of these arrows correlates with the rates of the processes taking place in *atg32Δ* cells. Arrows next to the names of lipid species denote those of them whose concentrations are elevated (red arrows) or reduced (blue arrows) in *atg32Δ* cells. Reproduced from ⁶².

5. Macromitophagy, neutral lipid synthesis and peroxisomal fatty acid oxidation protect yeast from “liponecrosis”, a previously unknown form of programmed cell death

5.1 Abstract

We identified a form of cell death called liponecrosis (see chapter 4). It can be elicited by an exposure of the yeast *Saccharomyces cerevisiae* to exogenous palmitoleic acid (POA). Our data imply that liponecrosis is (I) a programmed, regulated form of cell death rather than an accidental, unregulated cellular process; and (II) an age-related form of cell death. Cells committed to liponecrotic death: (I) do not exhibit features characteristic of apoptotic cell death; (II) do not display plasma membrane rupture, a hallmark of programmed necrotic cell death; (III) akin to cells committed to necrotic cell death, exhibit an increased permeability of the plasma membrane for propidium iodide; (IV) do not display excessive cytoplasmic vacuolization, a hallmark of autophagic cell death; (V) akin to cells committed to autophagic death, exhibit a non-selective *en masse* degradation of cellular organelles and require the cytosolic serine/threonine protein kinase Atg1p for executing the death program; and (VI) display a hallmark feature that has not been reported for any of the currently known cell death modalities – namely, an excessive accumulation of lipid droplets where non-esterified fatty acids (including POA) are deposited in the form of neutral lipids. We therefore concluded that liponecrotic cell death subroutine differs from the currently known subroutines of PCD. Our data suggest a hypothesis that liponecrosis is a cell death module dynamically integrated into a so-called PCD network, which also includes the apoptotic, necrotic and autophagic modules of PCD. Based on our findings, we propose a mechanism underlying liponecrosis.

5.2 Introduction

In multicellular organisms, the homeostasis of cell number in various tissues and in the entire organism is sustained via a regulated balance between the fundamental biological processes of cell division, cell differentiation and PCD. PCD refers to a genetically programmed, regulated form of cell death - as opposed to an accidental, unregulated cellular process³⁴. As a genetically programmed, regulated cellular process, a PCD subroutine should be intensified or attenuated by genetic manipulations that alter the abundance and/or activities of only certain

proteins^{34,108}. Furthermore, a PCD subroutine should be a cellular process comprised of a cascade of consecutive cellular events initiated in response to a certain stimulus, following each other in a certain order and orchestrated by a certain signaling pathway or network^{34,108}. Moreover, a PCD subroutine should be a cellular process that provides a certain benefit for development, survival and/or stress resistance of a cell population or an organism^{34,108}. Several PCD subroutines are presently known; these subroutines have different underlying mechanisms, exhibit different morphological and biochemical traits, and are orchestrated by different (although partially overlapping) signaling pathways^{34,108}. The initial classification of various types of PCD into apoptosis, autophagic cell death and necrosis was based mostly on morphological differences between cells committed to these different PCD subroutines^{34,108}. The most recent classification of PCD subroutines is based on a combination of numerous morphological and biochemical traits typical of each of them; the well-characterized PCD subroutines include extrinsic apoptosis, caspase-dependent or -independent intrinsic apoptosis, regulated necrosis, autophagic cell death and mitotic catastrophe.³ Some of the currently known PCD subroutines are characterized in much less details with respect to their morphological traits and biochemical features; these other PCD subroutines include anoikis, excitotoxicity, Wallerian degeneration, paraptosis, pyroptosis, pyronecrosis, entosis, parthanatos, netosis and cornification^{34,108}. Molecular mechanisms underlying these PCD subroutines and integrating them into a PCD network remain to be established.

The use of yeast as a model organism in cell death research has already greatly contributed to the current understanding of the molecular and cellular mechanisms underlying various PCD subroutines^{109–115}. We recently demonstrated that a short-term exposure of yeast cells to exogenously added palmitoleic fatty acid (POA) causes their death^{27,116}. In this study we provide evidence that POA-induced cell death in yeast is an age-related subroutine of genetically programmed, regulated cell death rather than an accidental, unregulated cellular process. We concluded that POA-induced cell death is a PCD subroutine because: (I) it is intensified or attenuated by genetic manipulations that eliminate only certain proteins involved in maintaining functional mitochondria, metabolizing lipids or macroautophagically degrading cellular constituents; and (II) it represents a cascade of consecutive cellular events that are initiated in response to POA and follow each other in a certain order. We call this previously unknown PCD subroutine “liponecrosis”. Based on our findings, we propose a model for molecular mechanisms

underlying liponecrosis. Our data suggest that liponecrosis represents a cell death module dynamically integrated into a so-called PCD network; this network also includes the apoptotic, necrotic and autophagic modules of PCD.

5.3 Materials and Methods

Yeast strains, media and growth conditions

The wildtype strain *Saccharomyces cerevisiae* BY4742 (*MAT α his3 Δ 1 leu2 Δ 0 lys2 Δ 0 ura3 Δ 0*) as well as the single-gene-deletion mutant strains *atg1 Δ* (*MAT α his3 Δ 1 leu2 Δ 0 lys2 Δ 0 ura3 Δ 0 atg1 Δ ::kanMX4*), *atg32 Δ* (*MAT α his3 Δ 1 leu2 Δ 0 lys2 Δ 0 ura3 Δ 0 atg32 Δ ::kanMX4*), *are2 Δ* (*MAT α his3 Δ 1 leu2 Δ 0 lys2 Δ 0 ura3 Δ 0 are2 Δ ::kanMX4*), *cyc3 Δ* (*MAT α his3 Δ 1 leu2 Δ 0 lys2 Δ 0 ura3 Δ 0 cyc3 Δ ::kanMX4*), *dga1 Δ* (*MAT α his3 Δ 1 leu2 Δ 0 lys2 Δ 0 ura3 Δ 0 dga1 Δ ::kanMX4*) and *fox1 Δ* (*MAT α his3 Δ 1 leu2 Δ 0 lys2 Δ 0 ura3 Δ 0 fox1 Δ ::kanMX4*) in the BY4742 genetic background (all from Thermo Scientific/Open Biosystems) were grown in YP medium (1% yeast extract, 2% peptone; both from Fisher Scientific; #BP1422-2 and #BP1420-2, respectively) initially containing 0.2% glucose (#D16-10; Fisher Scientific) as carbon source. Cells were cultured at 30°C with rotational shaking at 200 rpm in Erlenmeyer flasks at a “flask volume/medium volume” ratio of 5:1.

Cell viability assay for monitoring the susceptibility of yeast to a mode of cell death induced by palmitoleic acid (POA)

A sample of cells was taken from a culture at days 1, 2 and 4 of culturing. A fraction of the sample was diluted in order to determine the total number of cells using a hemacytometer. 8×10^7 cells were harvested by centrifugation for 1 min at $21,000 \times g$ at room temperature and resuspended in 8 ml of YP medium containing 0.2% glucose as carbon source. Each cell suspension was divided into 8 equal aliquots. Three pairs of aliquots were supplemented with POA (#P9417; Sigma) from a 50 mM stock solution (in 10% chloroform, 45% hexane and 45% ethanol; #650498, #248878 and #34852, respectively; all from Sigma). The final concentration of POA was 0.05 mM, 0.1 mM or 0.15 mM for each pair of aliquots; in all these aliquots, the final concentrations of chloroform, hexane and ethanol were 0.03%, 0.135% and 0.135%, respectively. One pair of aliquots was supplemented only with chloroform, hexane and ethanol

added to the final concentrations of 0.03%, 0.135% and 0.135%, respectively. All aliquots were then incubated for 2 h at 30°C on a Labquake rotator (#400110; Thermolyne/Barnstead International) set for 360° rotation. Serial dilutions of cells were plated in duplicate onto plates containing YP medium with 2% glucose as carbon source. After 2 d of incubation at 30°C, the number of colony forming units (CFU) per plate was counted. The number of CFU was defined as the number of viable cells in a sample. For each aliquot of cells exposed to POA, the % of viable cells was calculated as follows: (number of viable cells per ml in the aliquot exposed to POA/number of viable cells per ml in the control aliquot that was not exposed to POA) × 100.

Cell viability assay for monitoring the susceptibility of yeast to a mode of cell death induced by hydrogen peroxide

A sample of cells was taken from a culture at days 1, 2 and 4 of culturing. A fraction of the sample was diluted in order to determine the total number of cells using a hemacytometer. 8×10^7 cells were harvested by centrifugation for 1 min at $21,000 \times g$ at room temperature and resuspended in 8 ml of YP medium containing 0.2% glucose as carbon source. Each cell suspension was divided into 8 equal aliquots. Three pairs of aliquots were supplemented with hydrogen peroxide (#H325-500; Fisher Scientific) to the final concentration of 0.5 mM, 1.5 mM or 2.5 mM for each pair. One pair of aliquots remained untreated. All aliquots were then incubated for 2 h at 30°C on a Labquake rotator (#400110; Thermolyne/Barnstead International) set for 360° rotation. Serial dilutions of cells were plated in duplicate onto plates containing YP medium with 2% glucose as carbon source. After 2 d of incubation at 30°C, the number of CFU per plate was counted. The number of CFU was defined as the number of viable cells in a sample. For each aliquot of cells exposed to hydrogen peroxide, the % of viable cells was calculated as follows: (number of viable cells per ml in the aliquot exposed to hydrogen peroxide/number of viable cells per ml in the control aliquot that was not exposed to hydrogen peroxide) × 100.

Miscellaneous procedures

BODIPY 493/503 (4,4-Difluoro-1,3,5,7,8-Pentamethyl-4-Bora-3a,4a-Diaza-s-Indacene; #D-3922; Life Technologies/Molecular Probes) staining for monitoring neutral lipids deposited in lipid droplets, DAPI (4',6-Diamidino-2-phenylindole dihydrochloride; #D-9542; Sigma)

staining for visualizing nuclei, Annexin V (#630109; Clontech Laboratories, Inc.) staining for visualizing externalized phosphatidylserine (PS), and propidium iodide (PI; #P3566; Life Technologies/Molecular Probes) staining for visualizing the extent of plasma membrane permeability for small molecules were performed according to established procedures^{117,118}. Fluorescence and electron microscopies followed by morphometric analyses of the resulting images were performed according to established procedures^{13,65}.

Statistical analysis

Statistical analysis was performed using Microsoft Excel's (2010) Analysis ToolPack-VBA. All data are presented as mean \pm SEM. The *p* values were calculated using an unpaired two-tailed *t* test.

5.4 Results

5.4.1 Macromitophagy protects yeast from a mode of cell death triggered by exogenous palmitoleic fatty acid (POA)

An exposure of wildtype (WT) yeast cells to exogenous POA has been demonstrated to induce cell death, thereby significantly reducing clonogenic survival of these cells in a POA concentration-dependent manner^{27,116}. Noteworthy, the *pex5Δ* mutation previously known for its ability to impair peroxisomal fatty acid oxidation¹¹⁹ has been recently demonstrated not only to greatly reduce mitochondrial functionality but also to enhance the susceptibility of yeast to a form of cell death elicited by a brief exposure to exogenous POA²⁷. This finding suggested that the maintenance of a healthy population of functional mitochondria might protect yeast from POA-induced cell death modality. Macromitophagy, a selective macroautophagic degradation of dysfunctional mitochondria, is known to sustain such healthy population of functional mitochondria in chronologically aging yeast cells⁶². We therefore sought to investigate the importance of macromitophagy in protecting yeast from a mode of cell death triggered by exogenous POA. To attain this objective, we used the single-gene-deletion mutant strain *atg32Δ*. Because this mutant strain lacks a mitochondrial receptor for macromitophagy, it is known to be impaired only in the mitophagy pathway but not in other pathways of selective or non-selective macroautophagy^{84,120}. We found that the *atg32Δ* mutation significantly reduces clonogenic

survival of yeast cells briefly exposed to various concentrations of POA (Figure 17A-C). This indicated that by removing dysfunctional mitochondria, macromitophagy is a longevity assurance process that protects yeast from a form of cell death triggered by this monounsaturated fatty acid. Of note, the susceptibility of both WT and *atg32Δ* cells to a death mode elicited by exogenous POA increased with the chronological age of these cells (Figure 17A-C). Because the degree to which this death mode reduces cell viability appears to progress with the chronological age of a yeast cell, we concluded that it is an age-related modality of cell death.

Noteworthy, it was demonstrated that the *atg32Δ* mutation also significantly reduced clonogenic survival of yeast cells following their short-term (for 2 h) exposure to various concentrations of exogenous hydrogen peroxide (Figure 17D-F). The susceptibility of WT cells to a death mode elicited by exogenous hydrogen peroxide decreased with the chronological age of these cells, whereas the opposite trend was seen for chronologically aging *atg32Δ* cells (Figure 17D-F). Hence, a selective macroautophagic degradation of dysfunctional mitochondria protects yeast from an age-related form of cell death triggered by exogenous hydrogen peroxide.

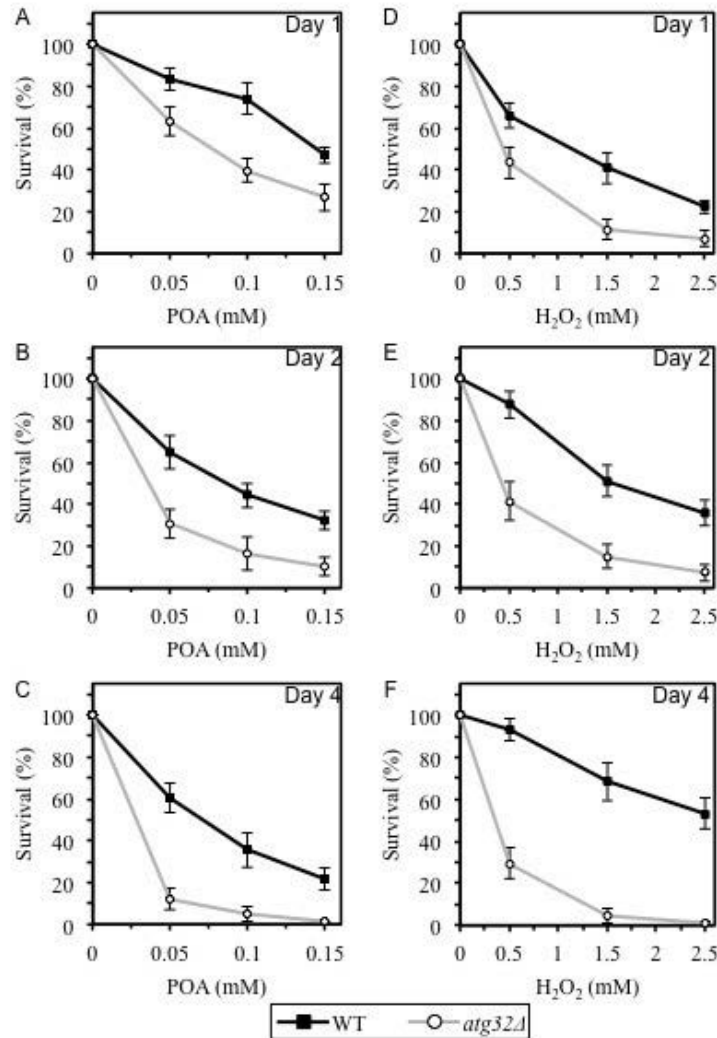


Figure 17 Deletion of Atg32p increases yeast susceptibility to cell death induced by palmitoleic acid (POA) and hydrogen peroxide. By removing dysfunctional mitochondria, macromitophagy protects yeast from age-related forms of cell death elicited by a short-term exposure to exogenous POA or hydrogen peroxide. WT and *atg32Δ* cells were recovered at days 1, 2 and 4 of culturing in a nutrient-rich YP medium initially containing 0.2% glucose as carbon source. Cell survival was assessed by measuring the clonogenicity of WT and *atg32Δ* cells after 2 h of treatment with various concentrations of exogenous POA (A-C) or hydrogen peroxide (D-F). Reproduced from ¹²¹.

5.4.2 POA induces “liponecrosis”, a mode of cell death that differs from apoptotic, regulated necrotic and autophagic cell death subroutines

To provide a mechanistic insight into the demonstrated essential role of macromitophagy in protecting yeast from a POA-induced mode of cell death, we used electron and fluorescence

microscopies (EM and FM, respectively) to examine WT and *atg32Δ* cells exposed to various concentration of this monounsaturated fatty acid. Our objectives were: (I) to define morphological traits characteristic of the cell death subroutine triggered by exogenous POA; and (II) to compare these traits to the well-established^{108–111,122} morphological features of the currently known apoptotic, regulated necrotic and autophagic cell death modalities.

We found that only minor fractions of WT and *atg32Δ* cells treated with various concentrations of POA exhibit such characteristic traits of a mitochondria-controlled mode of apoptotic cell death as nuclear fragmentation and phosphatidylserine (PS) translocation from the inner to the outer leaflet of the plasma membrane (Figure 18A, Figure 19A, Figure 20A,B). Thus, the mode of cell death elicited by the exposure of both WT and *an atg32Δ strain to exogenous POA* is not an apoptotic cell death subroutine.

Of note, significant portions of WT and *atg32Δ* cells exposed to exogenous hydrogen peroxide displayed fragmented nucleus and externalized PS (Figure 18B, Figure 20A, Figure 20A,B). Although the percentages of both WT and *atg32Δ* cells exhibiting these hallmarks of the apoptotic cell death subroutine following treatment with hydrogen peroxide were proportional to its concentration, the *atg32Δ* mutation significantly increased the fraction of such cells (Figure 18B, Figure 19A, Figure 20A,B). In sum, these microscopic analyses imply that (I) a short-term exposure of both WT and *atg32Δ* cells to exogenous hydrogen peroxide added at the concentrations ranging from 0.5 mM to 2.5 mM triggers an apoptotic form of cell death; and (II) macromitophagy protects yeast from this form of cell death.

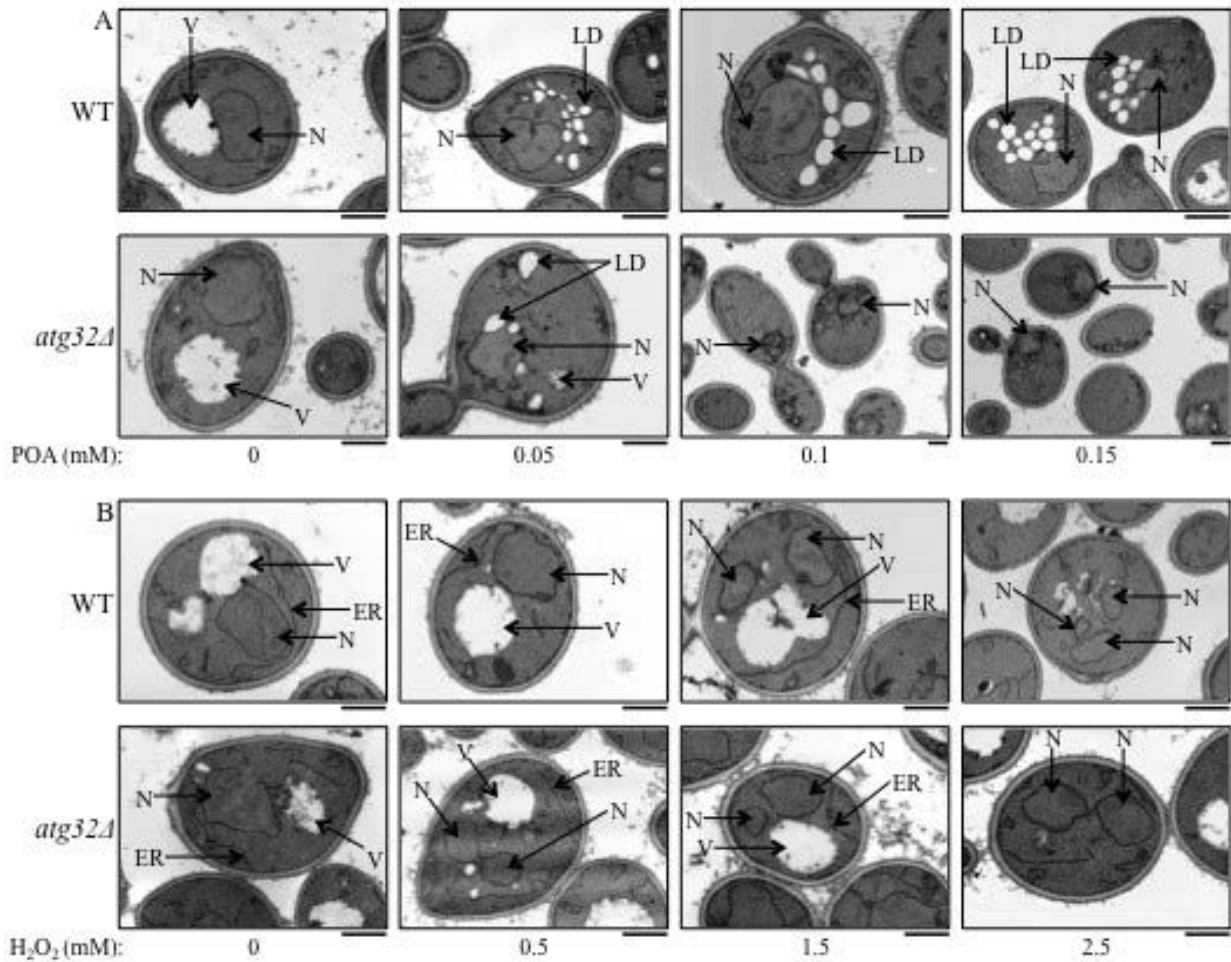


Figure 18 Morphological traits characteristic of the cell death subroutines triggered by a short-term exposure to exogenous POA or hydrogen peroxide. WT and *atg32Δ* cells were recovered at day 1 of culturing in a nutrient-rich YP medium initially containing 0.2% glucose as carbon source. Transmission electron micrographs of WT and *atg32Δ* cells after 2 h of treatment with various concentrations of exogenous POA (A) or hydrogen peroxide (B) are presented. Bar, 1 μ m. Abbreviations: ER, endoplasmic reticulum; LD, lipid droplet; N, nucleus; V, vacuole. Reproduced from ¹²¹.

Furthermore, our EM analysis revealed that WT and *atg32Δ* cells treated with various concentrations of POA do not exhibit rupture of the plasma membrane (Figure 18A, Figure 19B), a hallmark trait of a necrotic mode of PCD ^{109,123}. However, our FM analysis demonstrated that significant portions of WT and *atg32Δ* cells exposed to exogenous POA display propidium iodide (PI) positive staining (Figure 20C). This staining pattern is characteristic of a significantly increased permeability of the plasma membrane for PI and other small molecules, a hallmark trait of a necrotic mode of PCD ^{109,123}. Altogether, these EM and FM analyses demonstrate that a form of cell death triggered by an exposure of both WT and *atg32Δ* cells to exogenous POA is

not a typical necrotic cell death subroutine. Indeed: (I) unlike conventional necrotic cell death, this POA-induced form of cell death does not lead to plasma membrane rupture; but (II) akin to conventional necrotic cell death, this POA-induced form of cell death significantly increases plasma membrane permeability for PI and other small molecules.

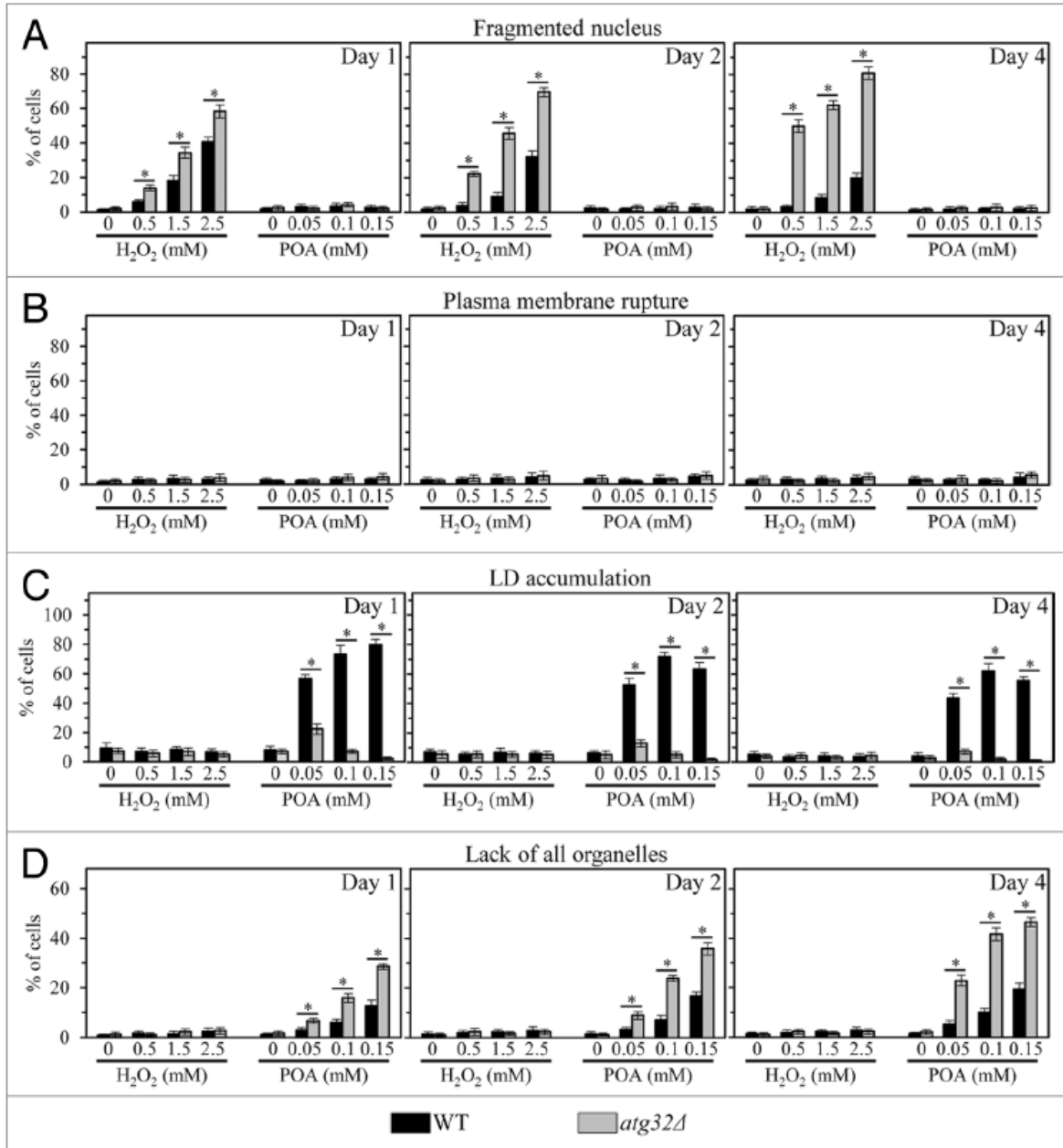


Figure 19 Percentage of WT and *atg32Δ* cells that display nuclear fragmentation (A), plasma membrane rupture (B), LD accumulation (C) or lack of all cellular organelles (D). WT and *atg32Δ* cells were recovered at days 1, 2 and 4 of culture in a nutrient-rich YP medium initially containing 0.2% glucose as carbon source. Transmission electron micrographs of WT and *atg32Δ* cells after 2 h of treatment with various concentrations of exogenous POA or

hydrogen peroxide were used for morphometric analysis; at least 100 cells of each strain were used for morphometric analysis at each time-point. Data are presented as means \pm SEM (n = 3; *p < 0.01). Reproduced from 121

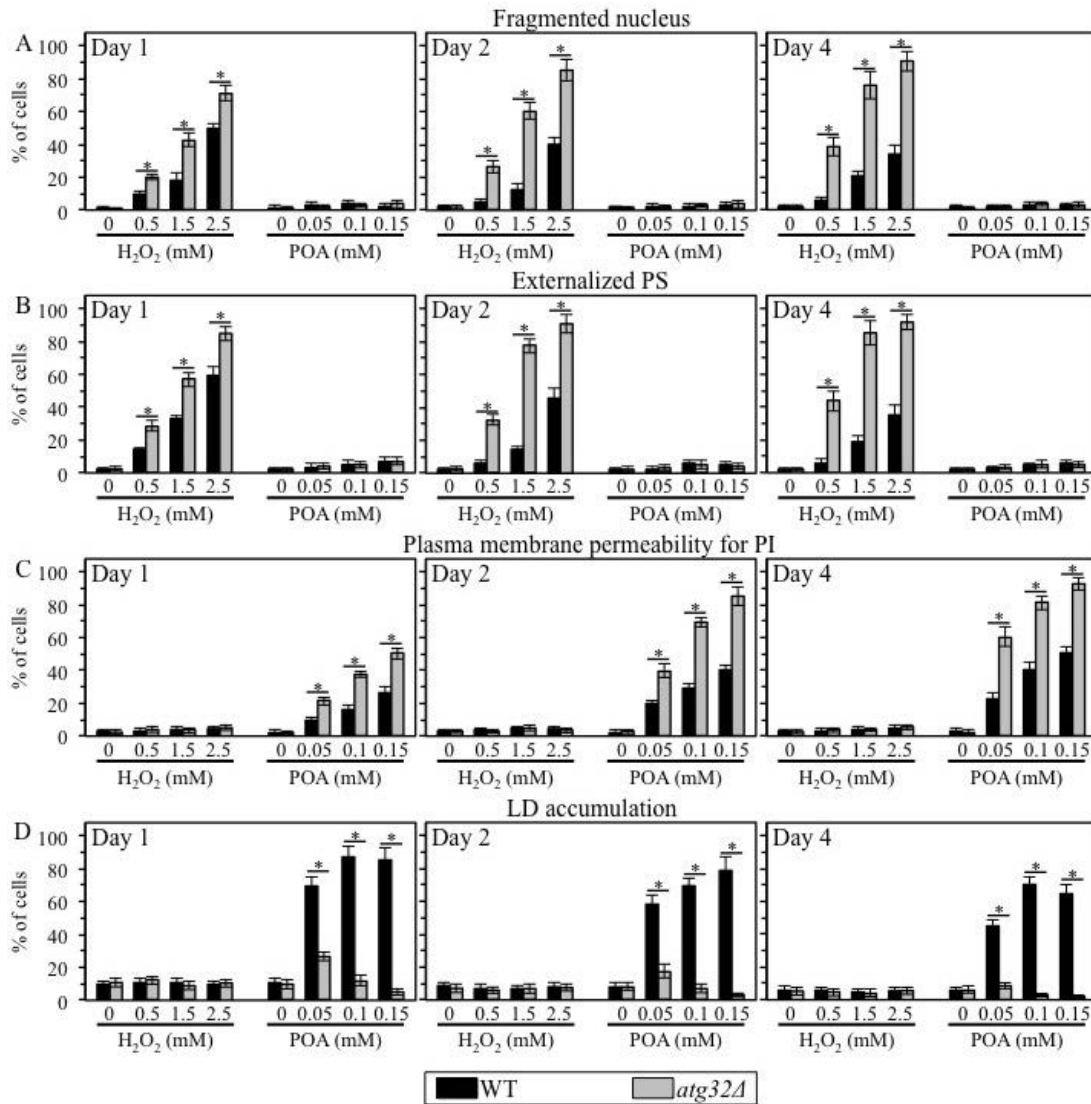


Figure 20 Percentage of WT and *atg32Δ* cells that display nuclear fragmentation (A), phosphatidylserine (PS) externalization (B), and propidium iodide (PI) positive staining (C) or LD accumulation (D). WT and *atg32Δ* cells were recovered at days 1, 2 and 4 of culturing in a nutrient-rich YP medium initially containing 0.2% glucose as carbon source. Fluorescence microscopy images of cells stained with DAPI (A), Annexin V (B), PI (C) or BODIPY 493/503 (D) were used for morphometric analysis; at least 800 cells of each strain were used for quantitation at each time-point. Data are presented as means \pm SEM (n = 3; *p < 0.01). Reproduced from ¹²¹.

Importantly, our EM and FM analyses uncovered that WT cells treated with various concentrations of POA exhibit an excessive accumulation of lipid droplets (LD) (Figure 18A,

Figure 19C and Figure 20D); LD are known to serve as a deposition site for stockpiling non-esterified (“free”) fatty acids and sterols in the forms of triacylglycerols (TAG) and ergosteryl esters (EE), the two major neutral lipids synthesized in the endoplasmic reticulum^{37,124}. This hallmark morphological feature of a POA-induced form of cell death has not been reported for any of the currently known apoptotic, regulated necrotic and autophagic cell death modalities^{108–111,122,125}. We therefore concluded that POA triggers a previously unknown form of cell death in yeast. We call this novel cell death modality “liponecrosis”.

5.4.3 Macromitophagy, functional mitochondria and neutral lipids synthesis protect yeast from liponecrotic cell death elicited by POA

It should be stressed that the *atg32Δ*-dependent mutational block of macromitophagy abolished the accumulation of LD in yeast cells committed to liponecrotic death triggered by cell exposure to POA (Figure 18A, Figure 19C and Figure 20D). Moreover, the *atg32Δ* mutation also significantly reduced clonogenic survival of yeast cells exposed to this monounsaturated fatty acid (Figure 17A, B, C). Based on these findings, we hypothesized that (I) the excessive accumulation of LD, a deposition site for stockpiling non-esterified fatty acids (including POA), protects yeast from a liponecrotic mode of cell death; (II) functional mitochondria are required for such accumulation of LD, likely because these organelles provide energy needed for a pro-survival process of depositing non-esterified fatty acids (including POA) within LD; and (III) macromitophagy protects yeast cells from liponecrotic death by sustaining a healthy population of functional mitochondria capable of providing energy for depositing non-esterified fatty acids (including POA) within LD. In support of this hypothesis, we found that the single-gene-deletion mutations *dga1Δ* and *are2Δ* reduce clonogenic survival of yeast cells committed to POA-induced liponecrotic death (Figure 21A, B); these two mutations are known to attenuate LD formation by eliminating redundant enzymes involved in the synthesis of TAG and EE (respectively), the two major neutral lipids synthesized in the ER¹²⁴. Furthermore, this hypothesis is also supported by our observation that the single-gene-deletion mutation *cyc3Δ* reduces clonogenic survival of yeast cells committed to liponecrotic death triggered by POA (Figure 21A, B); this mutation is known to abolish mitochondrial respiration by eliminating cytochrome *c* heme lyase and thereby impairing cytochrome *c* functionality¹²⁶.

In sum, these findings validate our hypothesis that macromitophagy protects yeast cells from liponecrosis by maintaining a healthy population of functional mitochondria capable of providing energy that is needed for a pro-survival process of depositing non-esterified fatty acids (including POA) within LD.

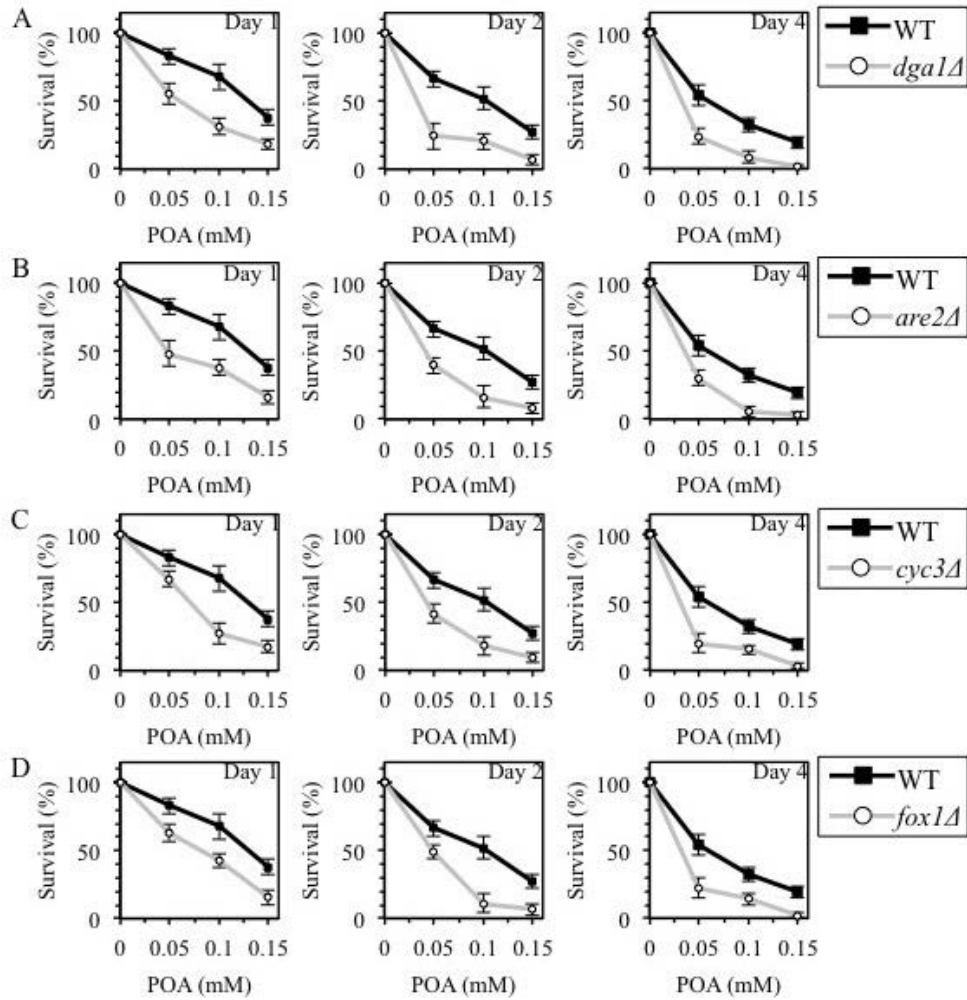


Figure 21 WT, *dga1Δ*, *are2Δ*, *cyc3Δ* and *fox1Δ* cells were recovered at days 1, 2 and 4 of culturing in a nutrient-rich YP medium initially containing 0.2% glucose as carbon source. Cell survival was assessed by measuring the clonogenicity of WT and mutant cells after 2 h of treatment with various concentrations of exogenous POA. Reproduced from ¹²¹.

5.4.4 Peroxisomal fatty acid oxidation protects yeast from liponecrotic cell death triggered by POA

We previously demonstrated that the single-gene-deletion mutation *pex5Δ* decreases clonogenic survival of yeast cells exposed to POA²⁷; this mutation is known to impair peroxisomal import of the first two enzymes of the fatty acid β -oxidation pathway¹¹⁹, thereby decelerating a conversion of immature (dysfunctional) peroxisomal precursors to mature (functional) peroxisomes¹²⁷. We therefore hypothesized that β -oxidation of non-esterified fatty acids (including POA) within functional peroxisomes may protect yeast from liponecrotic cell death by operating as a pro-survival process of reducing the cellular level of POA. In support of this hypothesis, we found that the single-gene-deletion mutation *fox1Δ* reduces clonogenic survival of yeast committed to POA-induced liponecrotic death (Figure 21D); this mutation is known to eliminate the first enzyme of the fatty acid β -oxidation pathway, thereby abolishing β -oxidation of non-esterified fatty acids (including POA) within functional peroxisomes¹¹⁹.

5.4.5 Non-selective macroautophagy executes liponecrotic cell death elicited by POA

Our EM analysis revealed that an exposure of WT cells to various concentrations of POA caused a POA concentration-dependent rise in the fraction of cells lacking all cellular organelles (Figure 18, Figure 19D). Importantly, we found that the *atg32Δ* mutation significantly increases the portion of such organelle-less cells that are committed to POA-induced liponecrotic death (Figure 18, Figure 19D). Of note, the percentages of WT and *atg32Δ* cells lacking all cellular organelles following an exposure to POA increased with the chronological age of these cells (Figure 18, Figure 19D). Based on these findings, we hypothesized that a non-selective *en masse* degradation of cellular organelles executes a liponecrotic form of cell death. This hypothesis is supported by our observation that the single-gene-deletion mutation *atg1Δ* increases clonogenic survival of yeast cells committed to liponecrotic death triggered by POA (Figure 22A-C). This mutation is known to abolish all pathways of non-selective and selective autophagic degradation of cellular organelles and macromolecules in yeast cells by eliminating a cytosolic serine/threonine protein kinase that governs these pathways¹²⁸. We therefore concluded that liponecrosis is an age-related form of PCD that is executed by a non-selective *en masse* autophagic degradation of cellular organelles and macromolecules in a process orchestrated by the cytosolic serine/threonine protein kinase Atg1p.

Of note, unlike the effect of *atg1Δ* on POA-elicited liponecrotic cell death, this mutation significantly reduced clonogenic survival of yeast cells following an exposure to various

concentrations of exogenous hydrogen peroxide (Figure 22D-F). This study demonstrated that a short-term exposure of yeast to exogenous hydrogen peroxide added at the concentrations ranging from 0.5 mM to 2.5 mM triggers an apoptotic form of cell death (see above). Thus, although a non-selective *en masse* autophagic degradation of cellular organelles and macromolecules executes an orchestrated by Atg1p form of POA-induced liponecrotic cell death, such degradation operates as a pro-survival process in yeast committed to apoptotic death that is triggered by cell exposure to exogenous hydrogen peroxide.

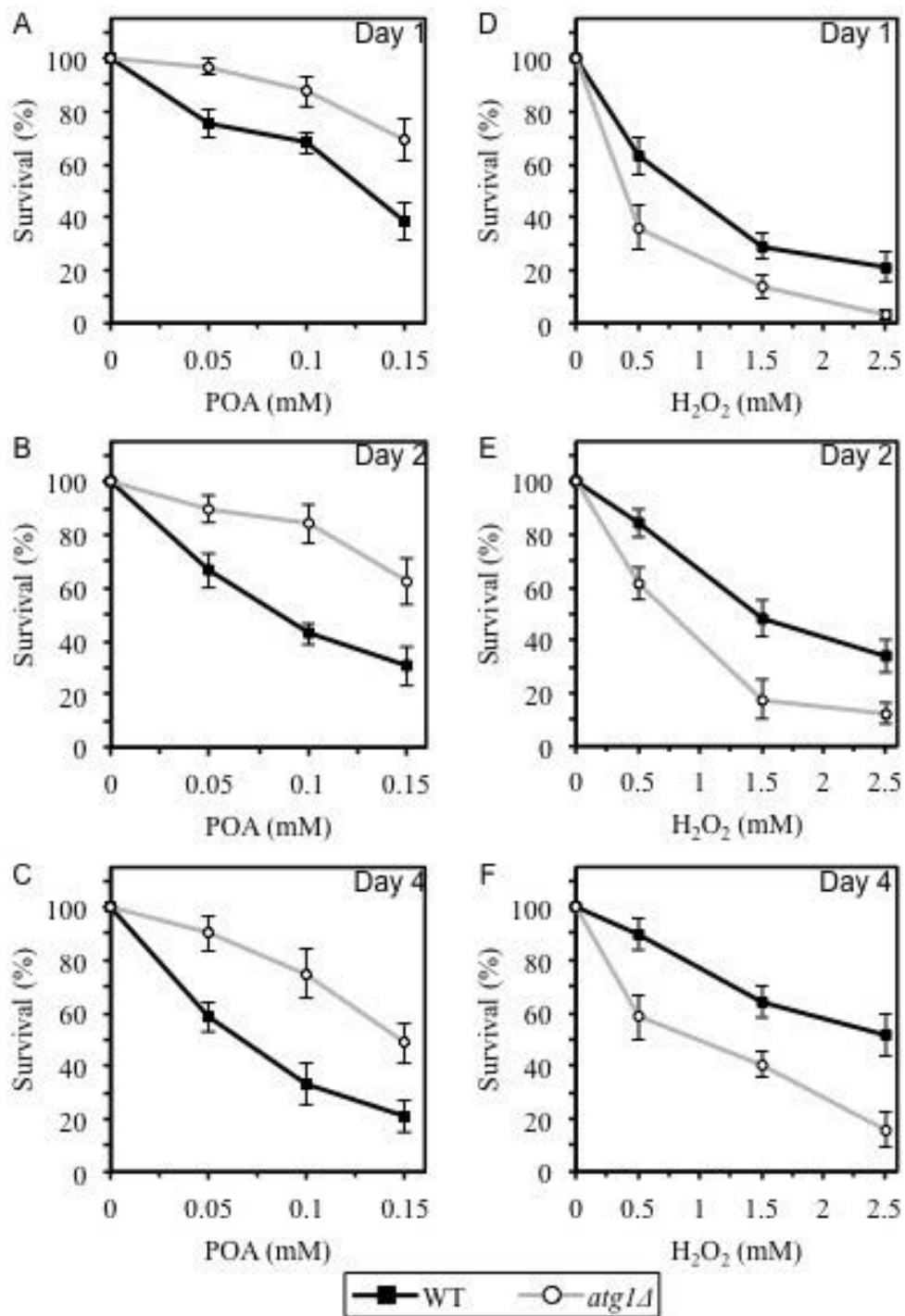


Figure 22 A non-selective en masse autophagic degradation of cellular organelles and macromolecules executes an orchestrated by Atg1p form of POA-induced liponecrotic cell death, whereas such degradation operates as a pro-survival process in yeast committed to apoptotic death that is triggered by cell exposure to exogenous hydrogen peroxide. WT and *atg1Δ* cells were recovered at days 1, 2 and 4 of culturing in a nutrient-rich YP medium initially containing 0.2% glucose as carbon source. Cell survival was assessed by measuring the clonogenicity of WT and

atg1Δ cells after 2 h of treatment with various concentrations of exogenous POA (A-C) or hydrogen peroxide (D-F).
Reproduced from ¹²¹.

5.5 Discussion

This study revealed a previously unknown form of cell death, which we call “liponecrosis”. Liponecrosis is initiated in response to a short-term exposure of yeast to exogenous POA, a monounsaturated fatty acid. We demonstrate that (I) mutations eliminating certain proteins involved in maintaining functional mitochondria, metabolizing lipids and macroautophagically degrading cellular constituents either enhance or attenuate liponecrosis; and (II) liponecrosis is a cascade of consecutive cellular events that are initiated in response to POA and follow each other in a certain order. Thus, akin to apoptotic, regulated necrotic and autophagic cell death modalities,^{108,110,111,123,125} liponecrosis is a programmed, regulated form of cell death rather than an accidental, unregulated cellular process. Moreover, liponecrosis is an age-related form of cell death. Indeed, we found that the degree to which it reduces cell viability progresses with the chronological age of a yeast cell.

Our conclusion that the liponecrotic cell death modality differs from the currently known apoptotic, regulated necrotic and autophagic cell death subroutines is based on the following findings. First, yeast cells committed to POA-induced liponecrotic death do not exhibit nuclear fragmentation and PS externalization; these two morphological features are known to be hallmarks of the apoptotic cell death subroutine¹¹¹. Second, yeast cells committed to POA-induced liponecrotic death do not display plasma membrane rupture, a morphological trait known to be characteristic of a necrotic cell death subroutine^{109,123}. However, it should be stressed that liponecrosis and regulated necrosis have at least one common feature, specifically a significantly increased permeability of the plasma membrane for PI^{109,123}. Our unpublished data suggest that the abnormally high permeability of the plasma membrane for PI and other small molecules in yeast cells committed to POA-induced liponecrotic death is likely due to (I) a specific remodeling of the plasma membrane lipidome; and (II) an excessive internalization of phosphatidylethanolamine caused by its translocation from the outer to the inner leaflet of the plasma membrane (Richard et al., in preparation). Third, yeast cells committed to POA-induced liponecrotic death do not exhibit excessive cytoplasmic vacuolization caused by the accumulation of autophagosomes; this morphological trait is known to be a hallmark of the

autophagic cell death subroutine^{108,110,123}. Interestingly, liponecrosis and autophagic cell death share at least two characteristic features, including (I) a non-selective *en masse* degradation of cellular organelles; and (II) a requirement for Atg1p, a cytosolic serine/threonine protein kinase that orchestrates both these subroutines of PCD^{108,110,123}. Fourth, yeast cells committed to POA-induced liponecrotic death exhibit an excessive accumulation of LD, a deposition site for stockpiling non-esterified fatty acids (including POA) in the form of neutral lipids. This characteristic morphological trait of the liponecrotic cell death subroutine has not been reported for any of the currently known apoptotic, regulated necrotic and autophagic cell death modalities^{108,110,111,123,125}.

A body of recent evidence supports the view that the individual pathways known to orchestrate the apoptotic, regulated necrotic and autophagic subroutines of cell death constitute modules that are dynamically integrated into a so-called PCD network^{115,129–135}. The concept of a PCD network provides a suitable explanation for the reported here and in several recent studies observations that (I) in response to some death triggers, in certain cell types and/or under specific circumstances a cell committed to a programmed death subroutine can exhibit a mix of morphological and biochemical traits that are characteristic of different currently known cell death modalities; and (II) several proteins can be actively involved in orchestrating more than one programmed death subroutine^{115,129–135}. From this it was hypothesized that liponecrosis is a previously unknown module dynamically integrated into the PCD network. In our hypothesis, the liponecrotic cell death module partially overlaps with three other modules comprising the network, namely the apoptotic, necrotic and autophagic modules of PCD.

5.6 Conclusions

Based on our findings, we propose the following model for molecular mechanisms underlying liponecrosis (Figure 23). This PCD subroutine is initiated in response to an excessive cellular stress that is created due to an incorporation of bulk quantities of POA into POA-containing phospholipids and the subsequent build-up of these POA-containing phospholipids in various cellular membranes. Our unpublished data support this hypothesis; as we found, excessive quantities of POA-containing phospholipids accumulate in both membranes of mitochondria as well as in the endoplasmic reticulum and the plasma membrane (see chapter 6). A non-selective *en masse* autophagic degradation of cellular organelles and macromolecules

executes the liponecrotic subroutine of PCD that is triggered by the extreme cellular stress caused by the excessive accumulation of POA-containing phospholipids in various cellular membranes (Figure 23). This autophagic execution of the liponecrotic cell death program is orchestrated by the cytosolic serine/threonine protein kinase Atg1p. Our model posits that several cellular processes play a pro-survival role in yeast exposed to POA by reducing the flow of POA into phospholipid synthesis pathways. These pro-survival processes protect yeast from liponecrosis by alleviating the excessive cellular stress caused by the build-up of POA-containing phospholipids in various cellular membranes. One of these pro-survival processes is an incorporation of POA into neutral lipids that are then deposited in LD (Figure 23). Indeed, we found that liponecrosis can be enhanced by genetic manipulations that impair neutral lipids synthesis and, thus, attenuate LD formation. Our model envisions that mitochondria provide energy driving the pro-survival process of depositing non-esterified fatty acids (including POA) within LD in the form of neutral lipids (Figure 23). This assumption is based on our findings that liponecrosis can be enhanced by genetic manipulations that abolish mitochondrial respiration by impairing cytochrome *c* functionality or impede a selective macroautophagic degradation of dysfunctional mitochondria. In our model, β -oxidation of non-esterified (“free”) fatty acids (including POA) within functional peroxisomes also plays a pro-survival role in yeast exposed to POA (Figure 23). By reducing the flow of POA into phospholipid synthesis pathways, this pro-survival process contributes to the alleviation of the excessive cellular stress that is elicited by the build-up of POA-containing phospholipids in various cellular membranes. Indeed, we found that liponecrosis can be enhanced by genetic manipulations that impair peroxisomal import of the first two enzymes of the fatty acid β -oxidation pathway or eliminate the first enzyme of this pathway normally confined to mature, functional peroxisomes.

Based on a unique combination of morphological traits characteristic of liponecrosis, this PCD modality differs from (I) a mitochondria-dependent necrotic cell death subroutine initiated in response to an exposure of the yeast *S. cerevisiae* to exogenous polyunsaturated fatty acids¹¹²; and (II) a mitochondria-dependent, metacaspase-independent cell death subroutine exhibiting morphological features of both apoptosis and necrosis following an exposure of the yeast *S. cerevisiae* to exogenous membrane-permeable C2-ceramide¹³⁶. Moreover, unlike cells of the yeast *S. cerevisiae* committed to liponecrosis, cells of the fission yeast *Schizosaccharomyces pombe* mutant strain deficient in TAG synthesis undergo a lipoapoptotic form of death upon

entry into stationary phase; these cells display hallmarks of an apoptotic cell death subroutine, including chromatin condensation, nuclear DNA fragmentation, PS externalization and reactive oxygen species accumulation ^{46,137}.

In the future, it would be important to identify other cellular processes that play essential pro-death or pro-survival roles in the liponecrotic cell death subroutine. These cellular processes may include (I) phospholipid synthesis in the endoplasmic reticulum and mitochondrial membranes and a bidirectional phospholipid exchange between them through membrane contact sites; (II) a transfer of phospholipids from the endoplasmic reticulum to the plasma membrane via membrane contact sites; (III) a maintenance of the non-random distribution of several phospholipid species within a bilayer of the plasma membrane; (IV) cellular signal transduction modulated by alterations in plasma membrane phospholipid asymmetry; and (V) cellular protein homeostasis. Another challenge for the future will be to explore mechanisms underlying the predicted here integration of the liponecrotic cell death module into the PCD network known to include the apoptotic, necrotic and autophagic modules of PCD.

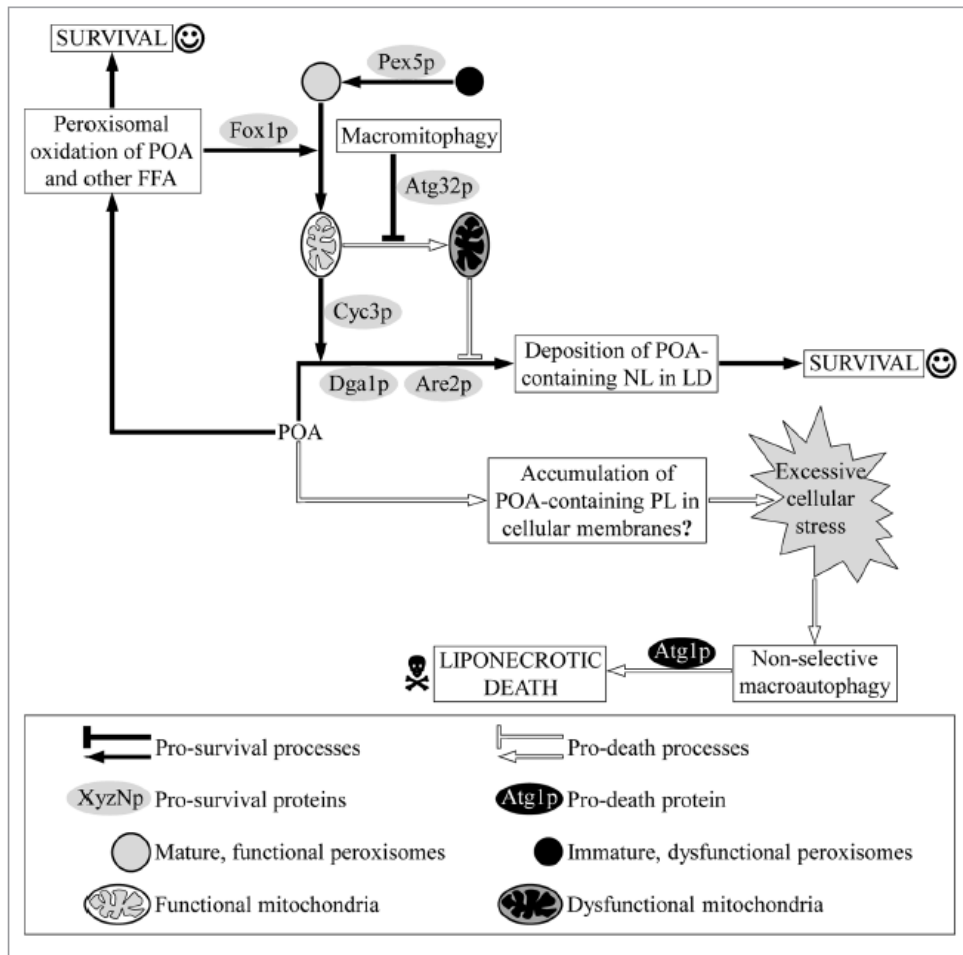


Figure 23 A model for molecular mechanisms underlying programmed liponecrotic cell death elicited by POA. An incorporation of POA into POA-containing phospholipids (PL) and their consequent accumulation in various cellular membranes may operate as pro-death processes that create excessive cellular stress, thereby triggering liponecrosis. This subroutine of PCD is executed by a non-selective en masse autophagic degradation of cellular organelles and macromolecules in a process orchestrated by the cytosolic serine/threonine protein kinase Atg1p. Alternatively, in a pro-survival process POA can be incorporated into neutral lipids (neutral lipids) that are then deposited in lipid droplets (LD). Macromitophagy protects yeast cells from liponecrosis by maintaining a healthy population of functional mitochondria capable of providing energy that is needed for a pro-survival process of depositing non-esterified fatty acids (including POA) within LD. Moreover, in a pro-survival process POA can be oxidized in peroxisomes. β -oxidation of non-esterified (“free”) fatty acids (FFA; including POA) within functional peroxisomes protects yeast from liponecrotic cell death by operating as a pro-survival process of reducing the cellular level of POA. Reproduced from ¹²¹.

6. Mechanism of liponecrosis, a distinct mode of programmed cell death

6.1 Introduction

We recently identified a form of PCD that differs from the currently known PCD subroutines, such as apoptosis, autophagic cell death and necrosis. We named this PCD subroutine “liponecrosis” since it can be instigated by a short-term exposure of yeast to exogenous palmitoleic acid (POA) ¹³⁸. The cell death modality in this case meets all of the criteria established for defining a PCD subroutine ^{34,108}. Specifically we discovered that liponecrotic PCD is a genetically programmed, regulated cellular process that can be modulated by genetic manipulations impairing functionality of only certain proteins. These proteins are important for enabling the maintenance of functional mitochondria, metabolism of certain molecular forms of lipids or autophagic degradation of some cellular constituents. The PCD modality induced by POA treatment also operates as a series of consecutive cellular processes that are triggered by POA and that follow each other in a certain order; and is likely to provide some benefits for the development and/or survival of a population of yeast cells because it represents an age-related mode of PCD - *i.e.*, the degree to which it reduces cell viability following an exposure to POA appears to progress with the chronological age of a yeast cell ¹³⁸. Additionally, yeast cells committed to liponecrotic PCD do not exhibit a combination of morphological traits and biochemical features characteristic of cells committed to any of the presently known apoptotic, autophagic or necrotic subroutines of PCD ¹³⁸. Moreover, yeast cells committed to liponecrotic PCD display an excessive accumulation of lipid droplets where non-esterified fatty acids are deposited in the form of neutral lipids; this hallmark feature of liponecrotic PCD has not been reported for any of the currently known PCD modalities ¹³⁸. Collectively, these findings imply that liponecrosis is a mode of PCD which differs from the currently known ones.

The data presented in this chapter reflect our attempts to establish a comprehensive model outlining how yeast cells commit to, and ultimately execute this particular cell death modality. To do this, we investigated how the commitment of yeast to POA-induced liponecrotic PCD alters lipid compositions of various cellular membranes, impacts the asymmetrical distribution of phospholipids across the plasma membrane bilayer, modulates a lipid-asymmetry-responsive signaling pathway, changes the extent of oxidative damage to cellular proteins and

lipids, affects the active maintenance of cellular protein homeostasis, and remodels various pathways for selective and non-selective autophagic degradation of “stressed”, damaged and dysfunctional organelles. Based on our findings, we propose a molecular mechanism underlying liponecrotic PCD subroutine.

6.2 Materials and Methods

Yeast strains and growth conditions

The WT strain BY4742 (*MAT α his3 Δ 1 leu2 Δ 0 lys2 Δ 0 ura3 Δ 0*) and single-gene-deletion mutant strains in the BY4742 genetic background (all from Thermo Scientific/Open Biosystems) were grown in YP medium (1% yeast extract, 2% peptone) initially containing 0.2% glucose as carbon source. Cells were cultured at 30°C with rotational shaking at 200 rpm in Erlenmeyer flasks at a “flask volume/medium volume” ratio of 5:1.

Cell viability assay for monitoring the susceptibility of yeast to liponecrotic PCD

A sample of cells was taken from a culture at days 1, 2 and 4 of culturing after one day of pre-culture in the same growth medium. A fraction of the sample was diluted in order to determine the total number of cells using a hemacytometer. 8×10^7 cells were harvested by centrifugation for 1 min at $21,000 \times g$ at room temperature and resuspended in 8 ml of YP medium containing 0.2% glucose as carbon source. Each cell suspension was divided into 8 equal aliquots. Three pairs of aliquots were supplemented with POA from a 50 mM stock solution (in 10% chloroform, 45% hexane and 45% ethanol). The final concentration of POA was 0.05 mM, 0.1 mM or 0.15 mM for each pair of aliquots; in all these aliquots, the final concentrations of chloroform, hexane and ethanol were 0.03%, 0.135% and 0.135%, respectively. One pair of aliquots was supplemented only with chloroform, hexane and ethanol added to the final concentrations of 0.03%, 0.135% and 0.135%, respectively. All aliquots were then incubated for 2 h at 30°C on a Labquake rotator set for 360° rotation. Serial dilutions of cells were plated in duplicate onto plates containing YP medium with 2% glucose as carbon source. After 2 d of incubation at 30°C, the number of colony forming units (CFU) per plate was counted. The number of CFU was defined as the number of viable cells in a sample. For each aliquot of cells exposed to POA, the % of viable cells was calculated as follows: (number of viable cells per ml

in the aliquot exposed to POA/number of viable cells per ml in the control aliquot that was not exposed to POA) $\times 100$.

Miscellaneous procedures

Mass spectrometry based lipidomics was carried out as described previously¹³⁹ and described in detail in appendix A.3. Measurement of changes in the pH of culture medium was carried out according to established methods¹³. Measurement of PE level in the extracellular leaflet of the PM was conducted by using a cinnamycin based assay described by Ikeda et al.¹⁴⁰. Immunodetection of carbonyl groups of oxidatively damaged cellular proteins was carried out using the OxyBlot assay kit (Millipore Corp.)¹⁴¹. Oxidatively damaged lipids were measured using the Lipid Hydroperoxide (LPO) assay kit (Cayman)¹³⁹. SDS-PAGE¹⁴² was performed as previously described.

Statistical analysis

Statistical analysis was performed using Microsoft Excel's (2010) Analysis ToolPack-VBA. All data are presented as mean \pm SEM. The *p* values were calculated using an unpaired two-tailed *t* test.

6.3 Result

6.3.1 The extent of POA incorporation into neutral lipids and phospholipids defines the susceptibility of yeast to liponecrotic PCD

We recently proposed a hypothesis for a mechanism that underlies liponecrotic PCD elicited by an exposure of yeast to exogenous POA¹³⁸. The hypothesis stipulated that (I) exogenous POA can be incorporated into membrane phospholipids that accumulate within various organellar membranes as well as into neutral lipids (neutral lipids) that amass in lipid droplets (LD); (II) exogenous POA can also be oxidized within peroxisomes; (III) an excessive accumulation of POA-containing phospholipids within various cellular membranes is a pro-death process which triggers liponecrotic PCD; (IV) both POA incorporation into neutral lipids and POA oxidation within peroxisomes are pro-survival processes since they prevent the buildup of POA-containing phospholipids within cellular membranes; and (V) mitophagy, an Atg32p-driven selective macroautophagic degradation of dysfunctional mitochondria^{120,143}, is a pro-

survival process which sustains a population of functional mitochondria needed for POA incorporation into neutral lipids and subsequent deposition of neutral lipids within LD¹³⁸.

To assess the validity of this hypothesis, mass spectrometry was used to compare the lipidomes of wildtype (WT) and mitophagy-deficient *atg32Δ* cells that were exposed to various concentrations of POA. It was observed that an exposure of WT cells to POA (0.05 mM) induced a dramatic shift in the relative proportions of neutral to polar phospholipids. Specifically, it was observed that POA treatment (0.05 mM) induced an increase in the relative proportion of TAG species, a major form of neutral lipids that are synthesized in the endoplasmic reticulum (ER) and then deposited within LD (Figure 24). Of interest, when WT cells were exposed to higher concentrations of POA (0.1 mM to 0.15 mM) the relative proportion of phospholipids to TAG was increased (Figure 24). Unsurprisingly, the major portion of molecular species of TAG and also phospholipids undergoing such characteristic changes in their levels following an exposure of WT cells to various concentrations of POA were their palmitoleic acid containing (C16:1) species (Figure 24, Figure 25). Of note, this effect was observed for all major forms of phospholipids, such as phosphatidic acid (PA), phosphatidylserine (PS), phosphatidylethanolamine (PE), phosphatidylcholine (PC), phosphatidylinositol (PI) and cardiolipin (CL) (Figure 26, Figure 27). Some of these phospholipids forms (such as PA, PS, PC and PI) are known to be synthesized exclusively in the ER and to be then transported to mitochondria via mitochondria-ER junctions and to the plasma membrane (PM) via PM-ER junctions^{47,67,78,94,96,139,144–146} (Figure 28). Other forms of phospholipid (such as PE and CL) have been shown to be formed only in the inner membrane of mitochondria; PE is then transported from mitochondria to the ER via mitochondria-ER junctions and from the ER to the PM via PM-ER junctions^{67,78,94,96,144–146} (Figure 28).

Using mass spectrometry together with clonogenic survival assays, it was demonstrated that the concentration of exogenous POA added to WT cells is inversely related to the accumulation of TAG species within these cells, and that the relative level of phospholipids containing POA increases (Figure 26, Figure 27). This trend also correlated with the susceptibility of these cells to liponecrosis¹²¹ (Figure 29). Taken together, the quantitative mass spectrometric and clonogenic survival analyses of WT cells treated with various concentrations of POA support the following key aspects of our hypothesis: (I) exogenous POA can be incorporated into phospholipids that accumulate within various cellular membranes, including

the ER, mitochondrial membranes and the PM (Figure 28); (II) exogenous POA can also be incorporated into TAG, a major form of neutral lipids that are synthesized in the ER and then deposited within LD (Figure 28); (III) an excessive accumulation of POA-containing phospholipids in the ER, mitochondrial membranes and the PM is a pro-death process which commits yeast to liponecrotic PCD; and (IV) an incorporation of POA into neutral lipids deposited within LD is a pro-survival process which protects yeast from liponecrotic PCD.

To assess the role of mitophagy in mitigating liponecrotic cell death, the same type of analyses were conducted using the *atg32Δ* mutant. In these analyses it was observed that inhibition of mitophagy (I) substantially reduced the extent to which an exposure to POA increases the cellular levels of all molecular species of TAG (Figure 25, Figure 24); and (II) significantly elevates the degree to which such an exposure increases the cellular levels of all molecular species of various forms of phospholipids - including POA containing species (Figure 26, Figure 27). As mentioned in the previous chapter, the *atg32Δ* mutation substantially increases the susceptibility of yeast to POA-induced liponecrotic PCD¹³⁸. In sum, these findings support a key aspect of our hypothesis on the essential pro-survival role of Atg32p-driven mitophagy in protecting yeast from the liponecrotic mode of PCD. Our mass spectrometry based lipidomic analysis of yeast treated with various concentrations of POA suggests that mitophagy acts as a pro-longevity process through its ability to sustain a population of functional mitochondria. These functional mitochondria are required for POA incorporation into neutral lipids (Figure 25, Figure 24), a process that prevents the buildup of POA-containing phospholipids within various cellular membranes (Figure 26, Figure 27) - likely by reducing the flow of POA into pathways for phospholipids synthesis and interorganellar transport^{78,124,147} (Figure 28).

The hypothesis was further validated by examining how various single-gene-deletion mutations (each eliminating an enzyme involved in POA transport to the ER or in POA incorporation into phospholipids and/or neutral lipids within the ER) influence the susceptibility of yeast to POA-induced liponecrotic PCD. Importantly, all these enzymes are redundant and none of them is an essential protein in yeast^{78,124}. Thus, although none of these single-gene-deletion mutations completely abolishes the incorporation of POA into phospholipids and/or neutral lipids, each of them causes significant changes in the cellular levels of phospholipids and/or neutral lipids^{78,124}. Deletion of *Fat1p* results in loss of a fatty acyl-CoA synthetase and

fatty acid transporter that activates imported fatty acids for use in the biosynthesis phosphatidic acid – a central metabolite in lipid metabolism⁷⁸. This mutant showed a reduction in susceptibility to POA-induced liponecrotic PCD (Figure 29). Deletion of *Fat1p* decreases the cellular uptake of POA and, thus, mitigates the incorporation of POA into both phospholipids and neutral lipids¹⁴⁸ (Figure 28). Furthermore, the *gpt2Δ*, *ayr1Δ* and *ale1Δ* mutations make yeast less susceptible to POA-induced liponecrotic PCD (Figure 29B-D); all these mutations attenuate POA incorporation into phospholipids^{78,124} (Figure 28). Moreover, the *dga1Δ* and *lro1Δ* mutations increase the susceptibility of yeast to POA-induced liponecrotic PCD (Figure 29 E, F); both these mutations have been shown to decrease the incorporation of POA into TAG, a major form of neutral lipids^{78,124} (Figure 28). In addition, it was recently demonstrated that the *are2Δ* mutation makes yeast more susceptible to POA-induced liponecrotic PCD¹²¹. This mutation is known to mitigate POA incorporation into ergosteryl esters, a form of neutral lipids^{78,124}.

Altogether, the data of our analysis of how various single-gene-deletion mutations having the opposite effects on the extent of POA incorporation into phospholipids and neutral lipids impact the susceptibility of yeast to POA-induced liponecrotic PCD strongly support the proposed hypothesis that: (I) an excessive accumulation of POA-containing phospholipids in the ER (and then in mitochondrial membranes and in the PM) is a pro-death process which commits yeast to liponecrotic PCD; and (II) an incorporation of POA into neutral lipids deposited within LD is a pro-survival process which protects yeast from liponecrotic PCD - likely because it prevents the buildup of POA-containing phospholipids within various cellular membranes by attenuating the flow of POA into pathways for phospholipid biosynthesis and interorganellar transport.

Noteworthy, it was found that the extent to which exogenous POA alters the cellular levels of neutral lipids and phospholipids in WT and *atg32Δ* cells increases with the chronological age of these cells (Figure 25, Figure 26, Figure 24, Figure 27). Moreover, these findings imply that the degree to which the liponecrotic mode of PCD reduces cell viability appears to progress with the chronological age of WT and each of the single-gene-deletion mutant strains tested (Figure 29). Collectively, the data further support the notion that liponecrosis is an age-related modality of PCD¹²¹.

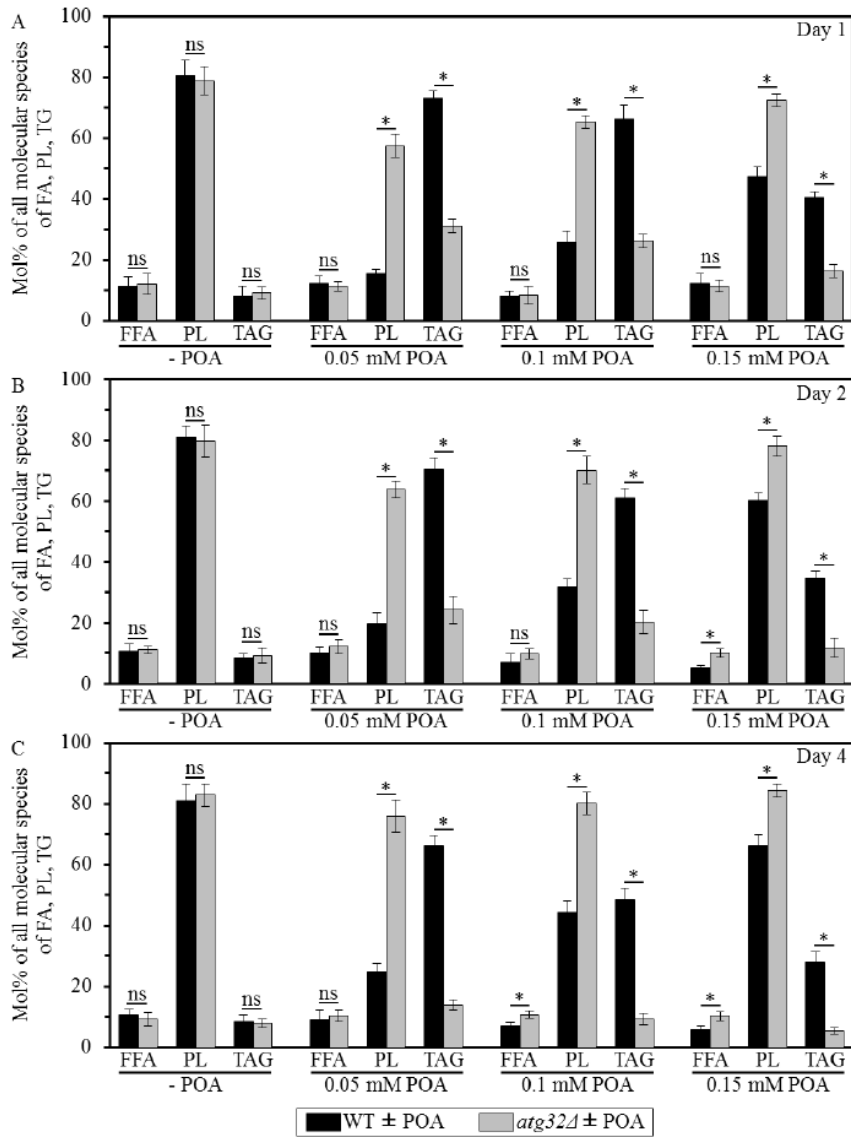


Figure 24 - An exposure of WT cells to various concentrations of exogenous POA elicits differential age-dependent effects on the relative levels of all molecular species of phospholipids and TAG, and the *atg32Δ*-dependent mutational block of mitophagy alters these effects. WT and *atg32Δ* cells were recovered at days 1, 2 and 4 of culturing in nutrient-rich YP medium initially containing 0.2% glucose as carbon source. Extraction of cellular lipids, and mass spectrometric identification and quantitation of various molecular species of non-esterified (“free”) fatty acids (FFA), phospholipids (PL) and triacylglycerols (TAG) were carried out as described in Materials and Methods. The relative level of all molecular species for each lipid form (i.e., FFA, phospholipids and TAG) was calculated as molar percentage of all these lipid forms. Data are presented as means \pm SEM ($n = 3$; $*p < 0.01$; ns, not significant).

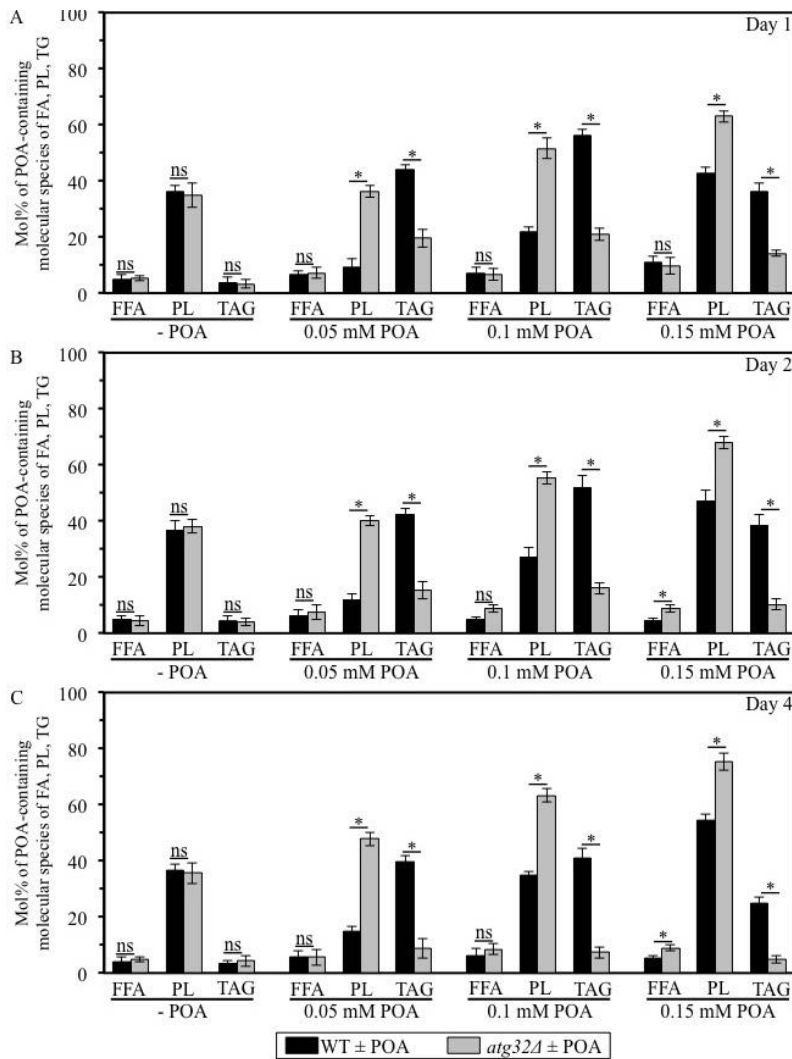


Figure 25 - An exposure of WT cells to various concentrations of exogenous POA elicits differential age-dependent effects on the relative levels of C16:1 molecular species (i.e., POA-containing species) of phospholipids and TAG, and the *atg32Δ*-dependent mutational block of mitophagy alters these effects. WT and *atg32Δ* cells were recovered at days 1, 2 and 4 of culturing in nutrient-rich YP medium initially containing 0.2% glucose as carbon source. The relative level of POA-containing molecular species for each lipid form (i.e., FFA, phospholipids and TAG) was calculated as molar percentage of all these lipid forms. Data are presented as means \pm SEM ($n = 3$; $*p < 0.01$; ns, not significant). For FFA, POA-containing molecular species are their POA-containing species. For the PA, PS, PE, PC and PI forms of PL, POA-containing molecular species are the C32:1, C32:2, C34:1 and C34:2 species of each of them. POA-containing cardiolipin species are its C64:4, C66:4, C68:4, C70:4 species. For TAG, POA-containing molecular species are their C48:2, C48:3, C50:2, C50:3, C52:2, C52:3 species.

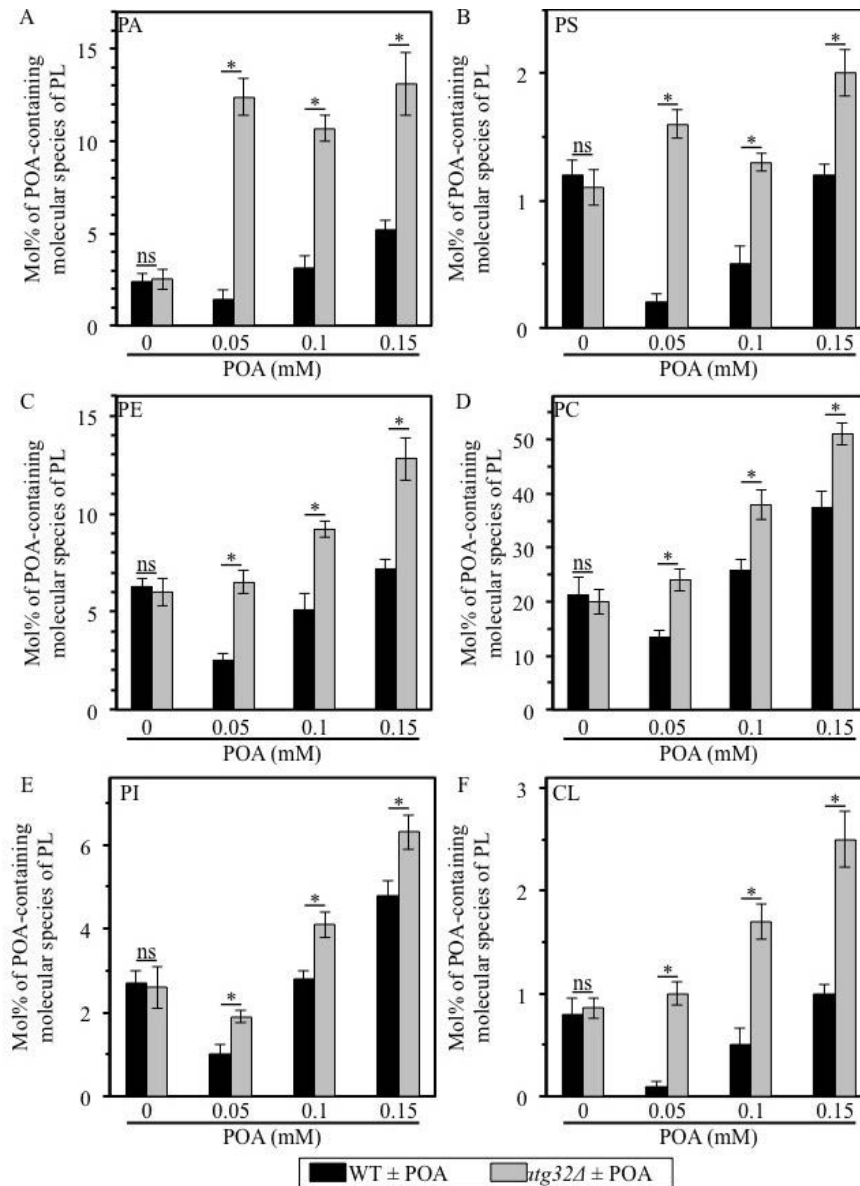


Figure 26 - An exposure of WT cells to various concentrations of exogenous POA elicits differential age-dependent effects on the levels of C16:1 molecular species (i.e., POA-containing species) of all major forms of phospholipids, and the *atg32Δ*-dependent mutational block of mitophagy alters these effects. WT and *atg32Δ* cells were recovered at days 1, 2 and 4 of culturing in nutrient-rich YP medium initially containing 0.2% glucose as carbon source. The relative level of POA-containing molecular species for each form of phospholipids (i.e., PA, PS, PE, PC, PI and CL) was calculated as molar percentage of all these phospholipids forms. Data are presented as means \pm SEM ($n = 3$; $*p < 0.01$; ns, not significant). For PA, PS, PE, PC and PI, POA-containing molecular species are the C32:1, C32:2, C34:1 and C34:2 species of each of them. For the CL form of PL, POA-containing molecular species are its C64:4, C66:4, C68:4, C70:4 species.

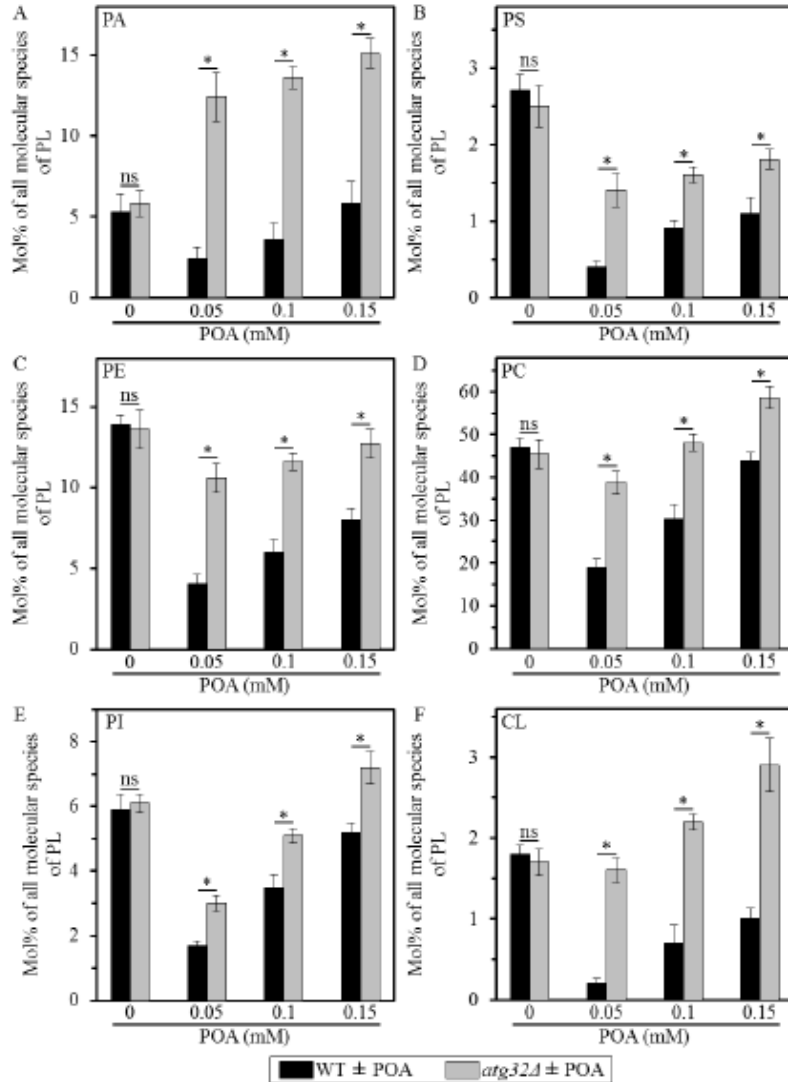


Figure 27 An exposure of WT cells to various concentrations of exogenous POA elicits differential age-dependent effects on the relative levels of all molecular species of all major forms of phospholipids, and the *atg32Δ*-dependent mutational block of mitophagy alters these effects. WT and *atg32Δ* cells were recovered at days 1, 2 and 4 of culturing in nutrient-rich YP medium initially containing 0.2% glucose as carbon source. The relative level of all molecular species for each form of phospholipids (i.e., PA, PS, PE, PC, PI and CL) was calculated as molar percentage of all these phospholipids forms. Data are presented as means \pm SEM (n = 3; *p < 0.01).

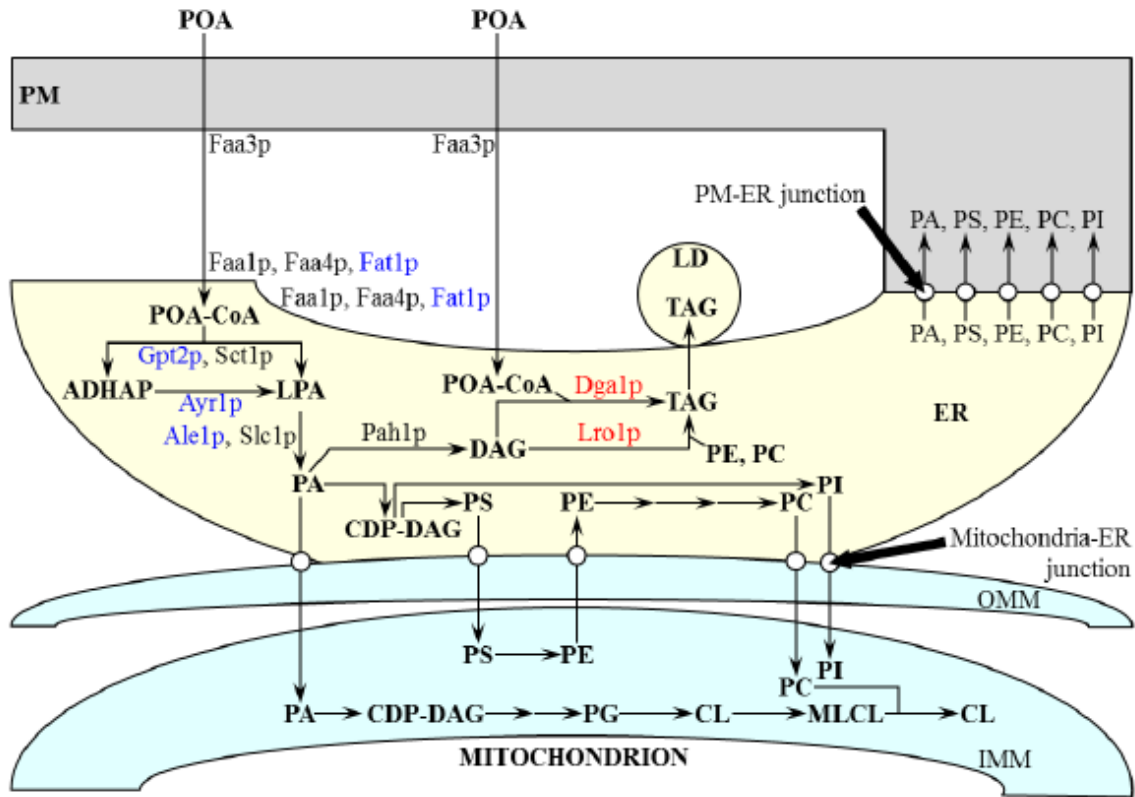


Figure 28 Outline of the flow of exogenous POA into pathways for phospholipids synthesis in the ER and mitochondria, phospholipid transport via mitochondria-ER and PM-ER junctions, TAG synthesis in the ER, and TAG deposition within LD. Following cellular uptake of POA, it is incorporated into various phospholipids. Some of these forms (such as PA, PS, PC and PI) are synthesized exclusively in the ER; these are then transported to mitochondria via mitochondria-ER junctions and to the PM via PM-ER junctions. Other forms of phospholipids (such as PE and CL) are formed only in the inner membrane of mitochondria; PE is then transported from mitochondria to the ER via mitochondria-ER junctions and from the ER to the PM via PM-ER junctions. In the ER, POA is also incorporated into TAG (as shown) and ergosteryl esters; these two forms of neutral lipids are then deposited within LD. The names of proteins that when deleted cause a decrease or increase of the susceptibility to POA-induced liponecrotic PCD are displayed in blue or red color, respectively.

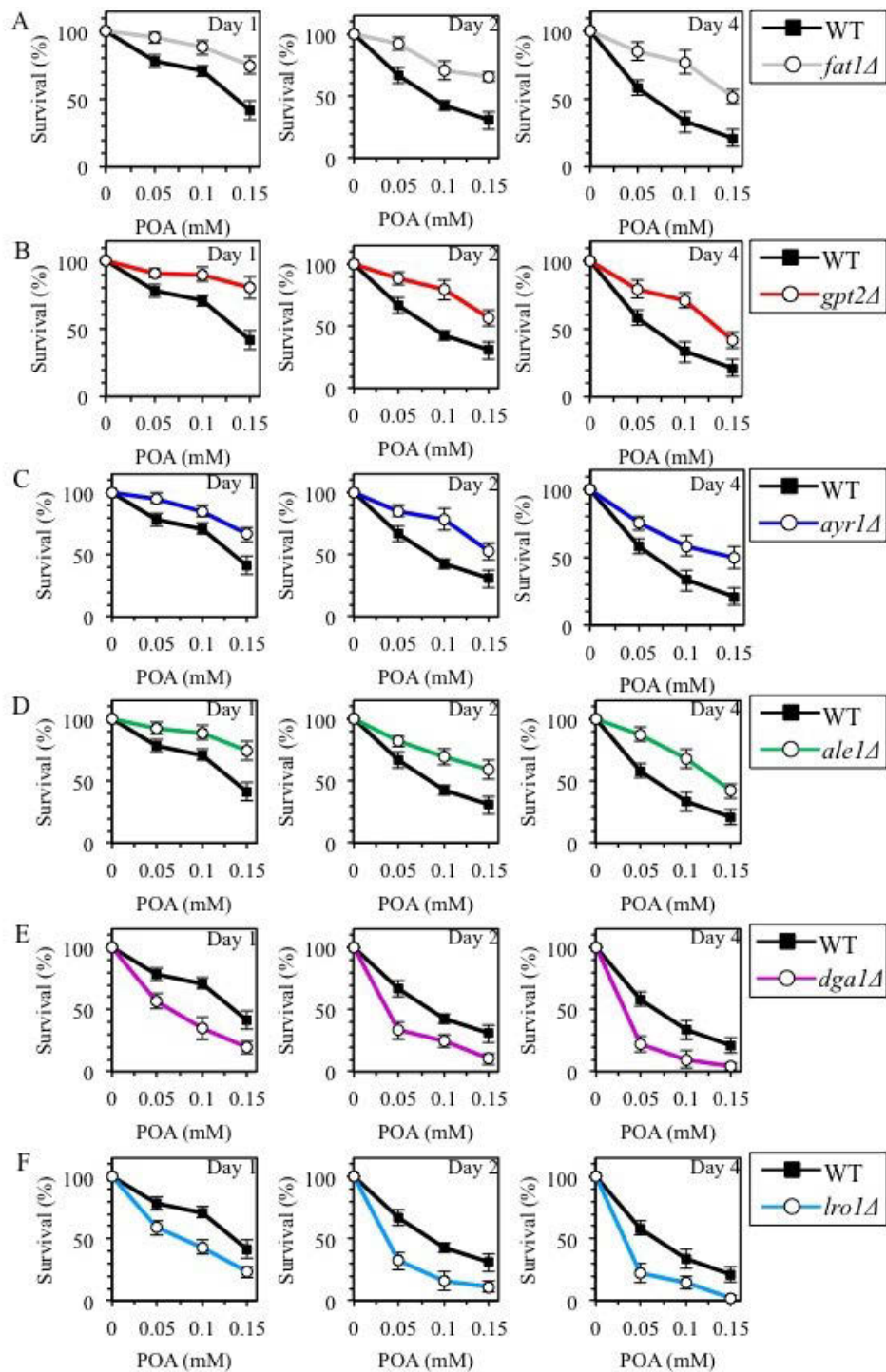


Figure 29 Various single-gene-deletion mutations eliminating enzymes involved in POA transport to the ER or lipid biosynthesis elicit differential age-dependent effects on the susceptibility of yeast to POA-induced liponecrotic PCD. WT, *fat1Δ*, *gpt2Δ*, *ayr1Δ*, *ale1Δ*, *dga1Δ* and *lro1Δ* cells were recovered at days 1, 2 and 4 of culture in a nutrient-rich YP medium initially containing 0.2% glucose. Cell survival was assessed by measuring the clonogenicity of WT and mutant cells after 2 h of treatment with various concentrations of exogenous POA. Data are presented as means \pm SEM (n = 12-19).

6.3.2 The alkaline-pH- and lipid-asymmetry-responsive Rim101 signaling pathway commits yeast to liponecrotic PCD by reducing the level of PE in the extracellular leaflet of the PM

The pH of culture media is known to affect phospholipid metabolism at a transcriptional level ¹⁴⁹. To assess whether alterations to culture media pH are important in the induction of liponecrotic cell death, the pH of culture medium following an exposure of WT cells to various concentrations of POA was measured. Medium alkalinisation was observed in a concentration-dependent manner (Figure 30A). To assess whether medium alkalinisation was essential for the commitment of yeast to liponecrotic PCD, susceptibility to POA was measured in buffered and unbuffered culture media. The pH of buffered culture media supplemented with different concentrations of POA was maintained at approximately 6.5 (Figure 30B) - *i.e.*, close to the initial pH of unbuffered culture media containing the same POA concentrations (Figure 30A). The data indicated that an exposure of WT yeast to POA commits these cells to liponecrotic PCD as efficiently in buffered media as it does in unbuffered media (Figure 30C), implying that the POA-induced medium alkalinisation is apparently unrelated to liponecrotic cell death. Unpublished data validated this conclusion; as it was found that a hypomorphic allele of the gene encoding the PM ATPase Pma1p ¹⁵⁰, a single-gene-deletion mutation eliminating the PM Na⁺ (K⁺)/H⁺ antiporter Nha1p ¹⁵¹, and a single-gene-deletion mutation removing the PM K⁺ transporter Trk1p ¹⁵² exhibit considerable differential effects on the extent of culture medium alkalinisation by cells exposed to POA but do not alter the susceptibility of yeast to POA-induced liponecrotic cell death.

In addition to medium alkalinisation, changes in the asymmetrical distribution of membrane phospholipids in the PM bilayer have been shown to induce the alkaline-pH- and lipid-asymmetry-responsive Rim101 signaling pathway in yeast cells ^{140,153}. Importantly, an active maintenance of the proper phospholipid asymmetry in the PM bilayer depends on the abundance and composition of different species of phospholipids in this bilayer ¹⁵⁴⁻¹⁵⁶. As we found, the POA-induced alkalinisation of culture medium by yeast cells does not elicit liponecrotic PCD despite the known ability of such alkalinisation to trigger the Rim101 signaling pathway. However, the observed buildup of different POA-containing species of phospholipids within the PM of cells treated with POA may perturb proper phospholipid asymmetry in the PM

bilayer resulting in the induction of the Rim101 pathway. We therefore hypothesized that the Rim101 signaling pathway may operate as a pro-death process that commits yeast to liponecrotic PCD.

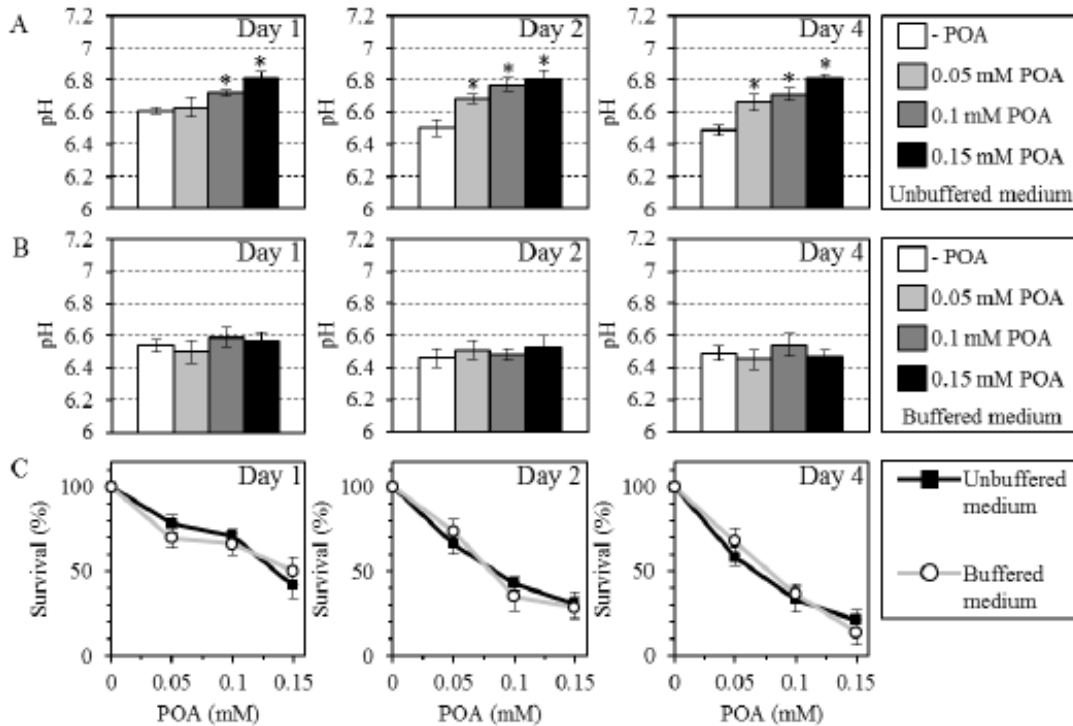


Figure 30 The alkalinisation of culture medium by yeast exposed to POA is not essential for the ability of POA to trigger liponecrotic PCD. WT cells were recovered at days 1, 2 and 4 of culturing in a nutrient-rich YP medium initially containing 0.2% glucose as carbon source; the medium was buffered (25 mM HEPES-KOH, pH 6.5) or remained unbuffered. (A, B) The pH of culture medium after 2 h of treatment with various concentrations of exogenous POA, either in unbuffered medium (A) or in buffered medium (B); data are presented as means \pm SEM (n = 5-7; *p < 0.01). (C) The survival of WT cells was assessed by measuring their clonogenicity after 2 h of treatment with various concentrations of exogenous POA, either in unbuffered medium or in buffered medium; data are presented as means \pm SEM (n = 6-9).

The Rim101 signaling pathway includes: (I) the pH sensing protein complex confined to the PM; and (II) the attached to the endosomal membrane proteolytic processing complex for the transcriptional factor Rim101p^{153,157}. The pH sensing protein complex on the PM consists of the integral membrane proteins Rim21p which senses extracellular pH, as well as Rim9p and Dfg16p, and the peripheral membrane protein Rim8p^{153,158,159} (Figure 31). Upon stimulation of the alkaline-pH- and lipid-asymmetry-responsive Rim101 signaling pathway, Rim8p promotes

endocytic internalization of the integral membrane components of the pH sensing protein complex^{153,160}. Following their internalization, Rim21p, Rim9p and Dfg16p stimulate the recruitment of the ESCRT (endosomal sorting complex required for transport) protein components Vps20p, Snf7p, Vps24p and Did4p of the ESCRT-III complex to the surface of the endosome^{153,161,162} (Figure 31). A subsequent recruitment of the ATPase Vps4p to the endosomal ESCRT-III complex initiates its Vps4p-, Vps24- and Did4p- dependent disassembly and the resulting accumulation of the Snf7p-Vps20p protein subcomplex on the surface of the endosome^{153,162,163}. This protein subcomplex then interacts with Rim20p and Rim13p, thereby activating the proteolytic processing of the transcriptional factor Rim101p by the cysteine protease Rim13p^{153,162,164} (Figure 31). The proteolytically cleaved form of Rim101p is delivered to the nucleus, where it activates transcription of the *RSBI* gene by suppressing its transcriptional repressor, Nrg1p^{153,162,165} (Figure 31). A protein product of the *RSBI* gene is a putative sphingoid long-chain base-specific translocase/transporter within the PM^{140,166}. Rsb1p has been shown to: (I) stimulate the Lem3p-dependent transport of PE from the extracellular (outer) leaflet of the PM to its intracellular (inner) leaflet; and (II) suppress the Yor1p-dependent transport of PE in the opposite direction^{137,157,164,165} (Figure 31).

Collectively, the above data suggest that an activation of the alkaline-pH- and lipid-asymmetry-responsive Rim101 signaling pathway is likely to reduce the level of PE in the extracellular (outer) leaflet of the PM (Figure 31). This prospect was investigated by measuring the relative levels of PE in the two leaflets of the PM. To attain this objective, we used the tetracyclic peptide antibiotic cinnamycin which specifically binds to PE in the extracellular (outer) leaflet of the PM and causes cell lysis^{167,169}. For this reason, the level of PE in the outer leaflet of the PM bilayer would correlate with the sensitivity of yeast to cinnamycin¹⁴⁰. We found that treatment with POA decreased the sensitivity of yeast to cinnamycin (Figure 32). This indicates that POA treatment resulted in the reduction of the level of PE in the extracellular leaflet of the PM. Moreover, the *yor1Δ* mutation eliminating a protein required for the transport of PE from the intracellular (inner) leaflet of the PM to its extracellular leaflet^{140,168} further decreased the sensitivity of pre-treated with POA cells to cinnamycin (Figure 32). In contrast, the *lem3Δ* mutation eliminating a protein required for the transport of PE from the extracellular leaflet of the PM to its intracellular leaflet^{140,167} increased the sensitivity of POA treated cells to cinnamycin (Figure 32). In sum, these findings imply that a depletion of PE in the extracellular

leaflet of the PM, likely due to its enhanced translocation to the intracellular leaflet of the PM, is a hallmark event of POA-induced liponecrotic PCD. It is conceivable that this characteristic trait of liponecrotic PCD is due to the ability of POA to trigger the Rim101 signaling pathway, thereby increasing the level of Rsb1p in the PM. The increased abundance of Rsb1p may enhance its stimulating effect on the Lem3p-dependent transport of PE from the extracellular leaflet to the intracellular leaflet of the PM and may also amplify its inhibitory effect on the Yor1p-dependent transport of PE within the PM bilayer in the opposite direction.

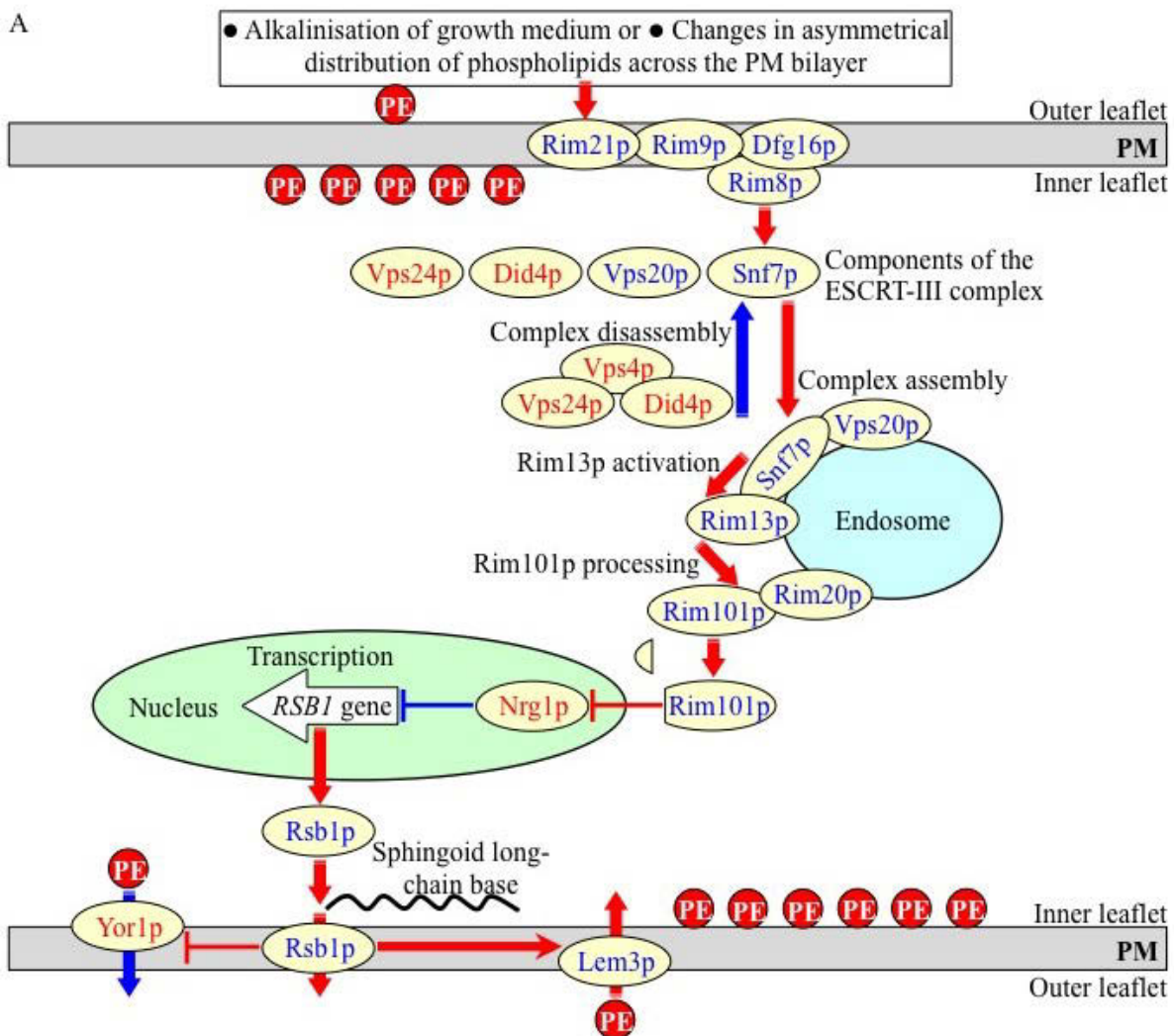


Figure 31 - Outline of the alkaline-pH- and lipid-asymmetry-responsive Rim101 signalling pathway operating in yeast cells. (A) This signalling pathway can be induced by alkalinisation of culture medium and/or in response to certain changes in asymmetrical distribution of some species of phospholipids across the PM bilayer. The Rim101 signalling pathway includes the pH sensing protein complex on the PM and the proteolytic processing complex for the transcriptional factor Rim101p on the endosomal membrane. After Rim101p is proteolytically processed by the

cysteine protease Rim13p on the surface of the endosome, its cleaved form is delivered to the nucleus. In the nucleus, cleaved Rim101p activates transcription of the *RSB1* gene by suppressing its transcriptional repressor, Nrg1p. A protein product of the *RSB1* gene is a putative sphingoid long-chain base-specific translocase/transporter within the PM. This protein stimulates the Lem3p-dependent transport of PE from the outer (extracellular) leaflet of the PM to its inner (intracellular) leaflet and suppresses the Yor1p-dependent transport of PE across the PM bilayer in the opposite direction. See text for additional details. The names of proteins whose lack causes a decrease or increase of the susceptibility of yeast to POA-induced liponecrotic PCD are displayed in blue or red color, respectively. Activation arrows and inhibition bars denote pro-death processes (displayed in red color) or pro-survival processes (displayed in blue color) for the liponecrotic mode of PCD.

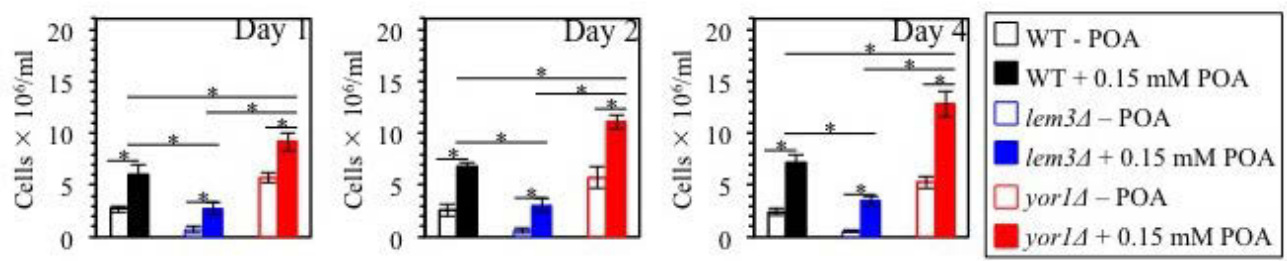


Figure 32 – Treatment of yeast cells with POA results in an altered asymmetric distribution of PE in the plasma membrane. WT, *lem3Δ* and *yor1Δ* cells were recovered at day 1 of culturing in nutrient-rich YP medium initially containing 0.2% glucose as carbon source. Each cell suspension was divided into two equal aliquots. Cells in one of these aliquots were treated for 2 h with 0.15 mM POA; cells in the other aliquot remained untreated. Cells in each aliquot were then diluted in YP medium containing 2% glucose and supplemented with 25 μ M cinnamycin. Both aliquots were incubated for 8 h, and the total number of cells in each aliquot was determined using a hemacytometer. Data are presented as means \pm SEM (n = 5-6). Because specific binding of cinnamycin to PE in the outer leaflet of the PM causes cell lysis, the level of PE in this leaflet of the PM bilayer positively correlates with the sensitivity of yeast to cinnamycin.

To further verify whether the Rim101 signaling pathway operates as a pro-death process that commits yeast to liponecrotic PCD, we examined how various single-gene-deletion mutations eliminating different protein components of this pathway influence the susceptibility of yeast to liponecrosis. It was found that the *rim21Δ*, *rim9Δ*, *dfg16Δ*, *rim8Δ*, *snf7Δ*, *vps20Δ*, *rim13Δ*, *rim20Δ* and *rim101Δ* mutations reduce the susceptibility of yeast to POA-induced liponecrotic PCD (Figure 33A-I). All these mutations are known to impair the ability of the transcriptional factor Rim101p to activate transcription of the *RSB1* gene^{153,162,165} (Figure 31), and are therefore expected to diminish the stimulating effect of Rsb1p on the Lem3p-dependent transport of PE from the extracellular leaflet of the PM to its intracellular leaflet^{153,167,168} (Figure

31). Moreover, all these mutations are also anticipated to lessen the inhibitory effect of Rsb1p on the Yor1p-dependent transport of PE across the PM bilayer in the opposite direction^{153,167,168} (Figure 31). In sum, the *rim21Δ*, *rim9Δ*, *dfg16Δ*, *rim8Δ*, *snf7Δ*, *vps20Δ*, *rim13Δ*, *rim20Δ* and *rim101Δ* mutations reducing the susceptibility of yeast to POA-induced liponecrotic PCD are likely to decrease the extent of PE depletion in the extracellular leaflet of the PM, a hallmark event of this PCD subroutine. Furthermore, the *rsb1Δ* and *lem3Δ* mutations made yeast less susceptible to POA-induced liponecrotic PCD (Figure 33 J, K). Because both these mutations are known to diminish the stimulating effect of Rsb1p on the Lem3p-dependent transport of PE from the extracellular leaflet of the PM to its intracellular leaflet^{153,167,168} (Figure 31), they are expected to lessen the degree of PE depletion in the extracellular leaflet of the PM. It was also observed that the *vps4Δ*, *vps24Δ* and *did4Δ* mutations increase the susceptibility of yeast to POA-induced liponecrotic PCD (Figure 34A-C). Because all these mutations have been shown to enhance the ability of Rim101p to activate transcription of the *RSB1* gene^{158,162} (Figure 31), they are likely to increase the extent of PE depletion in the extracellular leaflet of the PM. Additionally, the *nrg1Δ* mutation eliminating a transcriptional repressor of the *RSB1* gene^{153,162,165} (Figure 31) and the *yor1Δ* mutation impairing the transport of PE from the intracellular leaflet of the PM to its extracellular leaflet^{140,167,168} (Figure 31) were demonstrated to make yeast more susceptible to POA-induced liponecrotic PCD (Figure 34 D,E). Because the *nrg1Δ* mutation is known to attenuate the Yor1p-dependent transport of PE from the intracellular leaflet of the PM to its extracellular leaflet and the *yor1Δ* mutation has been shown to abolish it^{140,167,168} (Figure 31), both these mutations are expected to increase the extent of PE depletion in the extracellular leaflet of the PM. Altogether, the observation that mutations eliminating different protein components of the Rim101 signaling pathway influence the susceptibility of yeast to POA-induced liponecrotic PCD support the proposed hypothesis that this pathway operates as a pro-death process that commits yeast to this PCD subroutine.

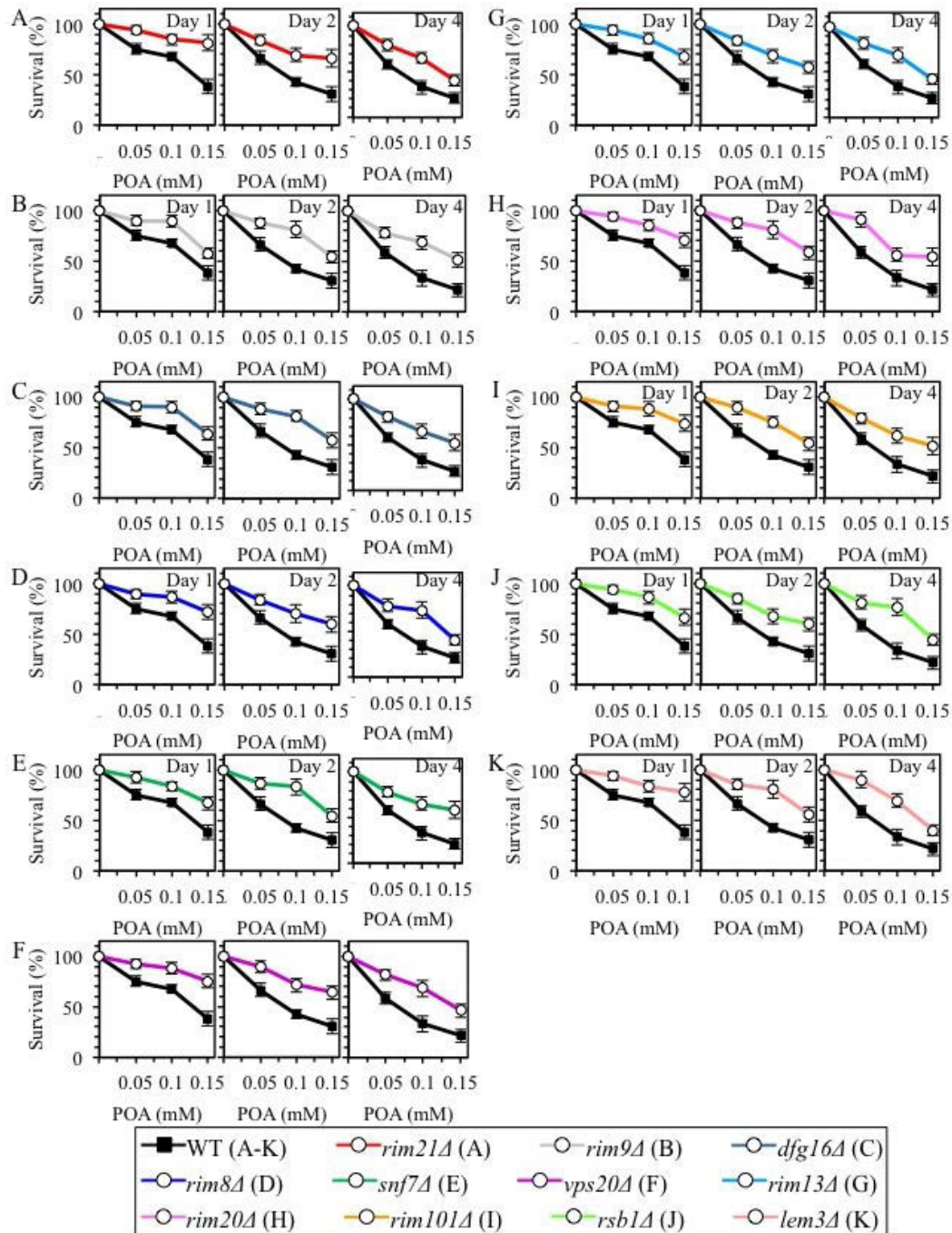


Figure 33 Various single-gene-deletion mutations eliminating different protein components of the Rim101 signalling pathway reduce the susceptibility of yeast to POA-induced liponecrotic PCD if they decrease the extent of PE depletion in the extracellular leaflet of the PM, a hallmark event of this PCD subroutine. WT, *rim21Δ*, *rim9Δ*, *dfg16Δ*, *rim8Δ*, *snf7Δ*, *vps20Δ*, *rim13Δ*, *rim20Δ*, *rim101Δ*, *rsb1Δ* and *lem3Δ* cells were recovered at days 1, 2 and 4 of culturing in a nutrient-rich YP medium initially containing 0.2% glucose as carbon source. Cell survival was assessed by measuring the clonogenicity of WT and mutant cells after 2 h of treatment with various concentrations of exogenous POA. Data are presented as means \pm SEM (n = 8-10).

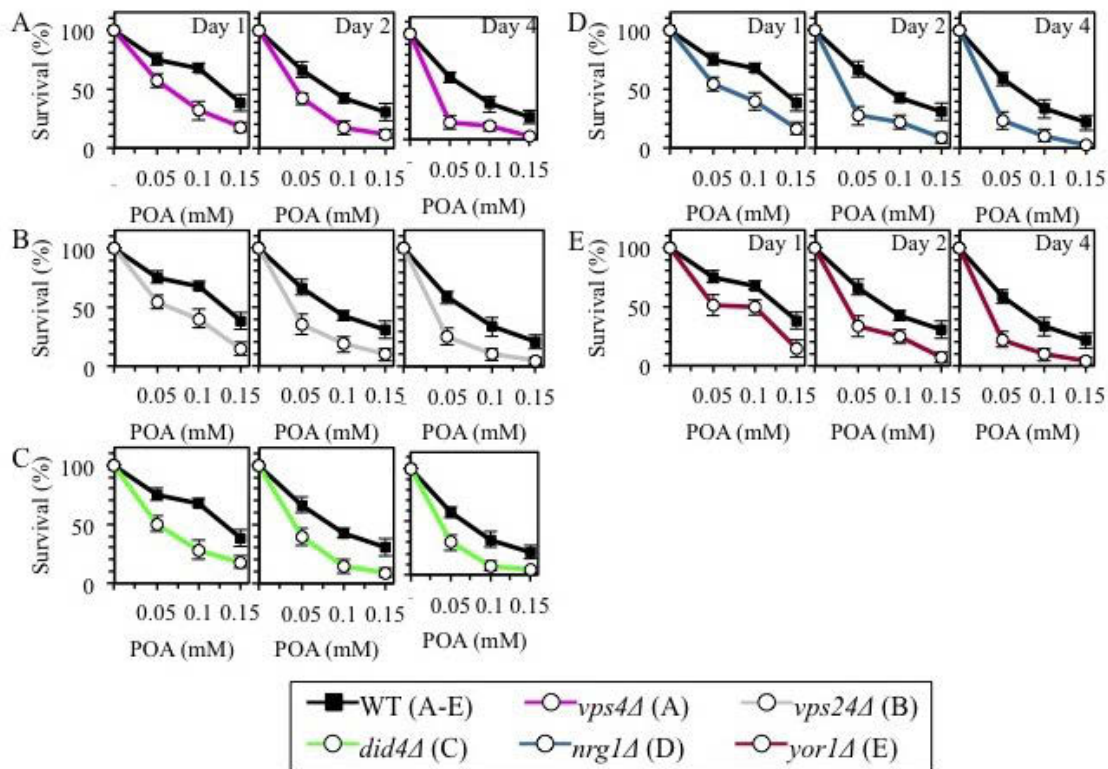


Figure 34 Various single-gene-deletion mutations eliminating different protein components of the Rim101 signalling pathway make yeast more susceptible to POA-induced liponecrotic PCD if they increase the degree of PE depletion in the extracellular leaflet of the PM, a hallmark event of this PCD modality. WT, *vps4Δ*, *vps24Δ*, *did4Δ*, *nrg1Δ* and *yor1Δ* cells were recovered at days 1, 2 and 4 of culturing in a nutrient-rich YP medium initially containing 0.2% glucose as carbon source. Cell survival was assessed by measuring the clonogenicity of WT and mutant cells after 2 h of treatment with various concentrations of exogenous POA. Data are presented as means \pm SEM (n = 6-13).

6.3.3 The commitment of yeast to liponecrotic PCD elevates the extent of oxidative damage to cellular proteins and lipids

Our lab has unpublished data indicating that liponecrotic PCD also results in the elevation of intracellular levels of ROS (courtesy of Adam Beach). To assess the role of elevated ROS production during liponecrotic cell death, the magnitude of oxidative damage to cellular proteins and lipids was measured. The data revealed that the concentration of exogenous POA added to WT cells positively correlates with both the degree of oxidative carbonylation of cellular proteins (Figure 35A,B) and the extent of oxidative damage to cellular lipids (Figure 35C). Moreover, disruption of mitophagy significantly elevated the magnitude of oxidative damage to cellular proteins (Figure 35A,B) and lipids (Figure 35C) in yeast exposed to POA.

Because Atg32p-driven mitophagy plays an essential pro-survival role in protecting yeast from liponecrotic PCD, one could envision that a rise in oxidative damage to cellular proteins and lipids above certain critical level contributes to the commitment of yeast to this PCD subroutine.

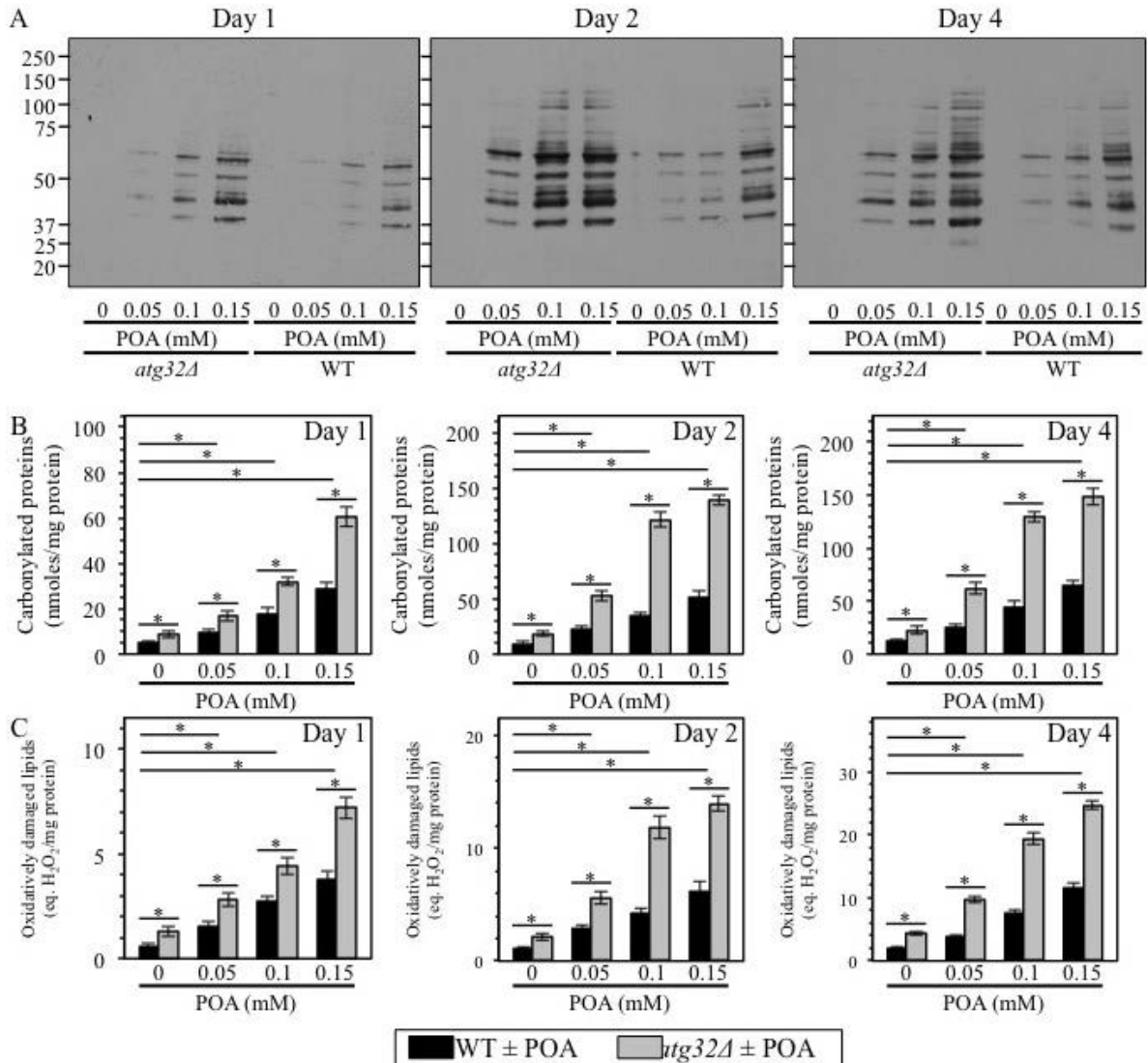


Figure 35 Yeast cells committed to liponecrotic PCD exhibit elevated oxidative damage to cellular proteins and lipids. WT and *atg32Δ* cells were recovered at days 1, 2 and 4 of culturing in nutrient-rich YP medium initially containing 0.2% glucose as carbon source. Immunodetection of carbonyl groups of oxidatively damaged cellular proteins (A) and biochemical assays for measuring oxidatively damaged cellular proteins (B) and lipids (C) were performed as described in Materials and Methods. Data are presented as means \pm SEM (n = 3-5; *p < 0.01).

6.3.4 Various pathways of macroautophagy differ in their roles in POA-induced liponecrotic PCD

Based on the devised model for the underlying mechanism of POA induced liponecrotic cell death (Figure 23), it was hypothesized that different macroautophagic processes may act in a conflicting manner in regulating this cell death modality¹³⁸. Macroautophagy is the major mode of autophagy initiated by the sequestration of cellular organelles and cytosolic proteins into double-membrane vesicles called autophagosomes^{128,170,171} (Figure 36). The ensuing fusion of autophagosomes with the vacuole enables them to deliver the sequestered cargo of organelles and proteins to the vacuole lumen for proteolytic degradation by resident hydrolases^{128,170,171} (Figure 36). The working model for the mechanism underlying liponecrosis suggests that (I) the cytosolic serine/threonine protein kinase Atg1p¹⁷² may orchestrate the execution of liponecrotic PCD by activating all currently known pathways for non-selective and selective autophagic degradation of dysfunctional and damaged organelles and macromolecules; and (II) Atg32p^{120,143}, may protect yeast from liponecrotic PCD by enabling the maintenance of a population of functional mitochondria needed for POA incorporation into neutral lipids¹³⁸ (Figure 36). The protein machinery orchestrating the diverse autophagic pathways in yeast is well known¹²⁸ (Figure 36).

To investigate the apparently contrasting roles of these different autophagic processes, clonogenic survival was measured in mutants in various pathways of non-selective or selective autophagic pathways. The *atg1Δ*, *atg11Δ* and *atg17Δ* mutations have been shown to impair all of the known pathways for non-selective or selective autophagy, including (I) the non-selective autophagy pathway for massive degradation of various cellular organelles and macromolecules^{128,170,171}; (II) the cytoplasm-to-vacuole (Cvt) pathway for the delivery of several resident hydrolases to the vacuole^{128,170,171}; (III) the cargo-specific pexophagy pathway for selective autophagic degradation of aged, dysfunctional, damaged or excessive peroxisomes^{128,170,171} and (IV) the cargo-specific mitophagy pathway for selective autophagic degradation of aged, dysfunctional, damaged or excessive mitochondria^{128,170,171} (Figure 36).

The *atg1Δ*, *atg11Δ* and *atg17Δ* mutations decreased the susceptibility of yeast to POA-induced liponecrotic PCD (Figure 37A-C). In contrast, the *atg19Δ* mutation, which is known to impair only the "biosynthetic" Cvt pathway^{128,170,171} (Figure 36), had no effect on the susceptibility of yeast to this mode of PCD (Figure 37D). Furthermore, the *atg36Δ* mutation,

which has been shown to eliminate only the cargo-specific pexophagy pathway¹⁷³ (Figure 36), did not affect the susceptibility of yeast to POA-induced liponecrotic PCD (Figure 37E). Moreover, we confirmed our recent finding¹³⁸ that the *atg32Δ* mutation, which is known to impair only the cargo-specific mitophagy pathway^{120,143} (Figure 36), increased the susceptibility of yeast to this mode of PCD (Figure 37F).

Altogether, these findings imply that various pathways of autophagy differ in their regulation of liponecrotic cell death. The "biosynthetic" Cvt pathway and the cargo-specific pexophagy pathway are not involved in committing yeast to this PCD subroutine. The non-selective autophagy pathway for massive degradation of various cellular organelles and macromolecules plays a pivotal role in executing the liponecrotic mode of PCD. In contrast, mitophagy is a crucial pro-survival process that protects yeast from liponecrotic cell death - likely by eliminating damaged and dysfunctional mitochondria, allowing for the sustenance of a population of functional mitochondria required for protective effect of fatty acid storage into neutral lipids.

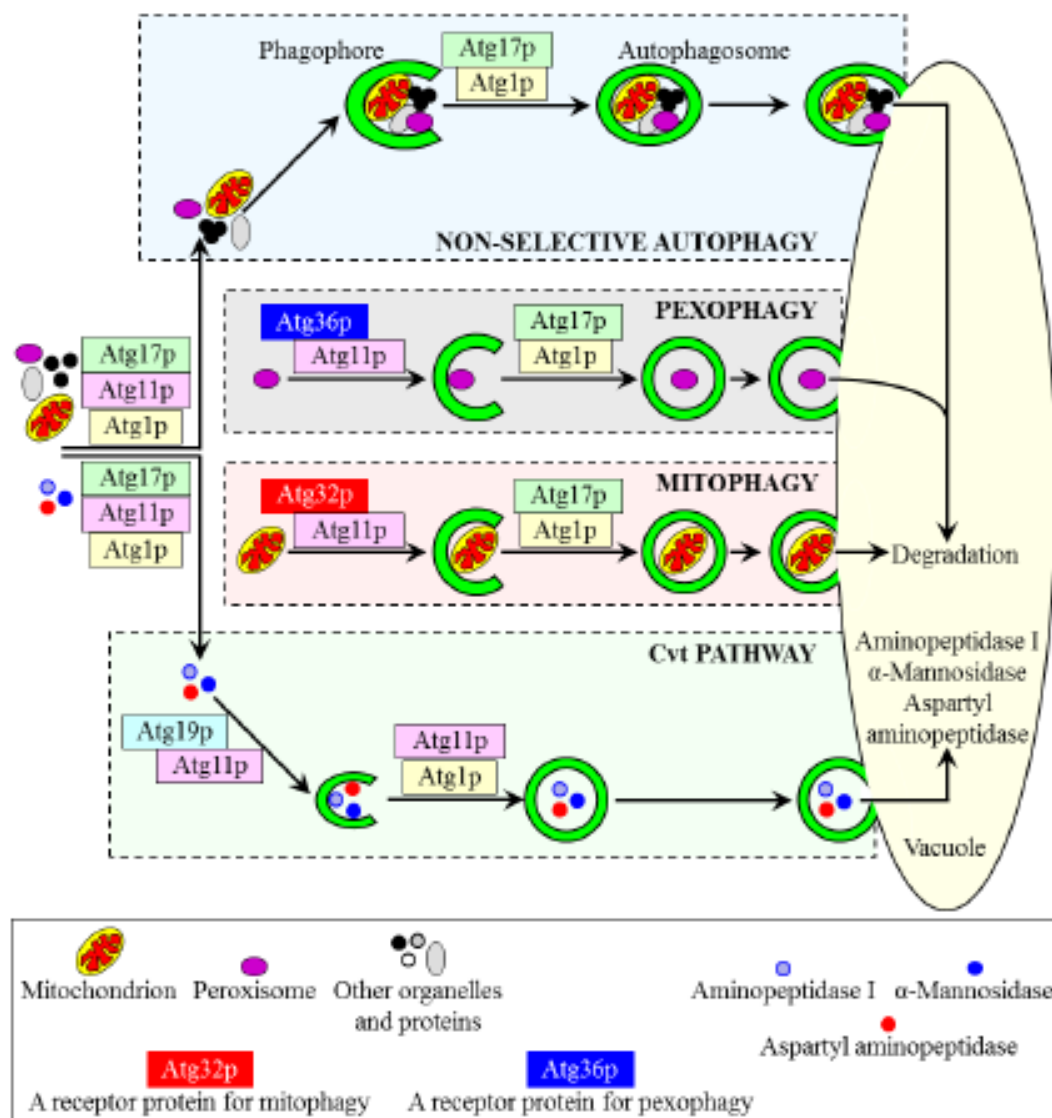


Figure 36 - Outline of the pathways for non-selective and selective macroautophagic delivery of cellular organelles and macromolecules to the vacuole in yeast. Macroautophagy, hereafter referred to as autophagy, is initiated when a precursor compartment known as the phagophore sequesters cellular organelles and cytosolic proteins into double-membrane vesicles called autophagosomes. Autophagosomes then fuse with the vacuole, thereby delivering the sequestered cargo organelles and proteins to the vacuole lumen for proteolytic degradation by resident hydrolases. These resident hydrolases, including aminopeptidase I, aspartyl aminopeptidase and α -mannosidase, are delivered to the vacuole via the "biosynthetic" cytoplasm-to-vacuole (Cvt) pathway of autophagy. Atg1p, Atg11p and Atg17p proteins play essential roles in all four pathways for non-selective and selective macroautophagic delivery of cellular organelles and macromolecules to the vacuole, including the non-selective autophagy pathway for massive degradation of various cellular organelles and macromolecules, the Cvt pathway, the cargo-specific pexophagy pathway for selective autophagic degradation of peroxisomes and the cargo-specific mitophagy pathway for

selective autophagic degradation of mitochondria. Atg19p is a protein essential only for the "biosynthetic" Cvt pathway of autophagy. Atg36p is involved only in the pexophagy pathway, whereas Atg32p plays an essential role only in the mitophagy pathway.

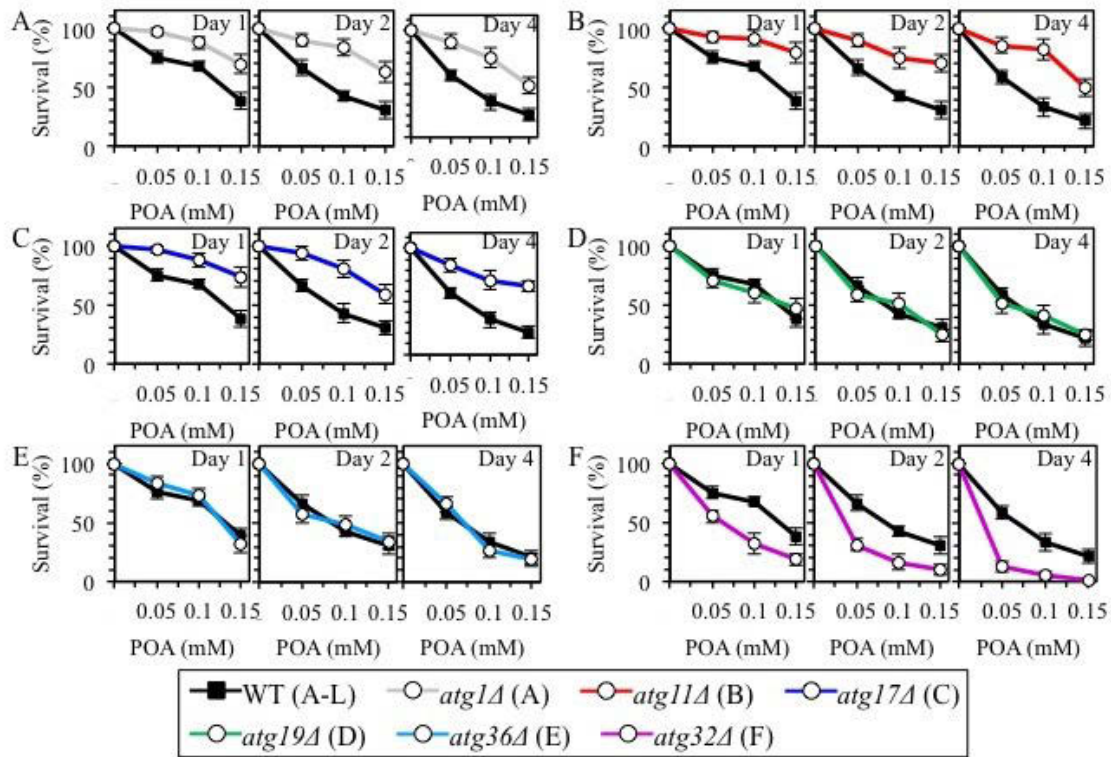


Figure 37 – Various pathways of autophagy play different roles in POA-induced liponecrotic PCD. WT, *atg1Δ*, *atg11Δ*, *atg17Δ*, *atg19Δ*, *atg36Δ* and *atg32Δ* cells were recovered at days 1, 2 and 4 of culturing in a nutrient-rich YP medium initially containing 0.2% glucose as carbon source. Cell survival was assessed by measuring the clonogenicity of WT and mutant cells after 2 h of treatment with various concentrations of exogenous POA. Data are presented as means \pm SEM (n = 11-19).

To verify whether non-selective autophagy plays an essential role in executing liponecrotic PCD, the recent finding of the ability of the natural polyamine called spermidine to extend yeast longevity by inducing autophagy was utilized¹²³. Noteworthy, the *spe1Δ* mutation which eliminates an enzyme catalyzing the first step of polyamine biosynthesis^{174,175} (Figure 38) has been shown to greatly reduce the intracellular level of spermidine and shorten yeast longevity¹²³. Thus, the efficiency of spermidine synthesis in yeast cells positively correlates with the efficiency of a systemic biological effect which spermidine causes by inducing the non-

selective autophagy pathway for massive degradation of various cellular organelles and macromolecules. We therefore first examined how the *spe1Δ*, *spe2Δ* and *spe3Δ* mutations influence the susceptibility of yeast cells to POA-induced liponecrotic PCD. Each of these single-gene-deletion mutations eliminates a different enzyme of the pathway for polyamine biosynthesis in yeast cells^{174,176,177} (Figure 38) and, thus, is expected to impair the ability of spermidine to induce the non-selective autophagy pathway of autophagy. We found that (I) the *spe1Δ*, *spe2Δ* and *spe3Δ* mutations reduce the susceptibility of yeast to liponecrotic PCD (Figure 38 B, D, F); (II) if added exogenously at the low concentration of 0.1 mM, spermidine reduces the protecting effect of each of these mutations against liponecrosis and restores the level of susceptibility to liponecrotic PCD seen for WT cells (Figure 38C,E, G); and (III) if added exogenously at the high concentration of 0.3 mM or 1 mM, spermidine makes *spe1Δ*, *spe2Δ* and *spe3Δ* cells even more susceptible to liponecrotic PCD than WT cells (Figure 38C,E,G). Moreover, we also found that while exogenous spermidine increases the susceptibility of WT cells to liponecrotic PCD in a concentration-dependent manner (Figure 38H), it does not alter the reduced susceptibility to liponecrosis of *atg1Δ* cells known to be deficient in the non-selective pathway of autophagy (Figure 38 I).

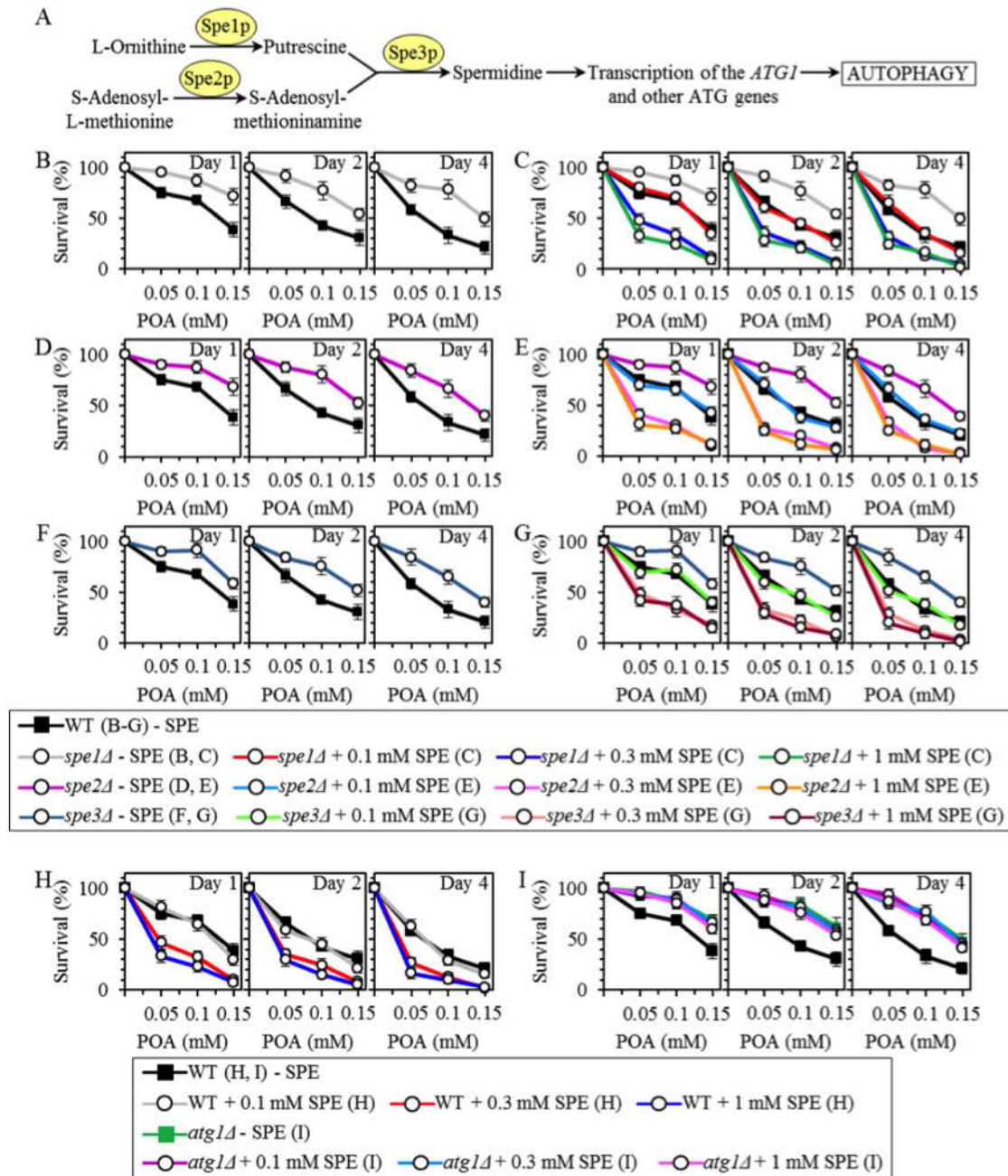


Figure 38 - The spermidine-inducible autophagy pathway for non-selective degradation of various cellular organelles and macromolecules plays an essential role in executing POA-induced liponecrotic PCD.

(A) Outline of the pathway for polyamine biosynthesis in yeast cells. The natural polyamine called spermidine has been shown to stimulate transcription of the *ATG1* and other *ATAG* genes, thereby inducing the non-selective autophagy pathway for massive degradation of various cellular organelles and macromolecules. (B-I) WT, *spe1Δ*, *spe2Δ*, *spe3Δ* and *atg1Δ* cells were recovered at days 1, 2 and 4 of culturing in a nutrient-rich YP medium initially containing 0.2% glucose, either in the absence of spermidine or in the presence of spermidine at the indicated final

concentration. Cell survival was assessed by measuring the clonogenicity of WT and mutant cells after 2 h of treatment with various concentrations of exogenous POA. Data are presented as means \pm SEM (n = 6-11).

Collectively, these findings further validate our conclusion that the non-selective autophagy pathway for massive degradation of various cellular organelles and macromolecules plays a pivotal role in executing the liponecrotic mode of PCD. In addition, these findings suggest that (I) the intracellular level of spermidine positively correlates with the extent of yeast susceptibility to liponecrotic PCD; and (II) spermidine may increase such susceptibility by activating the non-selective pathway of autophagy, thereby triggering the process which executes this mode of PCD.

Based on the findings reported here and in chapter 5¹³⁸, we propose the following model for molecular mechanisms that in yeast cells underlie the opposing roles of various autophagy pathways in POA-induced liponecrotic PCD (Figure 39). In WT cells treated with POA and in cells of various mutants exposed to exogenous POA, some mitochondria become “stressed”, damaged and dysfunctional - likely due to the observed in these cells excessive production of ROS as by-products of mitochondrial respiration. In *atg32Δ* mutant cells, these “stressed”, damaged and dysfunctional mitochondria cannot be selectively eliminated as efficiently as in WT cells, due to the *atg32Δ*-dependent mutational block of mitophagy (Figure 39A). This intensifies cellular processes that cause the buildup of ROS and oxidatively damaged organelles and macromolecules; the resulting amplification of processes that create an excessive level of cellular stress accelerates the onset of liponecrotic PCD in yeast impaired in Atg32p-driven mitophagy (Figure 39A). In *atg1Δ*, *atg11Δ*, *atg17Δ*, *spe1Δ*, *spe2Δ* and *spe3Δ* mutant cells exposed to POA (Figure 39B), Atg32p-driven mitophagy eliminates the “stressed”, damaged and dysfunctional mitochondria as selectively and efficiently as it does in WT, *atg19Δ* and *atg36Δ* cells treated with POA (Figure 39C). Therefore, the dynamics of cellular processes creating an excessive level of cellular stress in *atg1Δ*, *atg11Δ*, *atg17Δ*, *spe1Δ*, *spe2Δ* and *spe3Δ* mutant cells exposed to POA (Figure 39B) is similar to the one in WT, *atg19Δ* and *atg36Δ* cells treated with POA (Figure 39C). However, unlike WT, *atg19Δ* and *atg36Δ* cells undergoing liponecrotic PCD when the level of cellular stress exceeds a toxic threshold (Figure 39C), *atg1Δ*, *atg11Δ*, *atg17Δ*, *spe1Δ*, *spe2Δ* and *spe3Δ* mutant cells exhibit a decelerated rate of the execution of this PCD

subroutine because they are impaired in the non-selective autophagy pathway for massive degradation of various cellular organelles and macromolecules (Figure 39B).

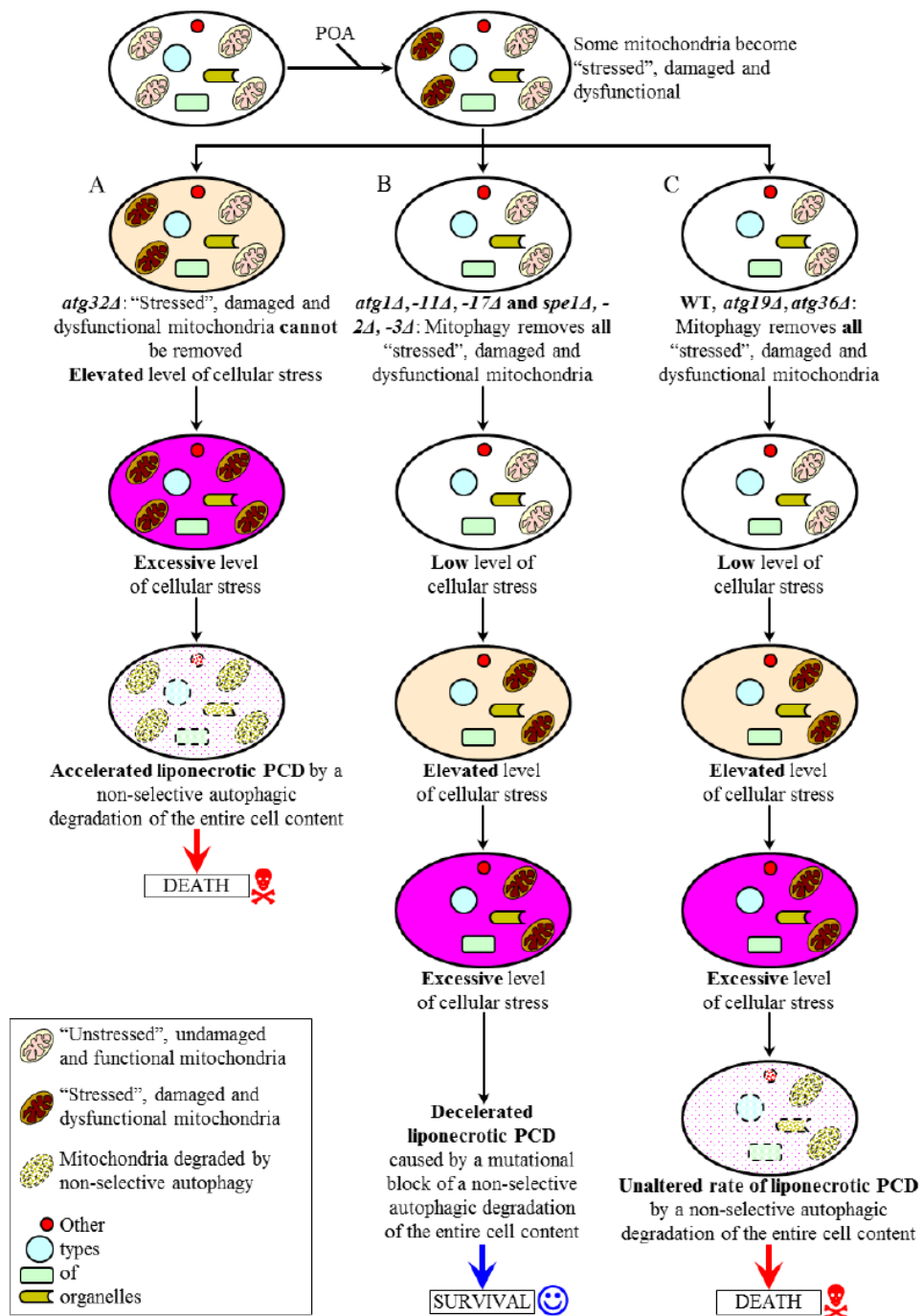


Figure 39 A model for molecular mechanisms that in yeast underlie the opposing roles of various autophagy pathways in POA-induced liponecrotic PCD.

6.4 Discussion

This study and our recent published data¹³⁸ suggest the following model for a mechanism underlying POA-induced liponecrotic PCD (Figure 40).

Exogenously added POA is incorporated into POA-containing PL. After being synthesized in the ER, excessive quantities of these POA-containing phospholipids initially accumulate in the ER membrane and then amass in mitochondrial membranes as well as in the PM. The buildup of the POA-containing phospholipids in the PM causes a reduction of PE level in its outer (extracellular) leaflet, thereby triggering the alkaline-pH- and lipid-asymmetry-responsive Rim101 signalling pathway (Figure 40). This pathway stimulates transcription of the *RSB1* gene; the resulting increased abundance of Rsb1p promotes further reduction of PE in the outer leaflet of the PM by (I) enhancing a stimulating effect of Rsb1p on the Lem3p-dependent transport of PE from the outer leaflet to the inner (intracellular) leaflet of the PM; and (II) amplifying an inhibitory effect of Rsb1p on the Yor1p-dependent transport of PE within the PM bilayer in the opposite direction. An ensuing depletion of PE in the outer leaflet of the PM elevates the permeability of this cellular membrane for small molecules (such as propidium iodide^{27,138}]), thereby contributing to the commitment of yeast to liponecrotic PCD.

The excessive accumulation of POA-containing phospholipids in both mitochondrial membranes of cells exposed to POA contributes to the commitment of yeast to liponecrotic PCD by impairing several mitochondrial processes that are indispensable for cell viability, such as respiration, membrane potential and ATP synthesis (Figure 40). These mitochondrial processes are essential for the ability of functional mitochondria to provide energy needed for the incorporation of POA into TAG, a pro-survival process which prevents the buildup of POA-containing phospholipids within the ER membrane, mitochondrial membranes and the PM by reducing the flow of POA into pathways for phospholipids synthesis and interorganellar transport (Figure 40).

Moreover, the buildup of POA-containing phospholipids in both mitochondrial membranes of cells exposed to POA contributes to the commitment of yeast to liponecrotic PCD also by causing the excessive production of ROS in mitochondria. A significant rise in cellular ROS above a critical level contributes to such commitment by: (I) oxidatively damaging protein and lipid constituents of various cellular organelles, thereby triggering a non-selective autophagic degradation of numerous “stressed”, damaged and dysfunctional organelles in a pro-

death process orchestrated by Atg1p, Atg11p and Atg17p; and (II) oxidatively damaging various cytosolic proteins, thereby impairing a pro-survival process of the maintenance of cellular proteostasis (Figure 40).

Several cellular processes in yeast exposed to POA can protect cells from liponecrosis. These pro-survival cellular processes include: (I) β -oxidation of POA within functional peroxisomes, which attenuates the excessive accumulation of POA-containing phospholipids in the ER membrane, mitochondrial membranes and the PM by lowering the flow of POA into pathways for phospholipids synthesis and interorganellar transport (Figure 40); (II) an incorporation of POA into TAG deposited in LD, which also prevents the buildup of POA-containing phospholipids within the ER membrane, mitochondrial membranes and the PM by reducing the flow of POA into pathways for phospholipids synthesis and interorganellar transport (Figure 40); and (III) mitophagy, a selective autophagic degradation of “stressed”, damaged and dysfunctional mitochondria in an Atg32p-driven process which sustains a healthy population of functional mitochondria capable of providing energy for POA deposition within LD in the form of TAG (Figure 40).

In the future, it would be important to explore a mechanism through which the observed depletion of PE in the outer (extracellular) leaflet of the PM enclosing yeast cells exposed to POA elevates the permeability of this cellular membrane for small molecules, thereby committing yeast to liponecrotic PCD. Another challenge for the future will be to define mechanisms by which the observed buildup of POA-containing phospholipids in both mitochondrial membranes of yeast cells exposed to POA alters such vital mitochondrial processes as respiration, membrane potential maintenance, ATP synthesis and ROS production – thus contributing to the commitment of yeast to liponecrotic PCD.

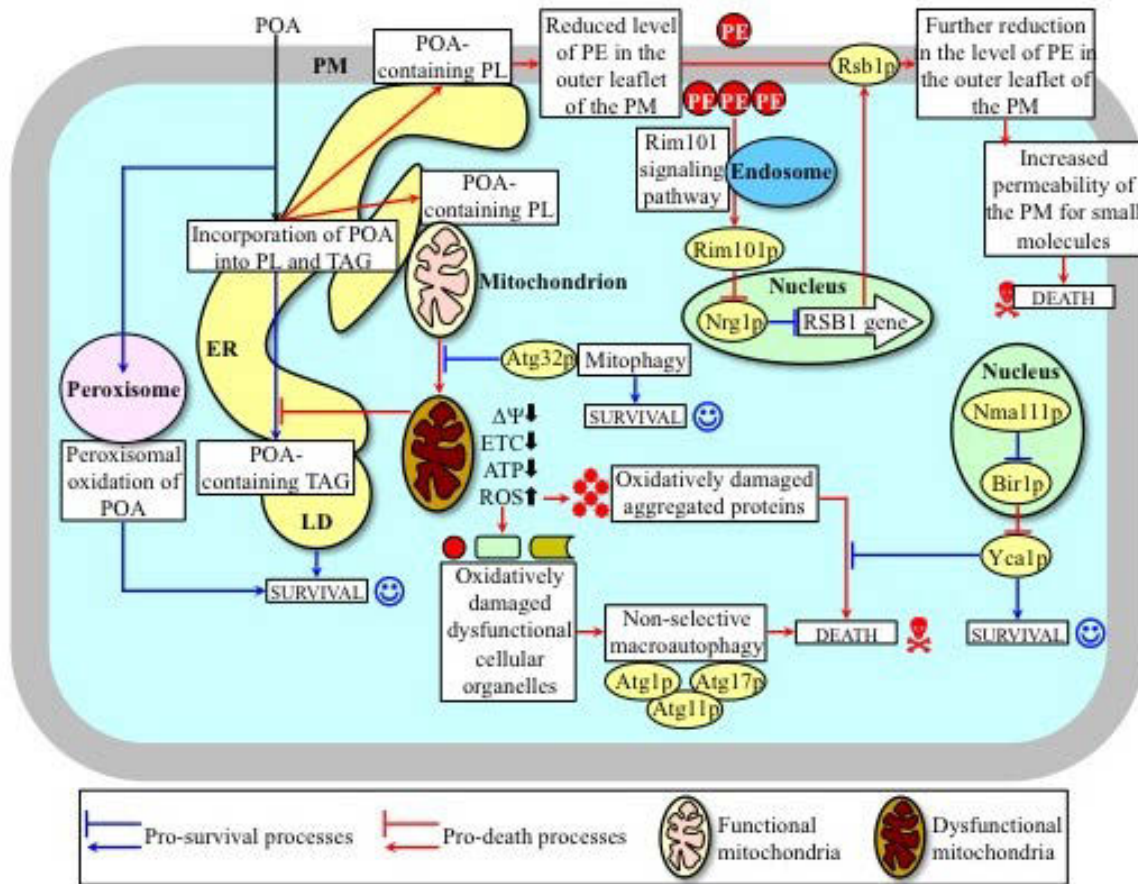


Figure 40 A model for a mechanism underlying POA-induced liponecrotic PCD in yeast. Exogenously added POA is incorporated into POA-containing phospholipids that then amass in the ER membrane, mitochondrial membranes and the PM. The buildup of the POA-containing phospholipids in the PM reduces the level of phosphatidylethanolamine (PE) in its outer leaflet, thereby increasing PM permeability for small molecules and committing yeast to liponecrotic PCD. The excessive accumulation of POA-containing phospholipids in mitochondrial membranes impairs mitochondrial functionality and causes the excessive production of reactive oxygen species (ROS) in mitochondria. The resulting rise in cellular ROS above a critical level contributes to the commitment of yeast to liponecrotic PCD by: (I) oxidatively damaging cellular organelles, thereby triggering their autophagic degradation; and (II) oxidatively damaging cytosolic proteins, thus impairing cellular proteostasis. Several cellular processes in yeast exposed to POA can protect cells from liponecrosis. They include: (I) POA oxidation in peroxisomes, which reduces the flow of POA into phospholipids synthesis pathways; (II) POA incorporation into triacylglycerols, which prevents the excessive accumulation of POA-containing phospholipids in cellular membranes; (III) mitophagy, a selective autophagic degradation of dysfunctional mitochondria, which sustains a population of functional mitochondria needed for POA incorporation into TAG; and (IV) a degradation of damaged, dysfunctional and aggregated cytosolic proteins, which enables the maintenance of cellular proteostasis. See Activation arrows and inhibition bars denote pro-death processes (displayed in red color) or pro-survival processes (displayed in blue color) for the liponecrotic mode of PCD elicited by POA.

7. Conclusions and Future Directions

Our data provide the first evidence in yeast of a programmed form of cell death that is controlled in a concentration dependent manner by the levels of exogenously added POA, and that this form of PCD is related to processes that maintain the normal lipid composition of the mitochondria, as well as other organelles. The cell death modality due to POA exposure appears to represent a previously uncharacterized type of PCD evidenced by the accumulation of lipid droplets, mass autophagic degradation of cellular organelles without the appearance of excessive vacuolization as in autophagic cell death, as well as loss of integrity of the PM without rupturing of the plasma membrane - typical of programmed necrotic cell deaths¹²¹. In addition to this, mitochondrial quality control through macromitophagy was shown to be a critical process for yeast cells to cope with POA induced liponecrosis as evidenced by the increased susceptibility of the *atg32Δ* mutant to POA induced liponecrosis. These mutants did not display the characteristic accumulation of lipid droplets when treated with any concentration of POA. This suggests that processes that maintain a functional pool of mitochondria are also required for the proper deposition of FFAs into LD as neutral lipids. Without these processes, we hypothesized that cell would exist in a state of energy deficit as evidenced by the lower levels of ATP production, as well as loss of proper redox homeostasis contributing to the age-related accumulation of oxidatively damaged proteins and lipids in the cell – all of which could contribute to promoting cell death. Because the susceptibility of yeast cells to POA and especially *atg32Δ* mutants was more pronounced at later time points, this could indicate that FFA mediated liponecrosis is an age related mode of cell death.

This effect corresponds to the changes in the lipidome, where we observed an increase in triglycerides when treated with lower concentrations of POA, yet when POA is in excess the tendency is toward the incorporation of POA into membrane phospholipids. This effect became more pronounced at later time points. In accordance with our electron microscopy data that showed that the *atg32Δ* mutant did not produce lipid droplets in response to POA, we also see that POA treated *atg32Δ* mutants tend to increase the molar proportion of their lipidome with POA containing phospholipids. This suggests that exogenously added POA enters yeast cells and is incorporated into triglycerides that are stored in lipid droplets when in present in the lowest tested concentrations. However, when POA is increased past a certain threshold, POA is instead incorporated into membrane phospholipids of the ER, Mitochondria, and PM. The extent

of this correlated with loss of clonogenicity as well as loss of membrane integrity as evidenced by permeability to propidium iodide²⁷. What is curious is that by genetically obstructing the cell from carrying out mitochondria specific macroautophagy, the extent of POA incorporation into phospholipids was greatly increased. This indicates that a functional pool of mitochondria is key to preventing this PCD modality. This could perhaps be due to an increase in the load of oxidatively stressed biomolecules as well as having lower net levels of ATP which would obstruct the capacity of the cell to store FFAs into neutral lipid stores in lipid droplets. More evidence from this came from our observation that the *atg32Δ* mutation completely abolished the presence of lipid droplets when cells were treated with POA.

Monitoring and maintenance of the proper asymmetrical distribution of membrane phospholipids is an essential cellular process which is controlled by the Rim101 pathway¹⁴⁰. We found that deletion of signalling components of the Rim101 pathway reduced susceptibility to POA induced liponecrotic cell death, while deletion of components that repress Rim101 signalling sensitized those cells to POA. This suggests that POA induced liponecrosis requires the Rim101 signalling pathway to commit to cell death. It is highly plausible that when the cellular concentration of POA exceeds a certain threshold, it is incorporated into phospholipids within the ER and then ultimately the plasma and mitochondrial membranes as well as potentially other biomembranes. In so doing, it changes the normal distribution of phospholipids in the plasma membrane causing an accumulation of negatively charged phospholipids in the outer leaflet of the plasma membrane. This was validated by our finding that treatment of cells with POA altered the proper asymmetry of phospholipids in the plasma membrane, namely a reduction of PE in the outer leaflet. This would likely induce the Rim101 pathway to commit yeast to PCD by further altering proper lipid asymmetry in the plasma membrane.

Because factors affecting lipid metabolism typically have pleiotropic effects it is likely that alterations to the cellular lipidome of POA treated cells will also have corresponding alterations to the mitochondrial lipidome. We found that a number of parameters of mitochondrial were altered by treatment with POA. In accordance with this model mitophagy plays an important role in maintaining a functional pool of mitochondria in the cell by maintaining their proper morphology, physiology, and lipid composition. This was demonstrated to be important for maintaining cellular redox homeostasis, where perturbations in mitochondrial quality control through mitochondria specific macroautophagy lead to increased accumulation of

protein carbonyls – which are indicative of oxidative stress to proteins – as well lipoperoxides – which are indicative of oxidatively damaged lipids. This may explain the observed increase in susceptibility of the *atg32Δ* mutant to liponecrotic cell death, as well as its generally shorter lifespan.

Our data also for the first time shows that mitophagy is necessary for caloric restriction to extend chronological lifespan in yeast, as well as for life extending bile acids to exert their effects. Lithocholic acid has previously been shown to greatly extend yeast chronological lifespan under both caloric restriction and normal conditions ²⁷. Our data indicates that loss of mitophagy results in deleterious alterations to the mitochondrial lipidome thus shortening CLS, whereas treatment of yeast cells with LCA resulted in alterations to the mitochondrial lipidome which extend yeast CLS. Together these data point towards a role for the mitochondrial lipidome in defining yeast longevity. Although the exact mechanisms still need to be elucidated we have shown that LCA accumulates primarily in the inner mitochondrial membrane, and that a number of measures of mitochondrial fitness are increased when cells are treated with LCA. This corresponds with the observed changes in mitochondrial morphology to further support the idea of a network regulating lipid metabolism, mitochondrial quality control, and longevity.

Based on our data we constructed the following model; POA enters yeast cells and initially is stored in LDs as neutral lipids (including TAGs). When the level of POA is above a certain threshold, the cell can no longer shunt FFA toward TAG biosynthesis, and POA inevitably accumulates in the membrane phospholipids of the ER. Because lipid metabolism is known to exist as a network spanning numerous organelles through membrane junctions, the change in lipid composition in the ER will lead to changes in the mitochondrial and plasma membranes. In so doing, this leads to loss in the functional integrity of the mitochondria resulting in a net energy deficit as well as the concomitant increase in ROS production leads to an increase in the abundance of oxidatively stressed biomolecules as well as insoluble protein aggregates. Furthermore, POA also alters the lipid composition of the PM that then will commit the cell to liponecrotic cell death. This is due to a change in the asymmetric distribution of PE across the outer leaflet of the plasma membrane. This imbalance in the proper lipid asymmetry homeostasis of the PM leads to the activation of the Rim101 signalling pathway which will activate the expression of Rsb1. Rsb1 then promotes a further exacerbation of the improper lipid asymmetry by negatively regulating Yor1 expression and negatively regulating Lem3 which is

known to be important for shuttling PE to outer or leaflet of the PM respectively. Thus, the extent of POA incorporation in phospholipids in the ER will determine the commitment of yeast cells to liponecrotic cell death.

Future Directions

- Left unmentioned was our findings that implicate components of both the apoptotic machinery (Richard et al. 2014 submitted) and the autophagic machinery¹²¹ in regulating liponecrosis. With this in mind another challenge for the future will be to try and explain whether and how liponecrosis is integrated into a PCD network that includes the apoptotic, necrotic, and autophagic modules of PCD.
- With regards to the importance of mitophagy as a pro-longevity process it would be interesting to understand which morphological and physiological features that dysfunctional mitochondria display are important for targeting these mitochondria for degradation via macromitophagy.
- Based on our model of how exogenously added POA induces liponecrosis, it would be interesting to understand how the observed depletion of PE in the outer (extracellular) leaflet of the PM of yeast cells exposed to POA elevates the permeability of this cellular membrane for small molecules. Since POA would also accumulate in the mitochondrial membrane phospholipidome, it would be interesting to see if this would alter vital mitochondrial processes such as respiration, membrane potential maintenance, ATP synthesis and ROS production.
- To further validate the role of the Rim101 pathway in committing yeast to liponecrotic cell death, it would be useful to use immunoblotting to verify that POA supplementation does in fact lead to the proteolytic activation of Rim101.
- With regards to the role of LCA in extending yeast CLS it would be critical to find out what are the identities of cellular proteins involved in the translocation of exogenously added LCA across the plasma membrane and its subsequent incorporation into the both the inner and outer mitochondrial membranes. Once discovered, genetic manipulations eliminating these components will allow us to know whether it really is the accumulation of LCA in the mitochondrial membranes that is necessary for its ability to extend longevity. If it really is the presence of LCA in the IMM, then does it specifically alter

the functions of proteins involved in mitochondrial phospholipid biosynthetic machinery like Psd1p and Crd1p ⁶⁶. Along these lines, it would be interesting to understand whether Ups1-dependent shuttling of PA from the OMM to the IMM, as well as the shuttling of PA from the MAM to the OMM would prove to be necessary for LCA to extend lifespan

8. References

1. Kirkwood, T. B. L. Understanding ageing from an evolutionary perspective. *J. Intern. Med.* **263**, 117–27 (2008).
2. Kaeberlein, M. Lessons on longevity from budding yeast. *Nature* **464**, 513–9 (2010).
3. Fontana, L., Partridge, L. & Longo, V. D. Extending healthy life span--from yeast to humans. *Science* **328**, 321–326 (2010).
4. Longo, V. D., Mitteldorf, J. & Skulachev, V. P. Programmed and altruistic ageing. *Nat. Rev. Genet.* **6**, 866–72 (2005).
5. Steinkraus, K. A., Kaeberlein, M. & Kennedy, B. K. Replicative aging in yeast: the means to the end. *Annu. Rev. Cell Dev. Biol.* **24**, 29–54 (2008).
6. Longo, V. D., Shadel, G. S., Kaeberlein, M. & Kennedy, B. Replicative and chronological aging in *saccharomyces cerevisiae*. *Cell Metab.* **16**, 18–31 (2012).
7. Johnson, S. C., Rabinovitch, P. S. & Kaeberlein, M. mTOR is a key modulator of ageing and age-related disease. *Nature* **493**, 338–45 (2013).
8. Greer, E. L. & Brunet, A. Signaling networks in aging. *J. Cell Sci.* **121**, 407–12 (2008).
9. Wei, M. *et al.* Life span extension by calorie restriction depends on Rim15 and transcription factors downstream of Ras/PKA, Tor, and Sch9. *PLoS Genet.* **4**, 0139–0149 (2008).
10. Wei, M. *et al.* Calorie restriction-induced life span extension depends on Rim15 and stress response transcription factors downstream of Ras/cAMP/PKA, Tor and Sch9. *PLoS Genet.* **preprint**, e13.eor EP – (2007).
11. Guevara-Aguirre, J. *et al.* Growth hormone receptor deficiency is associated with a major reduction in pro-aging signaling, cancer, and diabetes in humans. *Sci. Transl. Med.* **3**, 70ra13 (2011).
12. Lin, S.-J. Requirement of NAD and SIR2 for Life-Span Extension by Calorie Restriction in *Saccharomyces cerevisiae*. *Science (80-.)*. **289**, 2126–2128 (2000).
13. Goldberg, A. A. *et al.* Effect of calorie restriction on the metabolic history of chronologically aging yeast. *Exp. Gerontol.* **44**, 555–71 (2009).

14. Medvedik, O., Lamming, D. W., Kim, K. D. & Sinclair, D. A. MSN2 and MSN4 link calorie restriction and TOR to sirtuin-mediated lifespan extension in *Saccharomyces cerevisiae*. *PLoS Biol.* **5**, e261 (2007).
15. Kaeberlein, M. *et al.* Regulation of yeast replicative life span by TOR and Sch9 in response to nutrients. *Science* **310**, 1193–6 (2005).
16. Wei, M. *et al.* Life span extension by calorie restriction depends on Rim15 and transcription factors downstream of Ras/PKA, Tor, and Sch9. *PLoS Genet.* **4**, e13 (2008).
17. Blagosklonny, M. V. Calorie restriction: Decelerating mTOR-driven aging from cells to organisms (including humans). *Cell Cycle* **9**, 683–688 (2010).
18. Ingram, D. K. *et al.* Calorie restriction mimetics: an emerging research field. *Aging Cell* **5**, 97–108 (2006).
19. Lane, M. A., Roth, G. S. & Ingram, D. K. Caloric restriction mimetics: a novel approach for biogerontology. *Methods Mol. Biol.* **371**, 143–9 (2007).
20. Timmers, S. *et al.* Calorie restriction-like effects of 30 days of resveratrol supplementation on energy metabolism and metabolic profile in obese humans. *Cell Metab.* **14**, 612–22 (2011).
21. Wanke, V. *et al.* Caffeine extends yeast lifespan by targeting TORC1. *Mol. Microbiol.* **69**, 277–85 (2008).
22. Wood, J. G. *et al.* Sirtuin activators mimic caloric restriction and delay ageing in metazoans. *Nature* **430**, 686–9 (2004).
23. Baur, J. A. *et al.* Resveratrol improves health and survival of mice on a high-calorie diet. *Nature* **444**, 337–42 (2006).
24. Onken, B. & Driscoll, M. Metformin induces a dietary restriction-like state and the oxidative stress response to extend *C. elegans* Healthspan via AMPK, LKB1, and SKN-1. *PLoS One* **5**, e8758 (2010).
25. Bjedov, I. *et al.* Mechanisms of life span extension by rapamycin in the fruit fly *Drosophila melanogaster*. *Cell Metab.* **11**, 35–46 (2010).
26. McColl, G. *et al.* Pharmacogenetic analysis of lithium-induced delayed aging in *Caenorhabditis elegans*. *J. Biol. Chem.* **283**, 350–7 (2008).
27. Goldberg, A. *et al.* Chemical genetic screen identifies lithocholic acid as an anti-aging compound that extends yeast chronological life span in a TOR-independent manner, by modulating housekeeping longevity assurance processes. *Aging (Albany, NY)*. **2**, 393–414 (2010).

28. Zhao, J. *et al.* Short leukocyte telomere length predicts risk of diabetes in American Indians: the Strong Heart Family Study. *Diabetes* **63**, 354–62 (2014).
29. Zhao, J. *et al.* Metabolic profiles of biological aging in American Indians: the Strong Heart Family Study. *Aging (Albany, NY)*. **6**, 176–86 (2014).
30. Greenwood, M. T. & Ludovico, P. Expressing and functional analysis of mammalian apoptotic regulators in yeast. *Cell Death Differ.* **17**, 737–745 (2010).
31. Bitterman, K. J., Medvedik, O. & Sinclair, D. A. Longevity Regulation in *Saccharomyces cerevisiae*: Linking Metabolism, Genome Stability, and Heterochromatin. *Microbiol. Mol. Biol. Rev.* **67**, 376–399 (2003).
32. Beach, A. & Titorenko, V. I. In search of housekeeping pathways that regulate longevity. *Cell Cycle* **10**, 3042–4 (2011).
33. Eisenberg, T. & Büttner, S. Lipids and cell death in yeast. *FEMS Yeast Res.* 1–19 (2013). doi:10.1111/1567-1364.12105
34. Kroemer, G. *et al.* Classification of cell death: recommendations of the Nomenclature Committee on Cell Death 2009. *Cell Death Differ.* **16**, 3–11 (2009).
35. Kepp, O., Galluzzi, L., Lipinski, M., Yuan, J. & Kroemer, G. Cell death assays for drug discovery. *Nat. Rev. Drug Discov.* **10**, 221–37 (2011).
36. Edinger, A. L. & Thompson, C. B. Death by design: apoptosis, necrosis and autophagy. *Curr. Opin. Cell Biol.* **16**, 663–9 (2004).
37. Goldberg, A. A. *et al.* A novel function of lipid droplets in regulating longevity. *Biochem. Soc. Trans.* **37**, 1050–5 (2009).
38. Beach, A. *et al.* Integration of peroxisomes into an endomembrane system that governs cellular aging. *Front. Physiol.* **3**, 283 (2012).
39. Burstein, M. T. *et al.* Lithocholic acid extends longevity of chronologically aging yeast only if added at certain critical periods of their lifespan. *Cell Cycle* **11**, 3443–62 (2012).
40. Beach, A. *et al.* Mitochondrial membrane lipidome defines yeast longevity. *Aging (Albany, NY)*. **5**, 551–574 (2013).
41. Brown, L.-A. & Baker, A. Peroxisome biogenesis and the role of protein import. *J. Cell. Mol. Med.* **7**, 388–400
42. Bourque, S. D. & Titorenko, V. I. A quantitative assessment of the yeast lipidome using electrospray ionization mass spectrometry. *J. Vis. Exp.* (2009). doi:10.3791/1513

43. BLIGH, E. G. & DYER, W. J. A rapid method of total lipid extraction and purification. *Can. J. Biochem. Physiol.* **37**, 911–917 (1959).
44. Smets, B. *et al.* Life in the midst of scarcity: Adaptations to nutrient availability in *Saccharomyces cerevisiae*. *Curr. Genet.* **56**, 1–32 (2010).
45. Ptacek, J. *et al.* Global analysis of protein phosphorylation in yeast. *Nature* **438**, 679–684 (2005).
46. Low, C. P., Liew, L. P., Pervaiz, S. & Yang, H. Apoptosis and lipoapoptosis in the fission yeast *Schizosaccharomyces pombe*. in *FEMS Yeast Res.* **5**, 1199–1206 (2005).
47. Beach, A. *et al.* Mitochondrial membrane lipidome defines yeast longevity. *Aging (Albany. NY)*. **5**, 551–74 (2013).
48. Green, D. R., Galluzzi, L. & Kroemer, G. Mitochondria and the autophagy-inflammation-cell death axis in organismal aging. *Science* **333**, 1109–1112 (2011).
49. Breitenbach, M. *et al.* The role of mitochondria in the aging processes of yeast. *Subcell. Biochem.* **57**, 55–78 (2012).
50. Nunnari, J. & Suomalainen, A. Mitochondria: In sickness and in health. *Cell* **148**, 1145–1159 (2012).
51. Leonov, A. & Titorenko, V. I. A network of interorganellar communications underlies cellular aging. *IUBMB Life* **65**, 665–74 (2013).
52. López-Otín, C., Blasco, M. A., Partridge, L., Serrano, M. & Kroemer, G. XThe hallmarks of aging. *Cell* **153**, (2013).
53. Bratic, A. & Larsson, N.-G. The role of mitochondria in aging. *J. Clin. Invest.* **123**, 951–7 (2013).
54. Gomez, L. A. & Hagen, T. M. Age-related decline in mitochondrial bioenergetics: Does supercomplex destabilization determine lower oxidative capacity and higher superoxide production? *Semin. Cell Dev. Biol.* **23**, 758–767 (2012).
55. Schroeder, E. A., Raimundo, N. & Shadel, G. S. Epigenetic silencing mediates mitochondria stress-induced longevity. *Cell Metab.* **17**, 954–964 (2013).
56. Weyemi, U., Parekh, P. R., Redon, C. E. & Bonner, W. M. SOD2 deficiency promotes aging phenotypes in mouse skin. *Aging (Albany. NY)*. **4**, 116–8 (2012).
57. Barrientos, A. Complementary roles of mitochondrial respiration and ROS signaling on cellular aging and longevity. *Aging (Albany. NY)*. **4**, 578–9 (2012).

58. Ristow, M. & Schmeisser, S. Extending life span by increasing oxidative stress. *Free Radic. Biol. Med.* **51**, 327–336 (2011).
59. Pan, Y., Schroeder, E. A., Ocampo, A., Barrientos, A. & Shadel, G. S. Regulation of yeast chronological life span by TORC1 via adaptive mitochondrial ROS signaling. *Cell Metab.* **13**, 668–678 (2011).
60. Trinei, M. *et al.* P66Shc signals to age. *Aging (Albany, NY. Online)* **1**, 503–510 (2009).
61. Sheibani, S. *et al.* Supplemental Material to : **13**, 1–4 (2014).
62. Richard, V. R. *et al.* Macromitophagy is a longevity assurance process that in chronologically aging yeast limited in calorie supply sustains functional mitochondria and maintains cellular lipid homeostasis. *Aging (Albany, NY)*. **5**, 234–69 (2013).
63. Gregg, C., Kyryakov, P. & Titorenko, V. I. Purification of mitochondria from yeast cells. *J. Vis. Exp.* (2009). doi:10.3791/1417
64. Klose, C. *et al.* Flexibility of a eukaryotic lipidome - insights from yeast lipidomics. *PLoS One* **7**, (2012).
65. Guo, T. *et al.* A signal from inside the peroxisome initiates its division by promoting the remodeling of the peroxisomal membrane. *J. Cell Biol.* **177**, 289–303 (2007).
66. Osman, C., Voelker, D. R. & Langer, T. Making heads or tails of phospholipids in mitochondria. *J. Cell Biol.* **192**, 7–16 (2011).
67. Rowland, A. A. & Voeltz, G. K. Endoplasmic reticulum–mitochondria contacts: function of the junction. *Nat. Rev. Mol. Cell Biol.* **13**, 607–625 (2012).
68. Connerth, M. *et al.* Intramitochondrial transport of phosphatidic acid in yeast by a lipid transfer protein. *Science* **338**, 815–8 (2012).
69. Tamura, Y. *et al.* Tam41 is a CDP-diacylglycerol synthase required for cardiolipin biosynthesis in mitochondria. *Cell Metab.* **17**, 709–718 (2013).
70. Schulz, T. J. *et al.* Glucose Restriction Extends *Caenorhabditis elegans* Life Span by Inducing Mitochondrial Respiration and Increasing Oxidative Stress. *Cell Metab.* **6**, 280–293 (2007).
71. McMahon, H. T. & Gallop, J. L. Membrane curvature and mechanisms of dynamic cell membrane remodelling. *Nature* **438**, 590–6 (2005).
72. Zimmerberg, J. & Kozlov, M. M. How proteins produce cellular membrane curvature. *Nat. Rev. Mol. Cell Biol.* **7**, 9–19 (2006).

73. Klose, C. *et al.* Flexibility of a eukaryotic lipidome - insights from yeast lipidomics. *PLoS One* **7**, (2012).
74. Zimmerberg, J. Membrane biophysics. *Curr. Biol.* **16**, (2006).
75. Van Meer, G., Voelker, D. R. & Feigenson, G. W. Membrane lipids: where they are and how they behave. *Nat. Rev. Mol. Cell Biol.* **9**, 112–124 (2008).
76. Joshi, A. S., Thompson, M. N., Fei, N., Hüttemann, M. & Greenberg, M. L. Cardiolipin and mitochondrial phosphatidylethanolamine have overlapping functions in mitochondrial fusion in *Saccharomyces cerevisiae*. *J. Biol. Chem.* **287**, 17589–97 (2012).
77. Claypool, S. M. & Koehler, C. M. The complexity of cardiolipin in health and disease. *Trends Biochem. Sci.* **37**, 32–41 (2012).
78. Henry, S. A., Kohlwein, S. D. & Carman, G. M. Metabolism and regulation of glycerolipids in the yeast *Saccharomyces cerevisiae*. *Genetics* **190**, 317–49 (2012).
79. Choi, S.-Y. *et al.* A common lipid links Mfn-mediated mitochondrial fusion and SNARE-regulated exocytosis. *Nat. Cell Biol.* **8**, 1255–1262 (2006).
80. Huang, H. & Frohman, M. A. Lipid signaling on the mitochondrial surface. *Biochim. Biophys. Acta - Mol. Cell Biol. Lipids* **1791**, 839–844 (2009).
81. McMahon, H. T. & Gallop, J. L. Membrane curvature and mechanisms of dynamic cell membrane remodelling. *Nature* **438**, 590–596 (2005).
82. Kanki, T. *et al.* A genomic screen for yeast mutants defective in selective mitochondria autophagy. *Mol. Biol. Cell* **20**, 4730–8 (2009).
83. Kondo-Okamoto, N. *et al.* Autophagy-related protein 32 acts as autophagic degron and directly initiates mitophagy. *J. Biol. Chem.* **287**, 10631–8 (2012).
84. Okamoto, K., Kondo-Okamoto, N. & Ohsumi, Y. Mitochondria-anchored receptor Atg32 mediates degradation of mitochondria via selective autophagy. *Dev. Cell* **17**, 87–97 (2009).
85. May, A. I., Devenish, R. J. & Prescott, M. The many faces of mitochondrial autophagy: making sense of contrasting observations in recent research. *Int. J. Cell Biol.* **2012**, 431684 (2012).
86. Bhatia-Kishore, I. & Camougrand, N. Mitophagy in yeast: Actors and physiological roles. *FEMS Yeast Res.* **10**, 1023–1034 (2010).
87. Kanki, T., Klionsky, D. J. & Okamoto, K. Mitochondria autophagy in yeast. *Antioxid. Redox Signal.* **14**, 1989–2001 (2011).

88. Yen, W.-L. & Klionsky, D. J. How to live long and prosper: autophagy, mitochondria, and aging. *Physiology (Bethesda)*. **23**, 248–262 (2008).
89. Kanki, T. & Klionsky, D. J. The molecular mechanism of mitochondria autophagy in yeast: MicroReview. *Mol. Microbiol.* **75**, 795–800 (2010).
90. Youle, R. J. & Narendra, D. P. Mechanisms of mitophagy. *Nat. Rev. Mol. Cell Biol.* **12**, 9–14 (2011).
91. Lee, J., Giordano, S. & Zhang, J. Autophagy, mitochondria and oxidative stress: cross-talk and redox signalling. *Biochem. J.* **441**, 523–540 (2011).
92. Hirota, Y., Kang, D. & Kanki, T. The physiological role of mitophagy: New insights into phosphorylation events. *Int. J. Cell Biol.* (2012). doi:10.1155/2012/354914
93. Vazquez-Martin, A. *et al.* Mitochondrial fusion by pharmacological manipulation impedes somatic cell reprogramming to pluripotency: new insight into the role of mitophagy in cell stemness. *Aging (Albany, NY)*. **4**, 393–401 (2012).
94. Friedman, J. R. & Voeltz, G. K. The ER in 3D: A multifunctional dynamic membrane network. *Trends Cell Biol.* **21**, 709–717 (2011).
95. Elbaz, Y. & Schuldiner, M. Staying in touch: The molecular era of organelle contact sites. *Trends Biochem. Sci.* **36**, 616–623 (2011).
96. Carrasco, S. & Meyer, T. STIM proteins and the endoplasmic reticulum-plasma membrane junctions. *Annu. Rev. Biochem.* **80**, 973–1000 (2011).
97. Rieder, S. E. & Emr, S. D. Isolation of subcellular fractions from the yeast *Saccharomyces cerevisiae*. *Curr. Protoc. Cell Biol.* **Chapter 3**, Unit 3.8 (2001).
98. Panaretou, B. & Piper, P. Isolation of yeast plasma membranes. *Methods Mol. Biol.* **313**, 27–32 (2006).
99. Lev, S. Non-vesicular lipid transport by lipid-transfer proteins and beyond. *Nat. Rev. Mol. Cell Biol.* **11**, 739–750 (2010).
100. Lebedzinska, M., Szabadkai, G., Jones, A. W. E., Duszynski, J. & Wieckowski, M. R. Interactions between the endoplasmic reticulum, mitochondria, plasma membrane and other subcellular organelles. *Int. J. Biochem. Cell Biol.* **41**, 1805–1816 (2009).
101. Levine, T. Short-range intracellular trafficking of small molecules across endoplasmic reticulum junctions. *Trends Cell Biol.* **14**, 483–490 (2004).
102. Titorenko, V. I. & Terlecky, S. R. Peroxisome Metabolism and Cellular Aging. *Traffic* **12**, 252–259 (2011).

103. Sorice, M. *et al.* Cardiolipin-enriched raft-like microdomains are essential activating platforms for apoptotic signals on mitochondria. *FEBS Lett.* **583**, 2447–2450 (2009).
104. Gonzalvez, F. *et al.* Cardiolipin provides an essential activating platform for caspase-8 on mitochondria. *J. Cell Biol.* **183**, 681–696 (2008).
105. Rubinsztein, D. C., Shpilka, T. & Elazar, Z. Mechanisms of autophagosome biogenesis. *Curr. Biol.* **22**, (2012).
106. Knøvelsrud, H. & Simonsen, A. Lipids in autophagy: Constituents, signaling molecules and cargo with relevance to disease. *Biochim. Biophys. Acta - Mol. Cell Biol. Lipids* **1821**, 1133–1145 (2012).
107. Hailey, D. W. *et al.* Mitochondria Supply Membranes for Autophagosome Biogenesis during Starvation. *Cell* **141**, 656–667 (2010).
108. Galluzzi, L. *et al.* Molecular definitions of cell death subroutines: recommendations of the Nomenclature Committee on Cell Death 2012. *Cell Death Differ.* **19**, 107–120 (2012).
109. Eisenberg, T., Carmona-Gutierrez, D., Böttner, S., Tavernarakis, N. & Madeo, F. Necrosis in yeast. *Apoptosis* **15**, 257–268 (2010).
110. Kourtis, N. & Tavernarakis, N. Autophagy and cell death in model organisms. *Cell Death Differ.* **16**, 21–30 (2009).
111. Carmona-Gutierrez, D. *et al.* Apoptosis in yeast: triggers, pathways, subroutines. *Cell Death Differ.* **17**, 763–773 (2010).
112. Rockenfeller, P. *et al.* Fatty acids trigger mitochondrion-dependent necrosis. *Cell Cycle* **9**, 2836–2842 (2010).
113. Carmona-Gutiérrez, D. *et al.* The propeptide of yeast cathepsin D inhibits programmed necrosis. *Cell Death Dis.* **2**, e161 (2011).
114. Dziejic, S. A. & Caplan, A. B. Autophagy proteins play cytoprotective and cytotoxic roles in leucine starvation-induced cell death in *Saccharomyces cerevisiae*. *Autophagy* **8**, 731–738 (2012).
115. Munoz, A. J., Wanichthanarak, K., Meza, E. & Petranovic, D. Systems biology of yeast cell death. *FEMS Yeast Res.* **12**, 249–265 (2012).
116. Burstein, M. T. *et al.* Lithocholic acid extends longevity of chronologically aging yeast only if added at certain critical periods of their lifespan. *Cell Cycle* **11**, 3443–3462 (2012).
117. Bascom, R. A., Chan, H. & Rachubinski, R. A. Peroxisome biogenesis occurs in an unsynchronized manner in close association with the endoplasmic reticulum in

- temperature-sensitive *Yarrowia lipolytica* Pex3p mutants. *Mol. Biol. Cell* **14**, 939–957 (2003).
118. Madeo, F., Fröhlich, E. & Fröhlich, K. U. A yeast mutant showing diagnostic markers of early and late apoptosis. *J. Cell Biol.* **139**, 729–734 (1997).
 119. Lison, S., Goodman, J. M. & Subramani, S. Uniqueness of the mechanism of protein import into the peroxisome matrix: Transport of folded, co-factor-bound and oligomeric proteins by shuttling receptors. *Biochim. Biophys. Acta - Mol. Cell Res.* **1763**, 1552–1564 (2006).
 120. Kanki, T., Wang, K., Cao, Y., Baba, M. & Klionsky, D. J. Atg32 Is a Mitochondrial Protein that Confers Selectivity during Mitophagy. *Dev. Cell* **17**, 98–109 (2009).
 121. Sheibani, S., Richard, V. & Beach, A. Macromitophagy, neutral lipids synthesis, and peroxisomal fatty acid oxidation protect yeast from “liponecrosis”, a previously unknown form of programmed cell. *Cell* ... 1–10 (2013). at <https://orphanresearch.org/journals/cc/2013CC5339R.pdf>
 122. Shen, H.-M. & Codogno, P. Autophagic cell death: Loch Ness monster or endangered species? *Autophagy* **7**, 457–465 (2011).
 123. Eisenberg, T. *et al.* Induction of autophagy by spermidine promotes longevity. *Nat. Cell Biol.* **11**, 1305–1314 (2009).
 124. Kohlwein, S. D., Veenhuis, M. & van der Klei, I. J. Lipid droplets and peroxisomes: key players in cellular lipid homeostasis or a matter of fat--store 'em up or burn 'em down. *Genetics* **193**, 1–50 (2013).
 125. Denton, D., Nicolson, S. & Kumar, S. Cell death by autophagy: facts and apparent artefacts. *Cell Death Differ.* **19**, 87–95 (2012).
 126. Ocampo, A., Liu, J., Schroeder, E. A., Shadel, G. S. & Barrientos, A. Mitochondrial respiratory thresholds regulate yeast chronological life span and its extension by caloric restriction. *Cell Metab.* **16**, 55–67 (2012).
 127. Titorenko, V. I. & Rachubinski, R. A. Chapter 5 Spatiotemporal Dynamics of the ER-derived Peroxisomal Endomembrane System. *Int. Rev. Cell Mol. Biol.* **272**, 191–244 (2008).
 128. Reggiori, F. & Klionsky, D. J. Autophagic processes in yeast: mechanism, machinery and regulation. *Genetics* **194**, 341–61 (2013).
 129. Gozuacik, D. *et al.* DAP-kinase is a mediator of endoplasmic reticulum stress-induced caspase activation and autophagic cell death. *Cell Death Differ.* **15**, 1875–1886 (2008).

130. Eisenberg-Lerner, A., Bialik, S., Simon, H.-U. & Kimchi, A. Life and death partners: apoptosis, autophagy and the cross-talk between them. *Cell Death Differ.* **16**, 966–975 (2009).
131. Bialik, S., Zalckvar, E., Ber, Y., Rubinstein, A. D. & Kimchi, A. Systems biology analysis of programmed cell death. *Trends Biochem. Sci.* **35**, 556–564 (2010).
132. Zalckvar, E., Bialik, S. & Kimchi, A. The road not taken: a systems level strategy for analyzing the cell death network. *Autophagy* **6**, 813–815 (2010).
133. Zalckvar, E. *et al.* A systems level strategy for analyzing the cell death network: implication in exploring the apoptosis/autophagy connection. *Cell Death Differ.* **17**, 1244–1253 (2010).
134. Rubinstein, A. D. & Kimchi, A. Life in the balance - a mechanistic view of the crosstalk between autophagy and apoptosis. *J. Cell Sci.* **125**, 5259–68 (2012).
135. Young, M. M., Kester, M. & Wang, H.-G. Sphingolipids: regulators of crosstalk between apoptosis and autophagy. *J. Lipid Res.* **54**, 5–19 (2013).
136. Carmona-Gutierrez, D. *et al.* Ceramide triggers metacaspase-independent mitochondrial cell death in yeast. *Cell Cycle* **10**, 3973–3978 (2011).
137. Zhang, Q. *et al.* Schizosaccharomyces pombe cells deficient in triacylglycerols synthesis undergo apoptosis upon entry into the stationary phase. *J. Biol. Chem.* **278**, 47145–47155 (2003).
138. Sheibani, S. *et al.* Macromitophagy, neutral lipids synthesis, and peroxisomal fatty acid oxidation protect yeast from “liponecrosis”, a previously unknown form of programmed cell death. *Cell Cycle* **13**, 138–47 (2014).
139. Richard, V. R. *et al.* Macromitophagy is a longevity assurance process that in chronologically aging yeast limited in calorie supply sustains functional mitochondria and maintains cellular lipid homeostasis. *Aging (Albany, NY)*. **5**, 234–69 (2013).
140. Ikeda, M., Kihara, A., Denpoh, A. & Igarashi, Y. The Rim101 pathway is involved in Rsb1 expression induced by altered lipid asymmetry. *Mol. Biol. Cell* **19**, 1922–31 (2008).
141. Kyryakov, P. *et al.* Caloric restriction extends yeast chronological lifespan by altering a pattern of age-related changes in trehalose concentration. *Front. Physiol.* **3**, 256 (2012).
142. Titorenko, V. I., Smith, J. J., Szilard, R. K. & Rachubinski, R. A. Pex20p of the yeast *Yarrowia lipolytica* is required for the oligomerization of thiolase in the cytosol and for its targeting to the peroxisome. *J. Cell Biol.* **142**, 403–420 (1998).

143. Okamoto, K., Kondo-Okamoto, N. & Ohsumi, Y. Mitochondria-Anchored Receptor Atg32 Mediates Degradation of Mitochondria via Selective Autophagy. *Dev. Cell* **17**, 87–97 (2009).
144. Horvath, S. E. & Daum, G. Lipids of mitochondria. *Prog. Lipid Res.* **52**, 590–614 (2013).
145. Tavassoli, S. *et al.* Plasma membrane--endoplasmic reticulum contact sites regulate phosphatidylcholine synthesis. *EMBO Rep.* **14**, 434–40 (2013).
146. Tatsuta, T., Scharwey, M. & Langer, T. Mitochondrial lipid trafficking. *Trends Cell Biol.* **24**, 44–52 (2014).
147. Markgraf, D. *et al.* An ER protein functionally couples neutral lipid metabolism on lipid droplets to membrane lipid synthesis in the ER. *Cell Rep.* **6**, 44–55 (2014).
148. Faergeman, N. J., DiRusso, C. C., Elberger, A., Knudsen, J. & Black, P. N. Disruption of the *Saccharomyces cerevisiae* homologue to the murine fatty acid transport protein impairs uptake and growth on long-chain fatty acids. *J. Biol. Chem.* **272**, 8531–8538 (1997).
149. Young, B. P. *et al.* Phosphatidic acid is a pH biosensor that links membrane biogenesis to metabolism. *Science* **329**, 1085–1088 (2010).
150. Porat, Z., Wender, N., Erez, O. & Kahana, C. Mechanism of polyamine tolerance in yeast: Novel regulators and insights. *Cell. Mol. Life Sci.* **62**, 3106–3116 (2005).
151. Sychrov??, H., Ram??rez, J. & Pe??a, A. Involvement of Nha1 antiporter in regulation of intracellular pH in *Saccharomyces cerevisiae*. *FEMS Microbiol. Lett.* **171**, 167–172 (1999).
152. Orij, R., Brul, S. & Smits, G. J. Intracellular pH is a tightly controlled signal in yeast. *Biochim. Biophys. Acta - Gen. Subj.* **1810**, 933–944 (2011).
153. Maeda, T. The signaling mechanism of ambient pH sensing and adaptation in yeast and fungi. *FEBS J.* **279**, 1407–13 (2012).
154. Van Meer, G. Dynamic transbilayer lipid asymmetry. *Cold Spring Harb. Perspect. Biol.* **3**, (2011).
155. Mattiazzi, M. *et al.* Genetic interactions between a phospholipase A2 and the Rim101 pathway components in *S. cerevisiae* reveal a role for this pathway in response to changes in membrane composition and shape. *Mol. Genet. Genomics* **283**, 519–30 (2010).
156. Fadeel, B. & Xue, D. The ins and outs of phospholipid asymmetry in the plasma membrane: roles in health and disease. *Crit. Rev. Biochem. Mol. Biol.* **44**, 264–77

157. Manente, M. & Ghislain, M. The lipid-translocating exporter family and membrane phospholipid homeostasis in yeast. *FEMS Yeast Res.* **9**, 673–87 (2009).
158. Obara, K., Yamamoto, H. & Kihara, A. Membrane Protein Rim21 Plays a Central Role in Sensing Ambient pH in *Saccharomyces Cerevisiae*. *J. Biol. Chem.* (2012). doi:10.1074/jbc.M112.394205
159. Barwell, K. J., Boysen, J. H., Xu, W. & Mitchell, A. P. Relationship of DFG16 to the Rim101p pH response pathway in *Saccharomyces cerevisiae* and *Candida albicans*. *Eukaryot. Cell* **4**, 890–899 (2005).
160. Shukla, A. K., Xiao, K. & Lefkowitz, R. J. Emerging paradigms of ??-arrestin-dependent seven transmembrane receptor signaling. *Trends Biochem. Sci.* **36**, 457–469 (2011).
161. Xu, W., Smith, F. J., Subaran, R. & Mitchell, A. P. Multivesicular body-ESCRT components function in pH response regulation in *Saccharomyces cerevisiae* and *Candida albicans*. *Mol. Biol. Cell* **15**, 5528–5537 (2004).
162. Hayashi, M., Fukuzawa, T., Sorimachi, H. & Maeda, T. Constitutive activation of the pH-responsive Rim101 pathway in yeast mutants defective in late steps of the MVB/ESCRT pathway. *Mol. Cell. Biol.* **25**, 9478–9490 (2005).
163. Babst, M., Katzmann, D. J., Estepa-Sabal, E. J., Meerloo, T. & Emr, S. D. ESCRT-III: An endosome-associated heterooligomeric protein complex required for MVB sorting. *Dev. Cell* **3**, 271–282 (2002).
164. Weiss, P., Huppert, S. & Kölling, R. Analysis of the dual function of the ESCRT-III protein Snf7 in endocytic trafficking and in gene expression. *Biochem. J.* **424**, 89–97 (2009).
165. Lamb, T. M. & Mitchell, A. P. The transcription factor Rim101p governs ion tolerance and cell differentiation by direct repression of the regulatory genes NRG1 and SMP1 in *Saccharomyces cerevisiae*. *Mol. Cell. Biol.* **23**, 677–686 (2003).
166. Kihara, A. & Igarashi, Y. Identification and characterization of a *Saccharomyces cerevisiae* gene, RSB1, involved in sphingoid long-chain base release. *J. Biol. Chem.* **277**, 30048–30054 (2002).
167. Kato, U. *et al.* A novel membrane protein, Ros3p, is required for phospholipid translocation across the plasma membrane in *Saccharomyces cerevisiae*. *J. Biol. Chem.* **277**, 37855–37862 (2002).
168. Kihara, A. & Igarashi, Y. Cross talk between sphingolipids and glycerophospholipids in the establishment of plasma membrane asymmetry. *Mol. Biol. Cell* **15**, 4949–59 (2004).

169. Aoki, Y., Uenaka, T., Aoki, J., Umeda, M. & Inoue, K. A novel peptide probe for studying the transbilayer movement of phosphatidylethanolamine. *J. Biochem.* **116**, 291–297 (1994).
170. Nakatogawa, H., Suzuki, K., Kamada, Y. & Ohsumi, Y. Dynamics and diversity in autophagy mechanisms: lessons from yeast. *Nat. Rev. Mol. Cell Biol.* **10**, 458–467 (2009).
171. Inoue, Y. & Klionsky, D. J. Regulation of macroautophagy in *Saccharomyces cerevisiae*. *Semin. Cell Dev. Biol.* **21**, 664–670 (2010).
172. Matsuura, A., Tsukada, M., Wada, Y. & Ohsumi, Y. Apg1p, a novel protein kinase required for the autophagic process in *Saccharomyces cerevisiae*. *Gene* **192**, 245–250 (1997).
173. Motley, A. M., Nuttall, J. M. & Hettema, E. H. Pex3-anchored Atg36 tags peroxisomes for degradation in *Saccharomyces cerevisiae*. *EMBO J.* **31**, 2852–2868 (2012).
174. Fonzi, W. A. & Sypherd, P. S. The gene and the primary structure of ornithine decarboxylase from *Saccharomyces cerevisiae*. *J. Biol. Chem.* **262**, 10127–10133 (1987).
175. Minois, N., Carmona-Gutierrez, D. & Madeo, F. Polyamines in aging and disease. *Aging (Albany NY)* **3**, 716–32 (2011).
176. Hamasaki-Katagiri, N., Tabor, C. W. & Tabor, H. Spermidine biosynthesis in *Saccharomyces cerevisiae*: Polyamine requirement of a null mutant of the SPE3 gene (spermidine synthase). *Gene* **187**, 35–43 (1997).
177. Kashiwagi, K., Taneja, S. K., Liu, T. Y., Tabor, C. W. & Tabor, H. Spermidine biosynthesis in *Saccharomyces cerevisiae*. Biosynthesis and processing of a proenzyme form of S-adenosylmethionine decarboxylase. *J. Biol. Chem.* **265**, 22321–22328 (1990).
178. Narasimhan, S. D., Yen, K. & Tissenbaum, H. A. Converging Pathways in Lifespan Regulation. *Curr. Biol.* **19**, (2009).
179. Kaeberlein, M. Lessons on longevity from budding yeast. **464**, 513–519 (2010).
180. Kenyon, C. J. The genetics of ageing. *Nature* **464**, 504–12 (2010).
181. Kirkwood, T. B. L. *et al.* Towards an e-biology of ageing: integrating theory and data. *Nat. Rev. Mol. Cell Biol.* **4**, 243–249 (2003).
182. Murphy, M. P. & Partridge, L. Toward a control theory analysis of aging. *Annu Rev Biochem* **77**, 777–798 (2008).
183. Antebi, A. Physiology. The tick-tock of aging? *Science* **310**, 1911–3 (2005).

184. Blagosklonny, M. V. Paradoxes of aging. *Cell Cycle* **6**, 2997–3003 (2007).
185. Blagosklonny, M. V. Program-like aging and mitochondria: Instead of random damage by free radicals. *J. Cell. Biochem.* **102**, 1389–1399 (2007).
186. Budovskaya, Y. V. *et al.* An elt-3/elt-5/elt-6 GATA Transcription Circuit Guides Aging in *C. elegans*. *Cell* **134**, 291–303 (2008).
187. Kirkwood, T. B. L. Understanding the odd science of aging. *Cell* **120**, 437–47 (2005).
188. Lithgow, G. J. Why aging isn't regulated: A lamentation on the use of language in aging literature. *Exp. Gerontol.* **41**, 890–893 (2006).
189. Lin, S. Molecular mechanisms of aging: insights from budding yeast. *COLD SPRING Harb. Monogr. ...* (2008). at
<http://books.google.com/books?hl=en&lr=&id=Wgx4iBZ60RQC&oi=fnd&pg=PA483&dq=fob1+conservation&ots=ATsP_scgso&sig=4lhZe0rxPQn5Vh6od-zHIwgtWE4npapers2://publication/uuid/0C9C6D9E-19E1-4759-8627-1869514DC2DC>
190. Mair, W. & Dillin, A. Aging and survival: the genetics of life span extension by dietary restriction. *Annu. Rev. Biochem.* **77**, 727–754 (2008).
191. Fabrizio, P. *et al.* Sir2 blocks extreme life-span extension. *Cell* **123**, 655–667 (2005).
192. Burtner, C. R., Murakami, C. J., Kennedy, B. K. & Kaeberlein, M. A molecular mechanism of chronological aging in yeast. *Cell Cycle* **8**, 1256–1270 (2009).
193. Beach, A. *et al.* Integration of peroxisomes into an endomembrane system that governs cellular aging. *Front. Physiol.* **3**, 283 (2012).
194. Fran??ois, J. & Parrou, J. L. Reserve carbohydrates metabolism in the yeast *Saccharomyces cerevisiae*. in *FEMS Microbiol. Rev.* **25**, 125–145 (2001).
195. Trevisol, E. T. V., Panek, A. D., Mannarino, S. C. & Eleutherio, E. C. A. The effect of trehalose on the fermentation performance of aged cells of *Saccharomyces cerevisiae*. *Appl. Microbiol. Biotechnol.* **90**, 697–704 (2011).
196. Jain, N. K. & Roy, I. Trehalose and protein stability. *Curr. Protoc. Protein Sci.* (2010). doi:10.1002/0471140864.ps0409s59
197. Hu, J. *et al.* Tor-Sch9 deficiency activates catabolism of the ketone body-like acetic acid to promote trehalose accumulation and longevity. *Aging Cell* (2014). doi:10.1111/accel.12202
198. Simons, K. & Sampaio, J. L. Membrane organization and lipid rafts. *Cold Spring Harb. Perspect. Biol.* **3**, a004697 (2011).

199. Ejsing, C. S. *et al.* Global analysis of the yeast lipidome by quantitative shotgun mass spectrometry. *Proc. Natl. Acad. Sci. U. S. A.* **106**, 2136–2141 (2009).
200. Herzog, R. *et al.* Lipidexplorer: A software for consensual cross-platform lipidomics. *PLoS One* **7**, (2012).

Appendix

A. Metabolomic and Lipidomic Analyses of Chronologically Aging Yeast

Summary

Metabolomic and lipidomic analyses of yeast cells provide comprehensive empirical datasets for unveiling mechanisms underlying complex biological processes. In this chapter, we describe detailed protocols for using such analyses to study the age-related dynamics of changes in intracellular and extracellular levels of various metabolites and membrane lipids in chronologically aging yeast. The protocols for the following high-throughput analyses are described: (I) microanalytic biochemical assays for monitoring intracellular concentrations of trehalose and glycogen; (II) gas chromatographic quantitative assessment of extracellular concentrations of ethanol and acetic acid; and (III) mass spectrometric identification and quantitation of the entire complement of cellular lipids. These protocols are applicable to the exploration of the metabolic patterns associated not only with aging but also with many other vital processes in yeast. The described here methodology complements the powerful genetic approaches available for mechanistic studies of fundamental aspects of yeast biology.

A.1 Introduction

The replicative and chronological age of a eukaryotic cell is defined by the spatiotemporal dynamics of a plethora of cellular processes^{3,6,178–180}. To infer the relative contribution of each of these processes to cellular aging and to understand how certain genetic, dietary and pharmacological interventions delay cellular aging by modulating the chronology of critical cellular processes, the methodologies of metabolomic and lipidomic analyses can be advantageous^{6,13,126,181,182}. The application of metabolomics and lipidomics to the acquisition and quantitative analysis of vast empirical data on the metabolic history of a cell progressing through consecutive stages of aging process enables the systems level study of cellular aging

^{6,13,126,181,182}. It is conceivable that with the wealth of data that metabolomics and lipidomics can provide us, some of the most fundamental questions in cellular aging - such as whether it is a programmed process ^{4,183-186} or merely a result of the lifelong accumulation of unrepaired cellular and molecular damage ^{1,187,188} - can be answered.

Because longevity signaling pathways and mechanisms of their modulation by genetic, dietary and pharmacological interventions are evolutionarily conserved ^{3,6,178-180}, the budding yeast *Saccharomyces cerevisiae* is a valuable unicellular model organism for studying mechanisms underlying cellular aging in multicellular eukaryotes ^{3,6,178-180,189}. Due to the relatively short and easily monitored replicative and chronological lifespans of this genetically and biochemically manipulable unicellular eukaryote with annotated genome, it has been successfully used to (I) identify numerous novel longevity genes, many of which have been later implicated in regulating longevity of multicellular eukaryotic organisms; (II) establish the chemical nature of molecular damage that causes cellular and organismal aging and accelerates the onset of age-related diseases; and (III) identify a number of longevity-extending small molecules, many of which have been later shown to slow down aging, improve health, attenuate age-related pathologies and delay the onset of age-related diseases in multicellular eukaryotes ^{6,13,27,32,37,102,123,126,141,179,189-193}.

Recent metabolomic and lipidomic analyses of the metabolic history of chronologically aging yeast cells strongly suggest that their longevity is defined by a pattern of metabolism and organelle dynamics established prior to cell entry into a non-proliferative state in a genotype-, diet- and pharmacological intervention-dependent manner ^{13,32,37,102,123,126,141,191,193}. This chapter describes detailed protocols for such high-throughput analyses that have been used to measure the levels of trehalose, glycogen, ethanol and acetic acid as well as to quantitatively assess the entire complement of cellular lipids. These metabolites have been shown to play a pivotal role in defining the chronological lifespan of a yeast cell ^{13,32,37,102,123,126,141,191,193}. It should be emphasized that the metabolic and lipidomic analyses described here provide powerful empirical tools for studying mechanisms that underlie not only aging but also many other paradigms of yeast biology. As such, these high-throughput analyses are complementary to the great power of yeast genetics in exploring fundamental biological phenomena.

A.1.1 Trehalose Concentration Measurement

Trehalose is a nonreducing disaccharide that has been for a long time considered only as a reserve carbohydrate¹⁹⁴. However, recent findings suggested a role for trehalose metabolism in regulating a variety of cellular processes, including redox homeostasis and protein folding and aging^{126,195–197}. Our studies on the effect of caloric restriction on the metabolic history of chronologically aging yeast provided evidence for the essential role of trehalose in defining yeast lifespan through its effects on protein homeostasis (proteostasis)^{13,141}. Therefore, the existence of a modulated by trehalose regulatory network of cellular proteostasis has been suggested; by maintaining proper synthesis, post-translational modifications, folding, trafficking, degradation and turnover of proteins within a cell, this network defines its chronological and replicative age¹⁴¹. In this chapter, we describe a robust microanalytic biochemical assay for monitoring trehalose concentration in chronologically aging yeast cells.

A.1.2 Glycogen Concentration Measurement

Glycogen, which is known to be the major storage form of yeast glucose¹⁹⁴, has recently been implicated in defining yeast longevity. Our metabolomic and proteomic analyses of chronologically aging yeast provided evidence that a proper balance between the biosynthesis and degradation of glycogen are obligatory for lifespan extension by caloric restriction³. In this chapter, we describe a robust microanalytic biochemical assay for monitoring glycogen concentration in chronologically aging yeast cells.

A.1.3 Ethanol and Acetic Acid Concentration Measurement

A reduction of initial glucose concentration in nutrient-rich growth medium from 2% to 0.5% almost doubles the chronological lifespan of yeast³. Ethanol, a product of glucose fermentation by yeast cells, operates as a redox sink that regulates energy flux from deposited in lipid bodies neutral lipids to mitochondria^{32,37,102,193}. By suppressing peroxisomal enzymes involved in fatty acid oxidation, high ethanol concentrations reduce the energy flux to mitochondria^{3,32,37,102,193}. The resulting decline of the electrochemical potential across the inner mitochondrial membrane promotes mitochondrial fragmentation, which in turn stimulates the release of pro-apoptotic proteins from the mitochondrial intermembrane space and ultimately causes apoptotic cell death^{32,37,102,193}. Low ethanol concentrations promote peroxisomal fatty acid oxidation, thereby elevating the energy flux to mitochondria. The resulting increase of the electrochemical potential

across the inner mitochondrial membrane promotes mitochondrial fusion and maintains mitochondrially produced reactive oxygen species at a level that is insufficient to damage cellular macromolecules but can activate several longevity-extending stress response pathways^{3,32,37,102,193}.

Acetate is another product of glucose fermentation by yeast cells. Akin to ethanol amassed by yeast cultured in nutrient-rich growth medium, acetic acid accumulated by yeast cells grown in minimal medium accelerates chronological aging^{6,179,191,192}.

Both ethanol and acetic acid pass freely across the cell membrane and are thus easily assayed in the growth media. Gas chromatography (GC) is an ideal way to measure these two volatile species due to its speed, high sensitivity, large linear dynamic range and ease of sample preparation. Furthermore, ethanol and acetic acid can be monitored using a flame ionization detector (FID), with which virtually every GC system is equipped. Like other chromatographic techniques, GC relies on the differential solubility of molecules between the mobile (gas) phase and the stationary (liquid) phase on the inside surface of the column. Unlike other chromatographic techniques, however, changing the temperature of the GC oven, not by changing the mobile phase composition, controls the elution of molecules in GC. Thus, separation by GC is controlled by the vapor pressure of the separated molecules and the linear flow rate of the carrier gas. The described in this chapter quantitative assessment of extracellular concentrations of ethanol and acetic acid with the help of GC takes advantage of this fact to separate them from non-volatile contaminants, such as amino acids and sugars.

A.1.4 Mass Spectrometric Quantitative Assessment of the Yeast Lipidome

Lipids are one of the major classes of biomolecules and play important roles in membrane dynamics, energy storage and signaling¹⁹⁸. A body of evidence supports the view that lipid metabolism plays an important role in longevity regulation across phyla^{32,37,102,193}. The budding yeast *Saccharomyces cerevisiae* is a valuable model organism for studying molecular mechanisms linking cellular aging and metabolism of various lipid species in multicellular eukaryotes^{32,37,78,102,193}. In studying these mechanisms, it is crucial to have an analytical method for the robust and accurate quantitative assessment of the entire complement of yeast lipids (lipidome)^{64,199}. In this chapter we describe such a method, namely quantitative shotgun mass spectrometry (MS) using a high resolution Thermo Orbitrap Velos instrument. The method

employs a modified version of the Bligh and Dyer lipid extraction ⁴³ followed by Fourier transform tandem mass spectrometry (FT-MS/MS) to separate numerous lipid species. The raw data are then imported into the open source software LipidXplorer ²⁰⁰, which interprets extensive datasets of shotgun mass spectra to enable the quantitative characterization of all lipid species comprising the yeast lipidome.

A.2 Materials

A.2.1 Trehalose Concentration Measurement

7.2.1.1 Buffers, Solutions, and Growth Mediums

Prepare the following solutions in distilled water unless otherwise stated.

1. YP medium: 1% (w/v) yeast extract and 2% (w/v) bactopectone. Media should be autoclaved at 15 psi/121°C for 45 min prior to use. We typically use 0.2%, 0.5%, 1% or 2% glucose (w/v) as the carbon source.
2. PBS: 20 mM KH₂PO₄/KOH (pH 7.5) and 150 mM NaCl.
3. SHE solution: 50 mM NaOH and 1 mM EDTA.
4. THA solution: 100 mM Tris/HCl (pH 8.1) and 50 mM HCl.
5. Trehalose reagent: 25 mM KH₂PO₄/KOH (pH 7.5) and 0.02% BSA; with or without 15 mU trehalase (Sigma-Aldrich, St. Louis MO).
6. Glucose reagent: 100 mM Tris/HCl (pH 8.1), 2 mM MgCl₂, 1 mM DTT, 1 mM ATP, 0.2 mM NADP⁺, and mixture of hexokinase (7 U) and glucose-6-phosphate dehydrogenase (8 U) (Sigma-Aldrich, St. Louis MO).

A.2.1.2 Yeast Strains and Growth Conditions

Wild-type (WT) strain BY4742 (*MAT α his3 Δ 1 leu2 Δ 0 lys2 Δ 0 ura3 Δ 0*) and single-gene-deletion mutant strains in the BY4742 genetic background (all from Open Biosystems) can be grown in YP medium containing 0.2%, 0.5%, 1% or 2% glucose (w/v) as the carbon source. Cells should be cultured at 30°C with rotational shaking at 200 rpm in Erlenmeyer flasks at a flask volume/medium volume ratio of 5:1.

A.2.2 Glycogen Concentration Measurement

A.2.2.1 Buffers, Solutions, and Growth Mediums

Prepare the following solutions in distilled water unless otherwise stated.

1. YP medium: 1% (w/v) yeast extract and 2% (w/v) bactopectone. Media should be autoclaved at 15 psi/121°C for 45 min prior to use. We typically use 0.2%, 0.5%, 1% or 2% glucose (w/v) as the carbon source.
2. PBS: 20 mM KH₂PO₄/KOH (pH 7.5) and 150 mM NaCl.
3. SHE solution: 50 mM NaOH and 1 mM EDTA.
4. THA solution: 100 mM Tris/HCl (pH 8.1) and 50 mM HCl.
5. Glycogen reagent: 50 mM sodium acetate (pH 4.6) and 0.02% BSA; with and without 5 µg/ml amyloglucosidase 14 U/mg (Roche, Basel, Switzerland).
6. Glucose reagent: 100 mM Tris/HCl (pH 8.1), 2 mM MgCl₂, 1 mM DTT, 1 mM ATP, 0.2 mM NADP⁺, and mixture of hexokinase (7 U) and glucose-6-phosphate dehydrogenase (8 U) (Sigma-Aldrich, St. Louis MO).

A.2.2.2 Yeast Strains and Growth Conditions

Wild-type (WT) strain BY4742 (*MATα his3Δ1 leu2Δ0 lys2Δ0 ura3Δ0*) and single-gene-deletion mutant strains in the BY4742 genetic background (all from Open Biosystems) can be grown in YP medium containing 0.2%, 0.5%, 1% or 2% glucose (w/v) as the carbon source. Cells should be cultured at 30°C with rotational shaking at 200 rpm in Erlenmeyer flasks at a flask volume/medium volume ratio of 5:1.

A.2.3 Ethanol and Acetic Acid Concentration Measurement

1. Sample vials with cap/septum are available from many suppliers.
2. GC system equipped with an FID detector (*see Note 1*).
3. Column: The Equity-1 column from Supelco (0.32 mm I.D. × 30 m). This column has a simple stationary phase chemistry and provides good separation for ethanol and acetic acid. It is robust and widely available (*see Note 2*).

A.2.4 Mass Spectrometric Quantitative Assessment of the Yeast Lipidome

A.2.4.1 Yeast Strains and Growth Conditions

1. YP medium: 1% (w/v) yeast extract and 2% (w/v) bactopectone. Media should be autoclaved at 15 psi/121°C for 45 min prior to use. We typically use 0.2%, 0.5%, 1% or 2% glucose (w/v) as the carbon source.
2. Wild-type strain BY4742 (*MATa his3ΔI leu2Δ0 lys2Δ0 ura3Δ0*) and single-gene-deletion mutant strains in the BY4742 genetic background (all from Open Biosystems) can be grown in YP medium containing 0.2%, 0.5%, 1% or 2% glucose (w/v) as the carbon source. Cells should be cultured at 30°C with rotational shaking at 200 rpm in Erlenmeyer flasks at a flask volume/medium volume ratio of 5:1.

A.2.4.2 Lipid Extraction and Mass Spectrometry

1. Chromasolv HPLC (>99.9%) chloroform and methanol or equivalent (Sigma-Aldrich, St. Louis MO).
2. 28% ammonium hydroxide (Sigma-Aldrich, St. Louis MO).
3. Glass beads, acid-washed, 425-600 μM (Sigma-Aldrich, St. Louis MO).
4. Vortex with appropriate adapter.
5. 15 ml high-speed glass centrifuge tubes with Teflon lined caps (Fisher Scientific).
6. Chloroform/Methanol mixtures: 17:1, 2:1 and 1:2 mixtures of chloroform and methanol, as well as a chloroform/methanol (2:1) mixture with 0.1% ammonium hydroxide (v/v).
7. ABC: 155 mM ammonium bicarbonate (pH 8.0).
8. Internal Standards: Triacylglycerol (13:0/13:0/13:0) (Larodan, Malmo, Sweden) as well as various species of phospholipids - including phosphatidylcholine (13:0/13:0), phosphatidylethanolamine (14:0/14:0), phosphatidylserine (14:0/14:0), phosphatidic acid (14:0/14:0), and cardiolipin (14:0/14:0/14:0/14:0) (all from Avanti Polar Lipid, Alabaster, AL, USA).
9. Glass 2 mL sample vials with Teflon lined caps.

A.2.4.3 Software

1. LipidXplorer: (https://wiki.mpi-cbg.de/wiki/lipidx/index.php/Main_Page)
2. MSConvert: <http://proteowizard.sourceforge.net/>

A.3 Methods

A.3.1 Trehalose Concentration Measurement

A.3.1.1 Preparation of Alkali Cellular Extract

1. Measure the cell titer by taking 10 μL aliquots of cell culture, diluting appropriately, and counting cells with a hemacytometer.
2. Harvest 2×10^9 cells by centrifugation for 1 min at $16,000 \times g$ at 4°C .
3. Wash the cell pellet three times in ice-cold PBS and then resuspend in 200 μL of ice-cold SHE solution. Add an additional 800 μL of ice-cold SHE solution to the cell suspension (~ 1 ml total volume).
4. Incubate the resulting alkali extract at 60°C for 30 min to destroy endogenous enzyme activities and pyridine nucleotides.
5. Neutralize the extract by adding 500 μL of THA solution.
6. Divide the extract into 150 μL aliquots and quickly freeze them in liquid nitrogen. Store at -80°C prior to use.

A.3.1.2 A Microanalytic Biochemical Assay for Measuring Trehalose Concentration

1. Add 50 μL of alkali extract to 150 μL of trehalose reagent with and without trehalase.
2. Incubate the mixture for 60 min at 37°C . Add 800 μL of glucose reagent and incubate the mixture for 30 min at 25°C .
3. Measure the NADPH generated from NADP^+ fluorimetrically (excitation at 365 nm, emission monitored at 460 nm).

A.3.2 Glycogen Concentration Measurement

A.3.2.1 Preparation of Alkali Cellular Extract

1. Measure the cell titer by taking 10 μL aliquots of cell culture, diluting appropriately, and counting cells with a hemacytometer.
2. Harvest 2×10^9 cells by centrifugation for 1 min at $16,000 \times g$ at 4°C .

3. Wash the cell pellet three times in ice-cold PBS and then resuspend in 200 μL of ice-cold SHE solution. Add an additional 800 μL of ice-cold SHE solution to the cell suspension (~ 1 ml total volume).
4. Incubate the resulting alkali extract at 60°C for 30 min to destroy endogenous enzyme activities and pyridine nucleotides.
5. Neutralize the extract by adding 500 μL of THA solution.
6. Divide the extract into 150 μL aliquots and quickly freeze them in liquid nitrogen. Store at -80°C prior to use.

A.3.2.2 A Microanalytic Biochemical Assay for Measuring Glycogen Concentration

1. Add 50 μL of alkali extract to 500 μL of glycogen reagent and incubate at 25°C for 30 min.
2. Add 500 μL of glucose reagent and incubate at 25°C for 30 min.
3. Measure the NADPH generated from NADP^{+} fluorimetrically (excitation at 365 nm, emission monitored at 460 nm).

A.3.3 Ethanol and Acetic Acid Concentration Measurement

A.3.3.1 Yeast Strains and Growth Conditions

The wildtype strain BY4742 (*MAT α his3 Δ 1 leu2 Δ 0 lys2 Δ 0 ura3 Δ 0*) was grown in YP medium (1% yeast extract, 2% bactopectone) containing 0.2%, 0.5%, 1% or 2% glucose as carbon source. Cells were cultured at 30°C with rotational shaking at 200 rpm in Erlenmeyer flasks at a flask volume/medium volume ratio of 5:1.

A.3.3.2 Sample Preparation for Gas Chromatography

1. Collect aliquots of yeast cultures and harvest cells by centrifugation at $16,000 \times g$ for 2 min at room temperature.
2. The supernatant collected can either be used immediately or stored at -80°C prior to use.

A.3.3.3 Gas Chromatographic Measurement of Ethanol and Acetic Acid

1. Place 100 μL of supernatant in auto-sampler vials; to avoid growth in the vials, samples must be run at once for approximately 4 h. If you have a cooled auto sampler, you can load more samples.
2. Inject 1 μL of sample in a splitless injector (*see Note 3*), with constant back pressure, nitrogen as carrier gas and a temperature curve of:
 - a. 45 $^{\circ}\text{C}$ for 30 sec
 - b. 45-72 $^{\circ}\text{C}$ for 45 sec
 - c. 72-80 $^{\circ}\text{C}$ for 2 min
 - d. Increase to maximal temperature at highest rate and hold for 3 min to elute higher boiling point contaminants

Using this temperature profile, ethanol and acetic acid should elute after about 3 min, and the total run time will be about 20 min, including the cool-down time for the oven (*see Note 4*).

A.3.4 Mass Spectrometric Quantitative Assessment of the Yeast Lipidome

A.4.1 Yeast Culture Conditions and Glass Bead Lysate

1. Culture yeast in YPD medium (1% yeast extract, 2% bactopectone, 2% glucose) at 30 $^{\circ}\text{C}$ with rotational shaking at 200 rpm in Erlenmeyer flasks at a flask volume/medium volume ratio of 5:1. Cultures should be grown to whichever growth phase is desired for the study.
2. Harvest 5×10^7 cells (~5 mL of the culture for cells recovered in logarithmic growth phase) by centrifugation at $3000 \times g$ for 5 min at room temperature.
3. Wash the cell pellet with ice-cold ABC, transfer to a 2 mL microfuge tube; centrifuge at $16,000 \times g$ for 1 min at 4 $^{\circ}\text{C}$.
4. Resuspend the pellet in 1 ml of ice-cold ABC.
5. Add 200 μL of glass beads and vortex for 5 min, then place the sample on ice for 1 min. Repeat this step three times.
6. Assess protein content of cell lysate using standard methods.
7. The cell lysate should be stored at -80 $^{\circ}\text{C}$ until lipid extraction.

A.3.4.2 Lipid Extraction

1. Calculate the amount of the lysate needed for approximately 50 μg of protein equivalent per replicate. Transfer to 15 ml glass centrifuge tubes.
2. Add 1 mL of nanopure water.
3. Add 20 μL of internal standard mix prepared in chloroform according to **Table 1**.
4. Add 3 mL of chloroform/methanol (17:1) mixture and vortex at 4°C for 2 h (*see Notes 5, 6 and 7*).
5. Separate phases by centrifugation at $3000 \times g$ for 5 min at room temperature. Transfer the lower organic phase to a new 15 ml glass tube.
6. Add 1.5 ml of chloroform/methanol (2:1) mixture to the remaining aqueous phase and vortex at 4°C for 2 h.
7. Separate phases by centrifugation at $3000 \times g$ for 5 min at room temperature and combine with the organic phase from the chloroform/methanol (17:1) extract.
8. Evaporate off the solvent under nitrogen flow or in a vacuum evaporator.
9. Dissolve the lipid film in 100 μL of methanol/chloroform (2:1) mixture and transfer to a 2 ml glass sample vial with either Teflon or aluminum lined caps.
10. Samples should be stored at -20°C until ready to be analyzed by MS (*see Note 8*).

	Chain Composition	MW	M/Z	Concentration [mg/mL]	Ion
PA	14:0 / 14:0	592.41	591.40	0.1	M-H
PE	14:0 / 14:0	635.45	634.44	0.1	M-H
PG	14:0 / 14:0	666.45	665.44	0.02	M-H
PS	14:0 / 14:0	679.43	678.43	0.1	M-H
CL	14:0 / 14:0 / 14:0 / 14:0	1241.83	619.91	0.1	M-H
CM	17:0 / 18:1	551.53	550.52	0.05	M-H
FFA	19:0	298.28	297.27	0.02	M-H
DAG	14:0 / 14:0	512.44	511.44	0.05	M-H
TAG	13:0 / 13:0 / 13:0	680.60	698.63	0.1	M+NH ⁴
PC	13:0 / 13:0	649.47	650.48	0.1	M+H

Table 1 – Internal Standards

A.3.4.3 Mass Spectrometric Analysis of Yeast Lipids

1. Prior to running samples for the first time, it is recommended to run a standard curve for your lipid standards (*see Notes 9 and 10*). This can be done by preparing dilutions spanning ~ 0.005 to 50 μM and analyzing them in both negative and positive ion modes.
2. Dilute the lipid extract appropriately in chloroform/methanol (1:2) mixture with 0.1% NH_4OH , so that your signal falls within the range of your calibration curve.
3. Resolve lipids by direct injection using a Thermo Orbitrap Velos mass spectrometer equipped with a HESI-II ion source (Thermo Scientific, Waltham, MA, USA) at a flow rate of 5 $\mu\text{L}/\text{min}$ (*see Note 11*). Use an instrument method for data-dependent acquisition. The first segment is a full survey scan using the FT-MS; it is followed by 9 dependent MS/MS scans to sequentially perform MS/MS on all peaks above the set threshold from high to low intensity. Those peaks are then added to an exclusion list and the cycle will continue for 5 min (*see Note 12*). The tune settings and instrument methods that we routinely use are summarized in (**Table 2**, Table 3).

Tune Information		
Instrument Polarity	Positive	Negative
Source Voltage (kV)	3.9	4
Capillary Temp ($^{\circ}\text{C}$)	275	275
Sheath Gas Flow	5	5
Aux Gas Flow	1	1
FT-MS Injection Time (ms)	100	500
FTMS microscans	3	1

Table 2 – Orbitrap instrument settings

Acquisition Time (min)	5 (+0.25 delay)	
MS (segment 1)		
Instrument Polarity	Positive	Negative
Analyzer	FTMS	FTMS
Mass Range	Normal	Normal
Resolution	100,000	100,000
Data Type	centroid	centroid
Scan Range	400-1200	200-1400
Data Dependent MSMS (segments 2-10)		
Instrument Polarity	Positive	Negative
Analyzer	FTMS	FTMS
Resolution	30,000	30,000
Data Type	Centroid	Centroid
Activation	HCD	HCD
Activation Time (ms)	0.1	0.1
Isolation Width	1	1
Collision Energy	35	65
Mass Range	Normal	Normal
Data Type	centroid	centroid
Scan Range	-	-

Table 3 – Orbitrap instrument method summary

A.3.4.4 Identification and Quantitation of Lipids Following Their Separation by Mass Spectrometry

1. Convert mass spectra to an open format (mzXML, mzML) using the ProteoWizard MSConvert software, which is freely available from <http://proteowizard.sourceforge.net/>.
2. Spectra can then be imported into LipidXplorer for the automated detection of lipid species. (https://wiki.mpi-cbg.de/wiki/lipidx/index.php/Main_Page; see Figure 41).
3. Data are normalized by taking the ratio of signal intensity of precursor ions to that of their respective lipid class-specific internal standard (spiked standard), multiplied by the concentration of that standard to give a molar quantity. The ratio of an individual molar quantity by the sum of that contributed by all other detected lipid species will give the molar ratio, which should be expressed as a percentage.

A.4. Notes

1. Because the FID detects sample by burning it and reading the current across the flame, it is sensitive to how oxidized your analyte is - which is why it is more sensitive to ethanol than acetic acid.
2. The method and instrumentation are very robust and no further sample preparation is required beyond spinning down the cells. Unfortunately, this means the samples are quite dirty and your local GC owner may be hesitant to let you use their equipment. Offering to supply your own column, injection syringes and vaporization chambers may help.

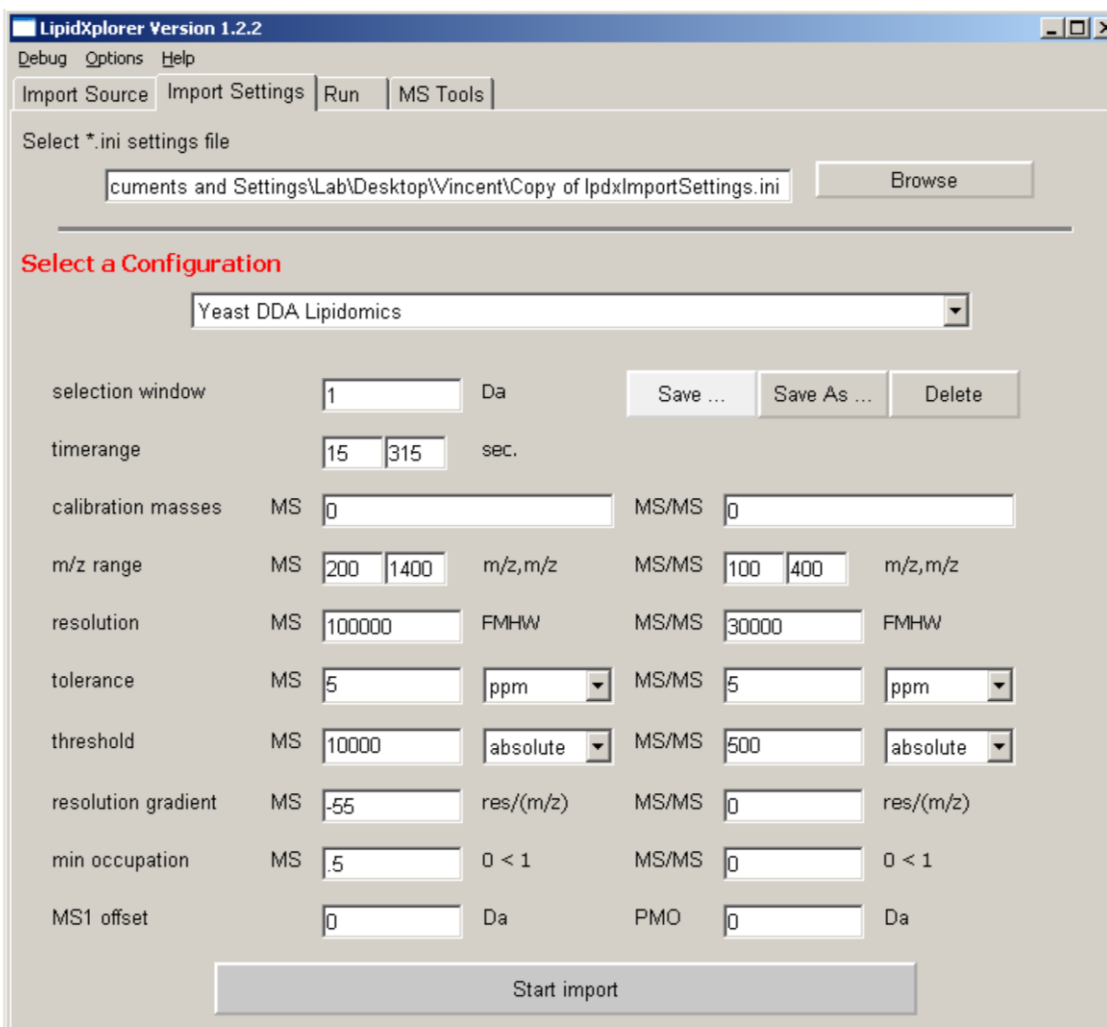


Figure 41 - Import setting for LipidXplorer

Following conversion to an open format (mzXML, mzML) using the ProteoWizard MSConvert software (<http://proteowizard.sourceforge.net/>), mass spectra can be imported into LipidXplorer

(https://wiki.mpi-cbg.de/wiki/lipidx/index.php/Main_Page) for the automated detection of lipid species.

3. Be sure to rinse the injection syringe several times after each run and, at the end of the day, remove it and clean it very well - otherwise sugars and other contaminants will render it unusable. It is good practice to run a standard curve at the beginning of each day. If many samples are analyzed, run a single point standard now and then to ensure the machine is operating properly; 0.1% (v/v) for both ethanol and acetic acid work well. If you start seeing drift in retention times or differences in sensitivity, you should replace the vaporization chamber or the glass fibre inside it. At worst you will have to remove a few centimetres at the beginning of the column, since you have 30 m to work with; it will not seriously affect its separation abilities. Vaporization chambers can also be rejuvenated with an intensive acid wash. Over the course of several hundred injections, we replaced or washed the vaporization chamber perhaps twice and never had to cut the column.

4. In nutrient-rich cultural media initially containing 2% glucose, we can see ethanol concentrations up to ~6%, and acetic acid ~0.3% in the cultures collected at logarithmic growth phase. Detection limits and linear dynamic range will vary from instrument to instrument, but 0.001% to 10%+ for ethanol and 0.01% to 10%+ for acetate are reasonable.

5. Handle chloroform and methanol with caution as they are both fairly toxic and readily leech contaminants from a number of sources including plastics, your skin, the air etc. If you have these solvents in large volumes (more than half a liter), it is advised to carefully transfer a smaller portion to a meticulously cleaned smaller glass container.

6. Never access solvents directly! Pour the appropriate volume into smaller glassware first. This will reduce the likelihood of accidental contamination of your solvents. Any contaminants within the solvent will be concentrated into the lipid film following extraction, so for that reason it is important to not skimp on the grade of solvents that you use!

7. It is very important to avoid the use of plastics in steps that involve any kind of manipulation of organic solvents - since they will leech contaminants into your samples, greatly complicating your spectra and potentially causing ion suppression effects. Use borosilicate glass pipettes for these steps. It is recommended to rinse pipettes with chloroform and methanol prior to use. When

handling lipid standards, it is a good idea to let them warm to room temperature and sonicate them prior to spiking your samples. This will help ensure the solubility of your standards.

8. Because the relative stabilities of different lipids are not very well known, it is important to be careful during all steps of the procedure to prevent sample degradation. Extraction and drying of lipid films should be done at 4°C. When injecting samples, try to keep those that will not be immediately run cold. When finished running the sample, it is advisable to return any remainder to -20°C for any further analysis.

9. Prior to running samples, it is a good idea to record baseline spectra of your solvents (in this case, it is a chloroform/methanol (1:2) mixture with 0.1% NH₄OH).

10. For the same reason as point 5, it is not recommended to store lipid extracts for extended periods of time prior to running. In our workflow, we try to arrange extractions to take place during the same week that we will be running the samples.

11. Although we have access to an LTQ Orbitrap Velos, any reasonably high-resolution mass spectrometer can be used with some modification to this protocol.

12. We typically use an instrument method for data-dependent acquisition, which automatically performs tandem MS on peaks in primary spectra. Depending on your specific needs, this may not be necessary.